Alma Mater Studiorum – Università di Bologna

DOTTORATO DI RICERCA IN

Scienze Biomediche: Progetto n.1 “Biotecnologie Mediche”

Ciclo XXV

Settore Concorsuale di afferenza: 06/A3

Settore Scientifico disciplinare: MED/07

Human papillomavirus (HPV) and associated diseases: between applied diagnostic and basic research

Presentata da: **Dott.ssa Daniela Barbieri**

Coordinatore Dottorato **Relatore**

Prof. Lucio Cocco **Prof.ssa Marialuisa Zerbini**

Esame finale anno 2013

Summary

1. Introduction

In 2008, Prof. Harald zur Hausen (German Cancer Research Center, Heidelberg, Germany) won the Nobel Prize in Medicine *"for his discovery of Human Papillomaviruses causing cervical cancer"* at the beginning of the '70s (zur Hausen et al., 1975), giving the necessary scientific grounds to the Italian physician Rigoni-Stern's observations in 1842 about the possible sexual transmission of cervical cancer. This event definitely underlined the global relevance of the research on HPV and associated diseases.

1.1 Human Papillomavirus (HPV)

1.1.1 Viral structure and genome organization

HPVs are small (55 nm of diameter), non-enveloped viruses with an icosahedral proteic capsid, belonging to the family of *Papillomaviridae*. The genome is a circular double stranded molecule of DNA (dsDNA) about 8000 bp long, which can be divided in three major regions separated by two polyadenilation sites (AE and AL) (Fig. 1) (Zheng & Baker, 2006). The early region contains six open reading frames (ORFs) expressed during the early phase of the viral cycle, which codify for functional proteins involved in cell cycle deregulation (E5, E6 and E7), control of viral genome replication and transcription (E1 and E2) and interactions with the cytoskeleton (E4). In the late region there are only two genes for the production of the major and minor structural proteins of the capsid (L1 and L2, respectively). These two regions are under the tight control of two different promoters, the early and the late promoters (P_{97} and P_{670} in HPV 16), whose activation is strictly dependent on cell differentiation status. The third region is the long control region or upper regulatory region (LCR or URR), a ~850bp long non-codifying region which contains sequences involved in the control of viral genes expression and replication (TATA box, enhancer and origin of replication). Here there are the four sequences specific for the binding of the viral protein E2 (E2 binding sites, E2BSs, 5'-$ACCN_6GGT$-3') which allow the transcriptional regulation of E6 and E7 (Androphy et al, 1987). When the concentration of E2 is low, it binds preferably to E2BS1 far from the early promoter, leading to E6/E7 expression. As E2 concentration increases, the other E2BSs will also be bound by E2, resulting in E6/E7 repression (Hegde, 2002). The interaction of E2 with E2BS1 was found to be the most stable interaction compared to binding

of E2 to the other binding sites, with E2BS2 in the origin of replication being the least stable. In addition to E1 and E2, other cellular transcription factors, such as TFIID, Sp1, Ap1, YY1 and NF1, can bind to this region influencing E2 binding and viral transcription (Lewis et al, 1999).

The viral genome is very compact and can encode multiple proteins by transcribing polycistronic transcripts which undergo alternative RNA splicing to express different proteins. For example, HPV 16 E6 and E7 pre-mRNAs are transcribed from the same P_{97} early promoter as bicistronic E6/E7 pre-mRNAs, and have an intron in the E6 coding region with one 5′ splice site and three alternative 3′ splice sites. Splicing of E6/E7 pre-mRNAs by alternative utilization of these three 3′ splice sites produce E6^E7, E6*I and E6*II mRNAs. If this intron remains unspliced, the resulting E6/E7 mRNA expresses the oncogenic full length E6 (Zheng & Baker, 2006).

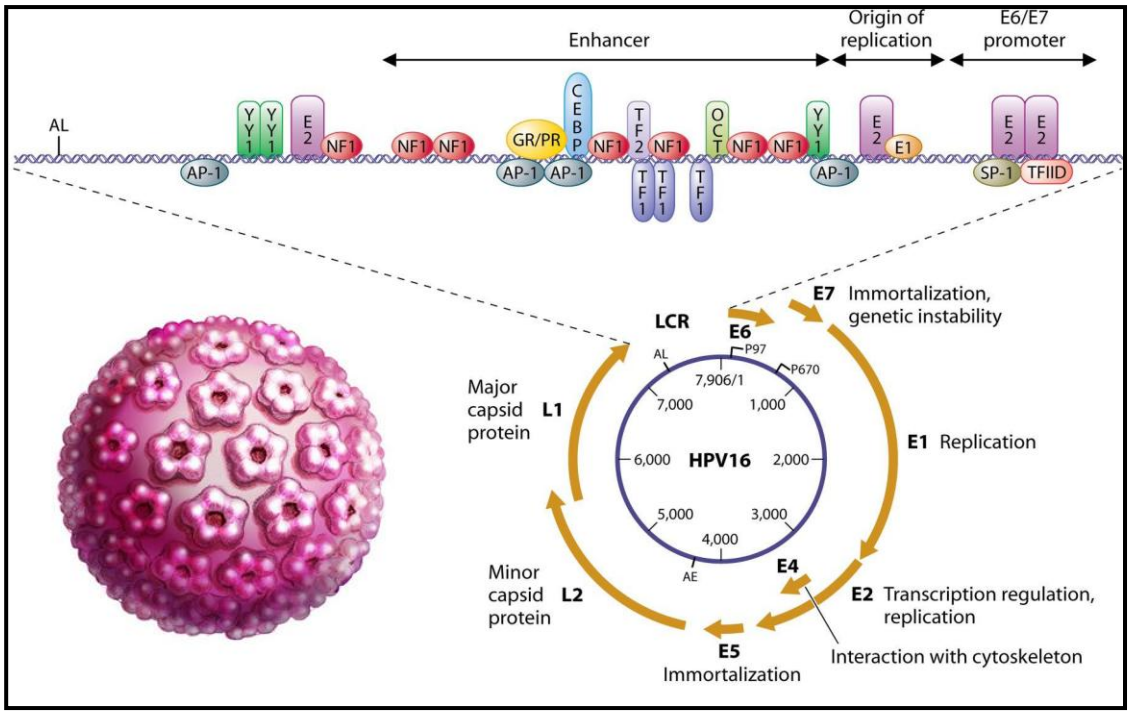

Figure 1 – Predicted structure and genomic organization of HPV 16: function of the codified proteins and cellular transcription factors which bind to the LCR (Lazarczyk et al, 2009).

1.1.2 Classification

Actually, more than 120 Papillomaviruses (PV) have been described based on the isolation of complete genome but more are probably to exit. The L1 ORF is the most conserved gene within the genome and has been used for the identification of new PV types over the past 20 years. A new PV isolate is recognized as such if the complete genome has been cloned and

the DNA sequence of the L1 ORF differs by more than 10% from the closest known PV type. Differences between 2% and 10% homology define a subtype and less than 2% a variant (de Villiers et al, 2004). The designation, HPV (number), is only given after isolation and characterization of the complete genome. This full-length genome is deposited at the Reference Centre for Papillomaviruses (in Heidelberg, Germany) where the genome organization and sequence is verified as a new PV type.

The *alpha-*, *beta-* and *gamma-genus* include the HPV types which have different genomic and biological properties (Fig. 2). In fact, HPVs can be divided in two major groups: the cutaneous and the mucosal HPV, depending on the type of epithelium which can preferentially infect. The *alpha-genus* include both mucosal and cutaneous HPVs with the E5 ORF, the *beta-* and *gamma-genus* only cutaneous HPVs without E5 ORF.

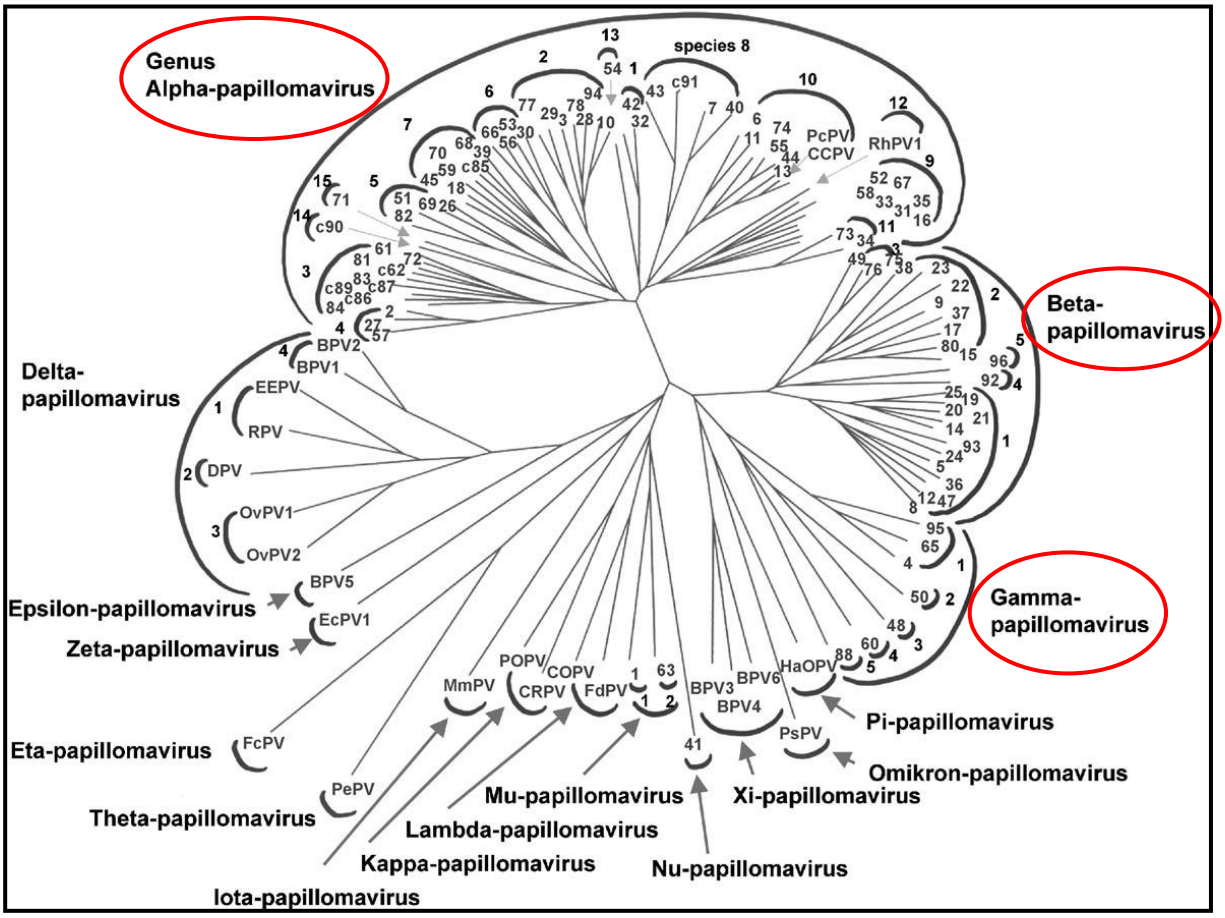

Figure 2 – Phylogenetic tree containing the sequences of 118 Papillomavirus types (human and non-human), based on the differences/similarities in the L1 ORFs (de Villiers et al, 2004). Red circles underline the genus which include the mucosal and cutaneous HPV types.

1.1.3 Viral cycle: productive infection and viral proteins

As previously mentioned, HPV viral cycle is strictly dependent on the differentiation status of the infected host cells and for this reason epithelial raft cultures has been developed to better investigate it *in vitro* (Andrei et al, 2010).

The normal productive infection starts when the virus reaches the dividing basal cells of the epithelium through small lesions, entering in the cytoplasm *via* clathrin- or caveolin-dependent endocytic mechanisms (Fig. 3) (Day et al, 2003). The major capsid protein L1 interacts with heparan sulfate proteoglycans on the cell surface with the involvement of a secondary receptor and a possible role for the minor capsid protein, L2. Particles disassemble in late endosomes and/or lysosomes, with the transfer of viral DNA to the nucleus being facilitated by L2 (Doorbar, 2006). In experimental systems, viral transcripts can be detected as early as 12 h post-infection, with mRNA levels increasing over the course of several days. In this early part of the infection, the viral genome is a stable episome (not integrated into the host genome) and acquires euchromatic structure (association with histones) allowing nuclear transcription factors to regulate the viral expression during the productive infection. The proteins E1 and E2 are required for its maintenance, replication with the cellular genome during the S-phase and segregation (Table 1). Moreover, E2 regulates transcriptional levels of E6 and E7 in a dose-dependent manner: these proteins are necessary to drive to and block the cell in the S-phase *via* interactions with p53 and pRb. Upon infection of basal cells, HPV genomes are replicated up to 50–100 copies per cell.

Suprabasal cells normally exit the cell cycle and begin the process of terminal differentiation in order to produce the protective barrier that is normally provided by the skin. At the same time, HPVs need to amplify their genome and produce new viral particles. What triggers the onset of late events is not yet fully understood, but appears to depend in part on changes in the cellular environment as the infected cell moves towards the epithelial surface, leading to the increase of viral proteins involved in replication (i.e. E1, E2, E4, E5). As E2 increases in abundance, occupancy of the remaining sites leads to the displacement of basal transcription factors, such as Sp1 and TBP (TATA-box-binding protein), that are necessary for promoter activation. It appears that the increase in E2 expression leads eventually to the down-regulation of E6/E7 expression and to the eventual loss of the replicative environment necessary for viral DNA synthesis. E5 is a transmembrane protein which resides predominantly in the endoplasmic reticulum, but it can associate with the vacuolar proton ATPase delaying the process of endosomal acidification. It is thought that this affects the

recycling of growth factor receptors on the cell surface, leading to an increase in epidermal growth factor (EGF)-mediated receptor signalling and the maintenance of a replication competent environment in the upper epithelial layers. On the other hand, E4 causes cell-cycle arrest in G2 phase and antagonizes E7-mediated cell proliferation.

The events that link genome amplification to the synthesis of the capsid proteins are not yet fully understood, but are dependent on changes in mRNA splicing and on the generation of transcripts that terminate at the late (rather than the early) polyadenylation site. The assembly of infectious virions in the upper epithelial layers is thought to require E2 in addition to the capsid proteins L1 and L2, and it has been suggested that E2 may improve the efficiency of genome encapsidation during natural infection. L2 localizes to the nucleus by virtue of nuclear localization signals located at its N- and C termini and, once there, it associates with PML (promyelocytic leukaemia) bodies. Although some PV L2 proteins can associate directly with DNA, the specific recruitment of viral genomes to PML bodies is thought to require E2, which can associate with viral DNA through its specific recognition sites. L1 assembles into capsomeres in the cytoplasm (360 copies of L1 organized into 72 capsomeres with 1 copy of L2 in the center) prior to nuclear relocation and is recruited into PML bodies only after L2 has bound and has displaced the PML component sp100.

In the end, virus release requires efficient escape from the cornified envelope at the cell surface, which may be facilitated by the E4 protein by disrupting the keratin network and affecting the integrity of the cornified envelope. The viral infectious cycle is exclusively intraepithelial: there is no viremia and no virus-induced cytolysis or cell death, and viral replication and release are not associated with inflammation.

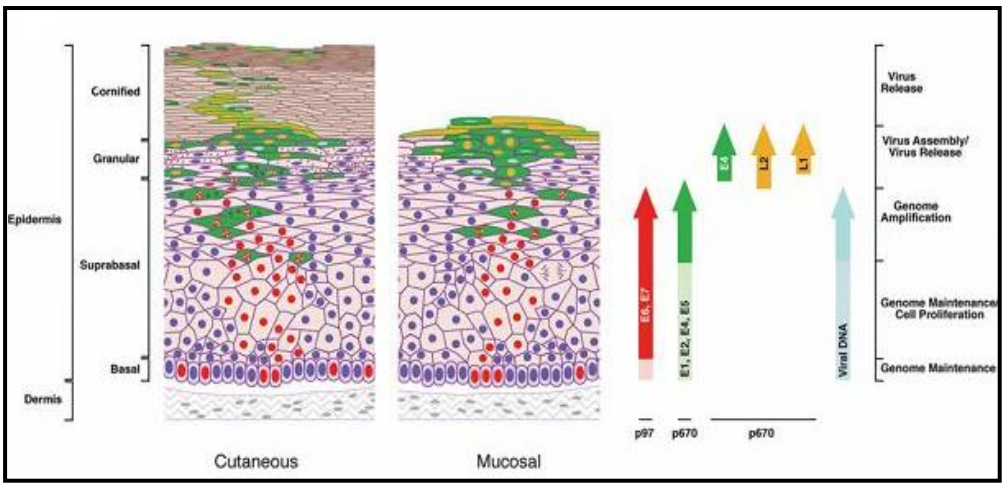

Figure 3 – Viral life cycle in cutaneous and mucosal epithelia and gene expression in different epithelial layers (Doorbar, 2006).

Table 1- Viral proteins and their functions (Doorbar, 2006; Ganguly & Parihar, 2009; Hegde, 2002; Miller et al, 2012).

Viral protein	Molecular Mass (kDa)	Functions and Interactions
L1	55-60	Major protein of the capsid (highly conserved among HPVs) Interaction with cell surface receptor
L2	70	Minor protein of the capsid Important for the efficacy packaging of new particles
E1	68-75	ATP-ase and Helicase (highly conserved among HPVs) Replication and maintenance of viral genome (binding site: 6 repeated AACNAT)
E2	50	DNA binding protein (binding site: 5'-ACCN$_6$GGT-3' in LCR) Replication, maintenance and segregation of viral genomes Regulation of E6 and E7 transcription Interaction with cellular RPA and DNA polymerase α
E4	17	Not fully clarified and mostly present as fusion protein E1^E4 Cell cycle arrest in G_2-phase
E5	8-10	Transmembrane protein which resides in the endoplasmatic reticulum Replication of the viral genome Maintenance of the competent replicative environment in the upper epithelial layers
E6	16-18	Oncoprotein (in high risk-HPV with C-term PDZ-binding domain) two zinc-binding domains with two CXXC motifs p53 ubiquitin-dependent degradation interacting with E6-associated protein (E6AP) Activation of cellular telomerase (hTERT) Inibition of IRF3 evading immune response, interaction with CBP/p300 Cell cycle deregulation
E7	11	Oncoprotein, low immunogenicity (C-terminus contains a zinc-binding domain composed of two CXXC motifs) N-term interacts with pRb avoiding its binding to transcription factor E2F Interaction with cellular HDACs, HATs, DMTs, AP1, p21, p27, p600 Inhibition of IRF1 and IRF9 evading immune response Cell cycle deregulation (targeting G_1/S checkpoint)

1.1.4 Molecular pathogenesis: transforming infection, integration and latency

In the previous paragraph, we described the productive infection of HPV, which does not cause a symptomatic effect nor a high immune response. However, the majority of HPV infections (90%) are cleared in 2 years without any complication for the host (Gravitt, 2011). But what happens if the infection persists? As we have seen, the key molecules during the viral replication are the oncoproteins E6 and E7, which interact with a great number of cellular proteins (Tab 1 and Fig 4). In experimental systems these interactions have been shown to induce proliferation and eventually immortalization and malignant transformation of cells, but the mechanisms which determine the "switch" from productive to transforming infection have not been completely understood yet. Since there are differences between E6/E7

proteins of different HPV types, actually we distinguish, among the mucosal group, high risk-HPVs (HR-HPVs), probably HR-HPVs and low risk-HPVs (LR-HPVs), depending on the different capacity of HPV types to establish a transforming infection. For example, HR-HPVs E6 protein contains a PDZ-binding domain targeting proteins in the cellular membrane-cytoskeleton interface, disrupting cell junctions and promoting transformation.

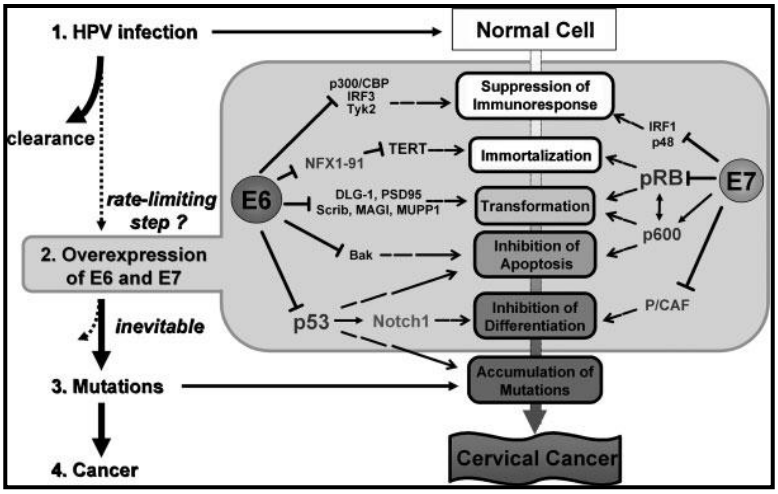

Figure 4 – Multi-step pathogenesis of HPV and some of the interactions of viral oncoproteins E6 and E7 with cellular proteins (Yugawa & Kiyono, 2009).

The crucial point during viral life cycle is the regulation of E6 and E7 expression. If these proteins are overexpressed, cell cycle/ mitosis deregulation and suppression of the immune response are increased as well, leading to genomic instability and accumulation of mutations at different sites (random) of the cellular chromosomes. Together, all these events are necessary for cancer development and define the malignant phenotype (multipolar mitoses are hallmark of HR-HPV-associated carcinomas) (Muñoz et al, 2006; Yugawa & Kiyono, 2009).

One of the main consequences of genomic instability during persistent HPV infection is random integration of the viral genome into cellular chromosomes through double strand breaks (DSBs) (Pett & Coleman, 2007; Pett et al, 2004; Wentzensen et al, 2004). Usually, this event occurs in the viral E2 ORF, leading to the complete or partial loss of E2 protein. Since E2 is fundamental for the correct regulation of E6 and E7 transcription, viral integration contributes to the overexpression of these oncoproteins. More rarely, concatameric integrants are observed, where viral copies (including intact E2) are arranged in a head-to-tail fashion with partially deleted copies at the 5'- and 3'- ends (Fig 5).

During the last 20 years, viral integration was thought to be the key mechanism for HPV-associated cancer development, but the findings of episomal viral DNA in late stage cancers

suggested the presence of alternative pathways for oncoproteins overexpression in the presence of active E2 (Arias-Pulido et al, 2006; Vinokurova et al, 2008). One of these mechanisms have been suggested to have an epigenetic nature, involving methylation of citosines (meC) by cellular DNA Methyltransferases (DMTs). In fact, not only DNA methylation is a mechanism commonly used by mammalian cells to drive and control gene expression, but it has been also shown that E7 can interact with DMT-1 (Burgers et al, 2007) and meC in CpG sites in the viral EBSs act as obstacle to E2 binding (Kim et al, 2003; Thain et al, 1996). DNA methylation in HPV infected cells may occur in both episomal and integrated viral genome as well as in cellular genes, having different roles (Szalmas & Konya, 2009). At the viral DNA level, it may act as a cellular defence mechanism avoiding foreign genes expression; at the host genome level, it may inactivate some key genes involved in the control of cellular signalling pathways.

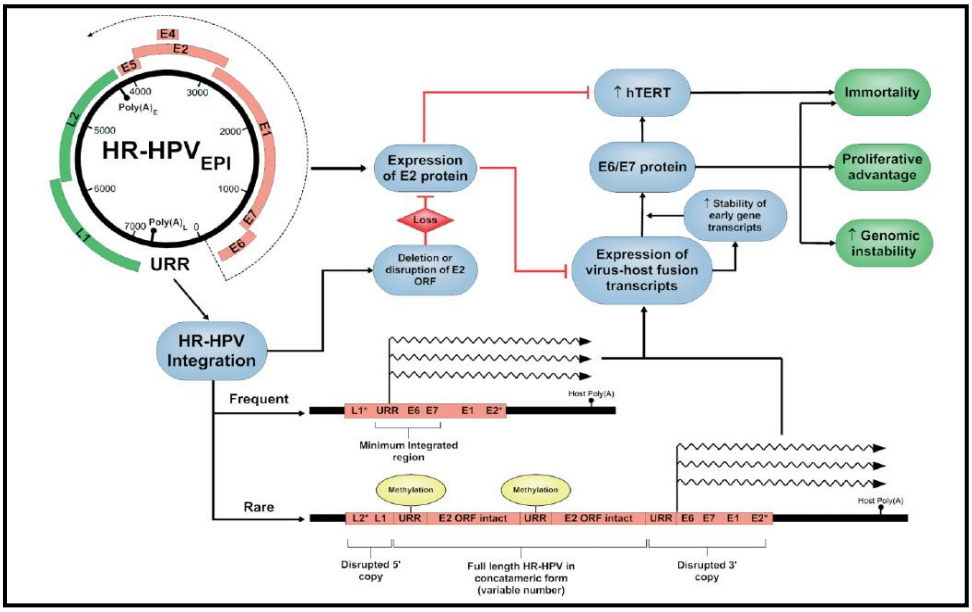

Figure 5 – Significance of HR-HPV integration detected in cervical carcinomas (Pett & Coleman, 2007).

Up to now, we described what happens during a persistent HPV infection, when the virus replicates with high titres which can be detected by common diagnostic techniques. However, sometimes in a basal stem cell HPV may persist and remain undetectable until triggered to differentiate by undetermined stimuli such as wound repair and hormonal regulation (Gravitt, 2011). This event is called viral latency and it has not been completely understood for HPV. It is thought that a few infected basal stem cells may retain HPV episomes, but do not differentiate, and these infected cells are unlikely to be sampled using standard exfoliative

techniques employed in most epidemiologic studies, which sample only the surface epithelium. Moreover, minor fraction of the episomal HPV DNA can be methylated *de novo* and can also be associated with transcriptionally inactive chromatin structure, providing a plausible mechanism for latent form of HPV infection (Szalmas & Konya, 2009). Wounding may stimulate latently infected basal cells to divide and trigger viral reactivation and stimulation of tissue-resident memory T cells.

1.2 Clinical relevance of mucosal *alpha*-HPVs infection

Transmission of HPV infection occurs primarily via sexual activity, most commonly vaginal and anal intercourse. Other forms of transmission have been occasionally reported such as skin-on-skin genital contact, and mother-to-child transmission, but their implication in cervical cancer is likely to be marginal. Oral sex can also be a route of HPV transmission.

HPV infection is very common. Most women in the world will be infected with genital HPV at some time in their lives, with a lifetime risk of infection of 50–80%, and peak incidence occurs in the 18–30 age group (Stanley, 2010). Even if HPV infection is mainly known worldwide for the causative relationship with cervical cancer, during the last 30 years it has been also associated to the development of many other diseases in both men and women, with different roles of HPV genotypes (Tab. 2).

The prevalence of genital HPV infection in men is not well established and results from studies are difficult to compare because of differences in sampling methods, differences in study population, and poor reporting of the presence or absence of clinical lesions. Here we describe the most important characteristics of HPV-associated diseases in the anogenital and aerodigestive tracts.

Table 2 – Sites of HPV-associated cancers (Kreimer & Chaturvedi, 2011).

Cancer site	% attributable to HPV infection	HPV-induced premalignant lesion	Screening modality
Cervix	100	Cervical intraepithelial neoplasia (CIN)	Cytology, colposcopy, primary screening
Anus	90	Anal intraepithelial neoplasia (AIN)	Cytology, High resolution anoscopy
Penis	40	Penile intraepithelial neoplasia (PIN)	Cytology/Histology
Vagina	40	Vaginal intraepithelial neoplasia (VAIN)	Cytology/Histology
Vulva	40	Vulvar intraepithelial neoplasia (VIN)	Cytology/Histology
Oropharynx	12-72	?	?

1.2.1 Cervical cancer and other HPV-associated diseases in the anogenital region

CERVICAL CANCER: SQUAMOUS CELL CARCINOMA (SCC) AND CERVICAL ADENOCARCINOMA (AdCa)

The cervix of the uterus is the preferential site of sexual infection by mucosal HPVs and undergoes physiological changes according to the age of the woman (before puberty, puberty, following puberty, after menopause) due to different hormonal levels. The area of the cervix with premalignant potential is the transformation zone, which is formed after puberty and corresponds to the site of transition from the columnar glandular epithelium (endocervix) and the squamous epithelium (esocervix) (Fig. 6).

According to World Health Organization (WHO) 2010 statistics, cervical cancer is the 3rd most common cancer among women worldwide, with 529 409 newly diagnosed cases and 274 883 deaths every year. However, global incidence and mortality rates vary geographically with 452 902 cases (85.5%) of cervical cancers occurring in low-income countries. It is more common in metropolitan areas than in rural areas, and the incidence is higher in populations with lower socio-economic status and level of education. Central and South America, southern and eastern Africa and the Carraiben have the highest incidence of the disease.

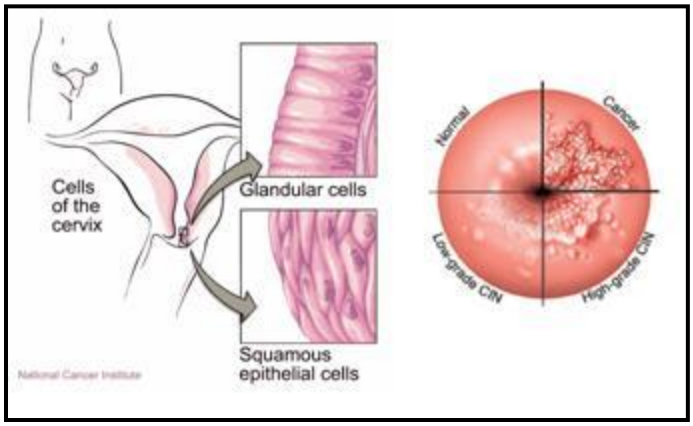

Figure 6 – Figures showing the location of the squamous epithelium in the exocervix or the glandular cells in the endocervix (left) and the spread of cervical cancer through the cervix (from normal cervix to cancer) which can be observed during a visual inspection (right).

Carvical cancer development is a long multistep process characterized by well-defined clinical stages and we can observe four main step: infection, persistence, progression, and invasion (Fig. 7). It is a rare complication of persistent infections with mucosal HPVs, which occur in 10% of the cases and are more likely to progress to premalignant lesions (CIN) in 5 years. Heterogeneity in biology (and definition) still exists in precancerous lesions: a) CIN 1 is a histopathological diagnosis of HPV infection, and should not be considered as a

precancerous lesion. Women with a persistent diagnosis of CIN 1 may progress to CIN 2/3 at a rate of 15% over 2 years, b) CIN2 is sometimes produced by non-carcinogenic HPV types, and has a sizable regression potential of 40% over an approximately 2-year period. Thus, CIN 2 represents an equivocal precancerous lesion, but it is treated in some regions to provide a safety margin against cervical cancer risk, c) CIN3 (*in situ* carcinoma, CIS) is the true precancerous lesion and progresses to cancer, if untreated, at a rate of around 30% over 20 years. When high-grade CIN (CIN 2 or worse) is diagnosed, treatment is mandatory. Overall treatments are more than 90% effective.

Virtually, all cervical cancer cases are linked to genital persistent infection with mucosal HPVs, which is the most common viral infection of the reproductive tract and its prevalence in the general population with normal cytology is 11.4% (14.3% in developing regions *vs* 10.3% in developed regions) (WHO HPV Summary Report Update 2010). In 1995, the IARC monograph working group concluded that there were sufficient evidences for the carcinogenicity of HPV 16 and 18 and limited evidences for the carcinogenicity of HPV 31 and 33. Actually, HR-HPV are HPV 16, 18, 31,33, 35, 39, 45, 51, 52, 56, 58, 59, 66 and 73, probably HR-HPV are HPV 26, 53, 68, 73 and 82, LR-HPV are HPV 6, 11, 13, 40, 42, 43, 44, 54, 61, 70, 72, 81 and 89 (Muñoz et al, 2006). HPV 16 and 18 are involved in 70.9% of all cervical cancers even if genotype-specific prevalence may vary geographically. Moreover, some recent studies have pointed out an important role of different HPV 16 variants, which sometimes have increased oncogenicity when compared to the main type (Quint et al, 2010; Sichero et al, 2012). The risk factors for acquisition of HPV infection have been historically linked to: a) early age at initiation of sexual activity, b) high number of new and recent sexual partners, c) high number of partners of the husband or male partner.

Although HPV is a necessary factor in cervical cancer development, there are also some cofactors playing a role in progression of HPV infection to cervical cancer. Cofactors influencing persistence and progression of HPV infection to advanced high-grade squamous intraepithelial lesions and cervical cancer include environmental cofactors, such as long-term use of hormonal contraceptives, tobacco smoking, co-infection with other sexually transmitted agents (i.e. HSV2 and *Chlamydia trachomatis*), high parity and diet, and host cofactors (i.e. HIV infection and immunosuppression) (Castellsagué et al, 2002; Veldhuijzen et al, 2010).

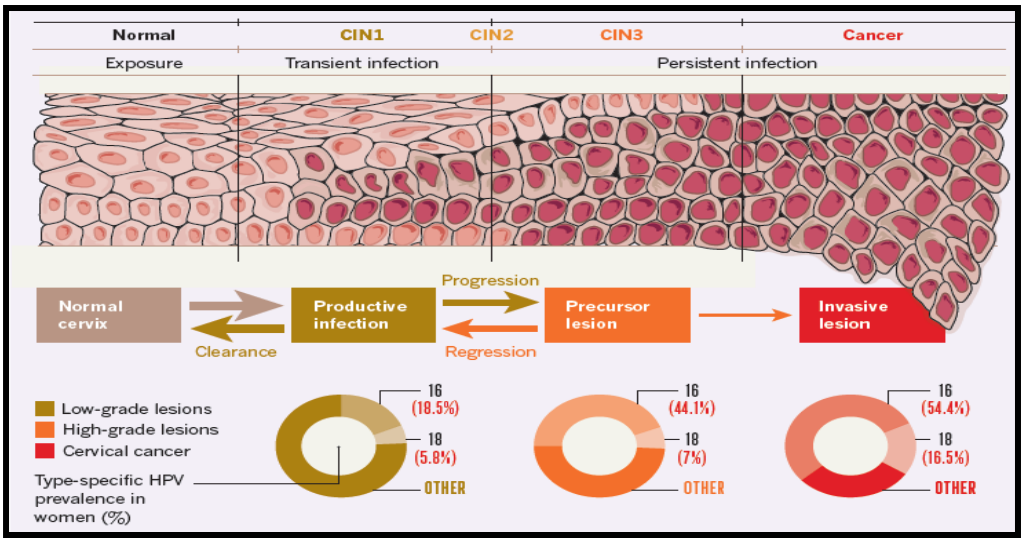

Fig. 7 – The phases of cervical cancer development, from normal epithelium to invasive cancer through precancerous lesions (CINs) . Infection with HPV 16 and 18 is more likely to lead to cancer than other genotypes.

From an histological point of view, cervical cancer can be divided in SCC (~80%) and AdCa (~20%). Carcinoma of the cervix has showed a marked decline in developed countries over the past 40 years, due to wider implementation of cytological screening and increased detection of premalignant disease. Although the decline is mainly attributable to a decrease in incidence of SCC, there has also been an increase in relative and absolute incidence of AdCa over the same period, especially among young women (age < 45 years). These two types of cervical cancers differ not only for epidemiology, but also for prognostic factors and survival (10–20% differences in 5-year overall survival rates, with AdCa being more aggressive), patterns of dissemination and recurrence, response to treatment and risk factors (AdCa more associated to obesity, nullipary and HPV 18) (Gien et al, 2010). Moreover, if for SCC and premalignant lesions of the esocervix a good classification and triage guidelines are available, it is not the same for AdCa and glandular lesions of the endocervix (Zaino, 2000). Glandular dysplasia (or atypical hyperplasia) has been proposed as a pathologic entity on the basis of the assumption that glandular lesions progress through a series of lesions of distinctive morphology as they acquire the genetic and phenotypic changes of carcinomas similar to squamous lesions of the cervix. *In situ* AdCa (AIS) has consistently been characterized by the following histological features: a) preservation of normal glandular architecture; b) involvement of part or all of the epithelium lining glands or forming the surface; c) nuclear enlargement, coarse chromatin, small single or multiple nucleoli; d) increased mitotic activity; and e) variable stratification of nuclei. There is no consensus regarding the criteria for the

diagnosis of microinvasive AdCa (MIA): authors generally have chosen a similar definition that restricts cases of MIA invasion to less than 5 mm from the basement membrane of the surface epithelium. To the situation, there is also a controversial classification for the histological types of invasive AdCa. Among mucinous AdCa, the most common is the endocervical type, followed by intestinal, signet ring, minimal deviation (MDA) and villoglandular type. Endometrioid AdCa may actually be more common than the endocervical type and histologically is indistinguishable from its counterpart in the uterine corpus. Other less common histotypes are clear cell, serous, mesonephric and adenosquamous AdCa.

VULVAR AND VAGINAL CANCER

Vulvar cancer accounts for 3-5% of all genital tract malignancies in women and is primarily a disease of the elderly (< 70 years). The aetiology is not well understood, but an association with HPV has been shown for multifocal warty or bowenoid lesions in younger populations (40%). Vulvar intraepithelial neoplasia (VIN) are the precursor lesions and the most important risk factors. On the other hand, SCC are the most common histotype (90%). A meta-analysis estimated a HPV prevalence of 76% for VIN and 36% for vulvar carcinomas. HPV 16 is the most common detected type (65-93% in VIN and 71% for vulvar cancer) followed by HPV 18 (WHO Summary Report Update 2010).

Primary cancer of the vagina constitutes 2% of all malignant neoplasm of the female genital tract, with the same risk factors for cervical neoplasia. Most vaginal carcinoma are secondary, arising from primary carcinoma of the cervix, endometrium or rectum and the association with HPV infection is around 40%. Vaginal intraepithelial neoplasia (VAIN) are the precursor lesions. HPV 16 is the most common type in at least 70% of HPV-positive carcinomas (WHO Summary Report Update 2010).

PENILE CANCER

Cancer of the penis represents less than 0.5% of cancers in men and the age at the diagnosis is > 60 years old. The aetiology seems to be multifactorial, but penile cancer with basaloid and warty features have shown the strongest association with HPV infection. Moreover, the geographical correlation between the incidence of penile and cervical cancers and the concordance of these two cancers among married couples suggested the common aetiology of HPV infection. Penile intraepithelial neoplasia (PIN) are the precursor lesions and HPV DNA is detectable in approximately 40% of all penile cancers. HPV DNA is detectable among PIN with the basoloid histological type, ranging from 75-80% of cases, and decreasing to 30-60% among invasive squamous cell carcinomas. HPV 16 is the most common genotype.

ANAL CANCER

Anal cancer is a rare malignancy arising in the anal canal, largely in the transitional zone separating the squamous epithelium of the canal and the mucosal epithelium of the rectum. The incidence is particularly high in men who have sex with men and among immunosuppressed men and women (HIV infected or transplant recipients). These cancers are predominantly squamous cell carcinoma, adenocarcinomas, or basaloid and cloacogenic carcinomas. Anal cancer is similar to cervical cancer with respect to overall HPV DNA positivity, with approximately 85% of cases associated with HPV infection worldwide. HPV 16 is the most common detected type, representing 87% of all HPV-positive tumours. HPV 18 is the second most common type detected and is found in approximately 9% of cases. HPV DNA is also detected in the majority of precancerous anal lesions (anal intraepithelial neoplasia, AIN) and the prevalence of HPV increases with the severity of the lesion.

NON-CANCEROUS DISEASE: GENITAL WARTS

Genital Warts (GWs) can involve the vulva, vagina, urethra, skin of anogenital tract, and penis. Having GWs is not associated with mortality and are related to both clinical symptoms (itching, burning, discharge, bleeding and pain) and psychosocial problems (embarrassment, anger, shame, anxiety and decreased self-esteem). Almost 100% of GWs are associated with either HPV 6 or 11. Although these HPV types give rise to benign changes, they can in rare cases be associated with malignant lesions such as the rare Buschke-Lowenstein tumours. HR-HPV types can be identified in up to 50% of cases, however, HPV 6 and 11 are considered the causative agents.

GWs represent not only a problem for the individual, but also imply significant healthcare costs for society. About 1% of the sexually active population harbours GWs at any given point in time and up to 17% of women aged 20-29 years have had at least one episode of GWs in the past (based on surveys in the Nordic countries of Europe).

1.2.2 Non-anogenital cancers: HPV-associated head and neck squamous cell carcinoma

The term “head and neck cancer” (HN) includes lesions at several anatomic sites, such as the lip, oral cavity, nose and paranasal sinuses, nasopharynx, oropharynx, hypopharynx, larynx, oesophagus, salivary glands, as well the soft tissues of the neck and ear and more than 95% of them are SCC (HNSCC) (Fig. 7). It is the sixth leading cancer by incidence worldwide. It is likely that approximately 600 000 cases will arise this year worldwide, and that only 40–50% of patients with HNSCC will survive for 5 years (Peter KC Goon, 2012). On clinical

examination, oral SCC lesions may be preceded by mucosal alterations with histologically detectable dysplastic changes. However, a malignancy involving a complex genetic process may also occur directly "*de novo*" without any pre-existing clinically detectable mucosal changes. All HNSCCs tend to be diagnosed late because there is no pain until the late stages. The most important risk factor of head and neck cancer worldwide is smoking, with alcohol coming second.

In 1983, Syrjanen and colleagues provided the first evidence on the presence of HPV infection in HNSCC, by analyzing the presence of HPV antigens in 40 oral carcinomas using immunohistochemistry, but, up to date, scientists have been able to support only an association, not an aetiological role (Syrjänen et al, 1983). Although, at present, HPV infection has been established in 20-25% of all HNSCC, the role of HPV in the pathogenesis of HNSCC has been controversial mainly because the detection rates of HPV DNA have been highly variable among the studies, ranging from 0% to 100% and HPV 16 has been identified in 20–90% of the oropharyngeal carcinomas (OPSCCs). These highly variable detection rates can be partly explained by variations in the sampling techniques and different HPV detection methods.

Several studies indicate that oral HPV infection is likely to be sexually acquired and it seems that HPV-positive tumours form a distinct group within HNSCCs. The aetiological factors differ, the tumours are different at the molecular level and the clinical outcome is different, in general HPV infected HNSCCs have a more favourable prognosis and response to chemo/radiotherapy (Tab. 3) (Leemans et al, 2011; Syrjanen, 2010; Worden et al, 2008). Oropharyngeal carcinomas, tonsillar cancers in particular, showed the strongest association with HPV, with some 60% being ascribed to HPV (Syrjanen, 2010).

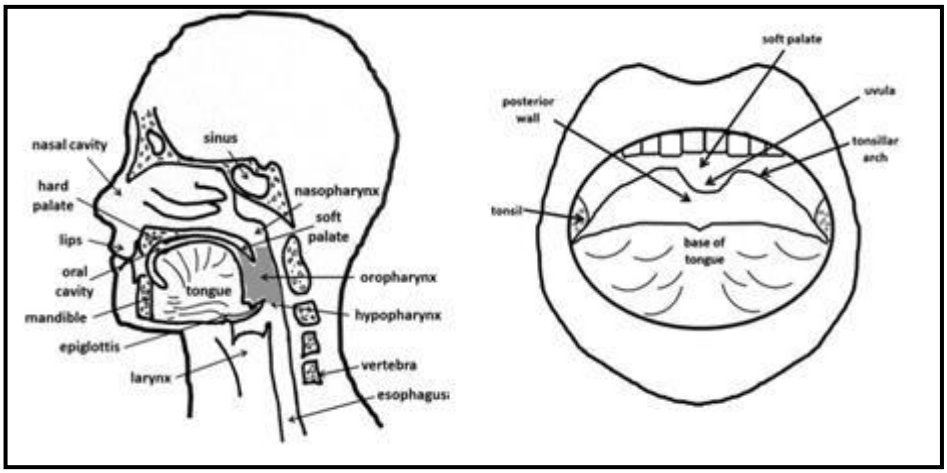

Figure 8 – Possible sites of incidence of HNSCCs (Miller et al, 2012).

HPV involvement in HNSCCs is supported by a series of observations. First, HPV is a virus with broad and essential tropism for epithelial tissues. *In vitro* studies clearly proved that viral oncoproteins belonging to HR-HPVs immortalize human keratinocytes, including oral keratinocytes. The HR-HPV genotypes can be detected in HNSCC with PCR techniques and fluorescence *in situ* hybridization. In addition, genotype-concordant viral DNA can be found in the lymph nodes of patients with metastatic oropharyngeal SCC (OPSCC) (Miller et al, 2012).

An interesting study compared gene expression profiles of HPV+ and HPV− oropharyngeal cancer and oral cavity cancer (Lohavanichbutr et al, 2009). In oral cavity tumours, no significant difference in gene expression was noted when comparing HPV+ and HPV− specimens. However, analysis of oropharyngeal tumours shows significant differences (347 differentially expressed genes) in HPV+ compared with HPV− lesions. Differences were particularly common among genes involved in DNA regulation and repair, cell cycle, and chemotherapy/radiotherapy sensitivity. These results underscore the observation that HPV+ oropharyngeal disease represents a divergent biological entity from HPV− disease.

Table 3 – Different clinical and biological characteristics of HPV-positive and HPV-negative HNSCCs (Kostareli et al, 2012; Leemans et al, 2011; Syrjanen, 2010).

Feature	HPV-related HNSCC	HPV negative HNSCC
Incidence	Increasing	Decreasing
Age	Young Adults	Adults
Aetiology	Sexual Behaviour (Sexual partners, Oral sex, age first intercourse)	Tobacco and/or Alcohol consumption
TP53	Wild type	Frequent mutations
p16	Overexpressed	Not expressed
Genomic aberrations	Few and some connected with improved survival	Many and widespread
Predilection site	Oropharynx	None
Immunosuppression	Related	Not related
5-years Overall Survival	~82%	~35%

However, according to data from different studies recently reviewed by Kostareli (Kostareli et al, 2012), also HPV-positive OPSCC are heterogeneous in both biological and clinical behaviour, possibly due to differences in viral load and/or viral oncoproteins expression. In fact, it has been recently shown that HPV DNA+/RNA- tumours have a worst prognosis compared to those HPV DNA+/RNA+ ones (Holzinger et al, 2012). These HPV-related

tumours have better survival maybe for the combined effect of phenomena occurring in epigenome, genome and expression pattern, which drive alterations in the intracellular signalling networks, and the components of tumour microenvironment (angiogenesis, immune system, inflammation, etc.) (Fig. 8). For example, wild type p53 enables HPV-related OPSCC to respond to DNA damage *via* apoptosis, making these tumours more sensitive to ionizing radiations therapy. On the other hand, infection by HPV may also render these cells more visible to the innate immune system leading to a synergistic effect with radiotherapy. But further studies are needed to confirm these hypothesis.

1.3 Control and prevention of cervical cancers: diagnosis, screening and vaccination

Cervical cancer is easily manageable through early diagnosis and treatment, which can drastically reduce incidence and mortality. More importantly, cervical cancer can be avoided to a large extent by action of both primary and secondary prevention.

1.3.1 Cervical cancer screening

Cancer screening is a public health intervention undertaken in an asymptomatic population to prevent invasive disease and resulting mortality through the early detection of precancerous lesions. It is generally accepted that organized screening is more effective and cost-effective than opportunistic screening and cervical cancer is the only gynaecologic malignancy that currently meets the criteria for screening: a) the time between the appearance of precancerous lesions and the occurrence of invasive cervical cancer is long (10-30 years), leaving time for detection and treatment, b) treatment of precancerous lesions is less expensive and more successful in avoiding death, as compared to the management of invasive cervical cancer.

A good screening test should be accurate, reproducible, inexpensive, easy to perform and follow-up, acceptable and safe and several tests are available for cervical cancer screening: cytology (conventional or liquid-based), visual inspection (with acetic acid or Lugol's iodine) and HPV testing (Cuzick et al, 2012). In 1952, Georgios Papanicolau described a cervical smear technique capable of detecting abnormal cervical cytology suggestive of cervical neoplasia, the Pap test (conventional cytology) (Fig. 9).

Guidelines for cervical cancer screening program are formulated depending on whether or not there is a program already in place, and if so, whether or not this program is successful. The most appropriate target age group for a screening program is 25-30-years, because younger women may have abnormalities, but they are likely to resolve spontaneously. An interval of 3

to 5 years between screening visits is considered appropriate in women with previous negative screening results. Women whose previous Pap smear was abnormal should follow the cervical diagnostic algorithm established locally.

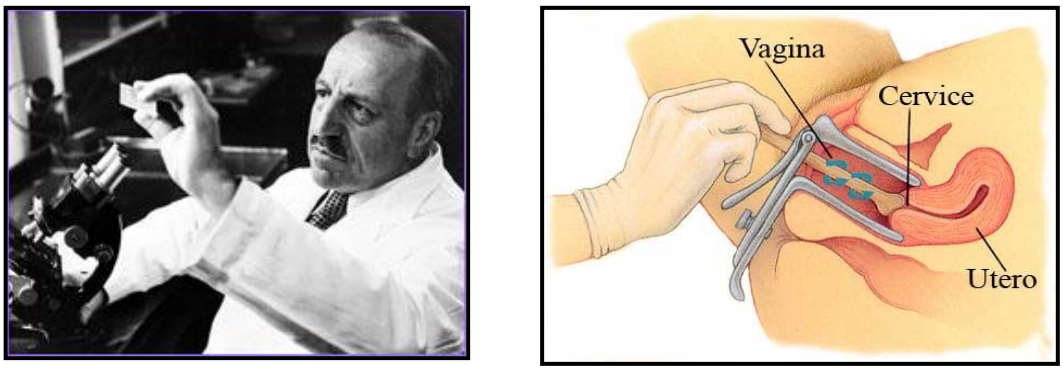

Figure 9 - Georgios Papanicolau (left) and a scheme showing how to collect cervical specimen for the Pap test (right).

1.3.2 Techniques for HPV detection in clinical samples: HPV-DNA test

Recently established guidelines recommend HR-HPV DNA testing in order to improve the efficacy of primary cytological screening programs or as triage tests. At present the Hybrid Capture 2 (HC2) assay (QIAGEN GmbH, Hilden, Germany), the Cervista test (Hologic, Madison, WI, USA), and the Roche Cobas 4800 HPV Test (Roche Inc., Branchburg, NJ, USA) are the only tests for the detection of HR-HPV DNA approved by U.S. Food and Drug Administration for cervical cancer screening (Tab. 4) (Poljak & Kocjan, 2010).

Furthermore, specific HPV typing is important for epidemiological studies, assessment of the clinical behaviour of particular genotypes, clinical management of women, clinical follow-up studies, evaluating prevention strategies, development of new therapies and prophylactic/therapeutic vaccines.

Difference in the carcinogenic potential between the different HR-HPV types and indicate the potential value of genotyping in cervical cancer screening. HPV 16, 18, 31 and 33 infection and especially HPV 16 persistence were associated with high absolute risks for progression to high-grade cervical lesions (Kjær et al, 2010). Moreover, clinical trials conducted to test the efficacy of prophylactic vaccines that target two HR-HPV types, HPV 16 and HPV 18, as well as the low-risk (LR) HPV 6 and 11 (see next paragraph), require accurate detection of genotype-specific HPV infections associated with cancer and precancerous lesions.

Sequencing of DNA is the gold standard method for accurate viral typing. However, DNA sequencing techniques have been facing limitations in typing HPV when the specimen

harbours multiple genotypes resulting in non-interpretable sequence data. (Gharizadeh et al, 2005).

The most widely used PCR-based methods employ consensus primers that amplify highly conserved regions of the L1 or E1 gene or E6 gene, followed to genotype specific hybridization by reverse line blot hybridization or microchip format. All hybridization-based methods can discriminate HPV types in multiple infections, but can identify only HPV types represented by probes.

Actually, many commercially available CE-marked genotyping HPV DNA tests exist. HPV-typing assays, such as INNO-LiPA HPV (Innogenetics), Linear Array (Roche) and PapilloCheck (Greiner Bio-One GmbH), are commonly used in the follow-up of persistent infections to monitor the presence of specific HPV genotypes. Many studies comparing different methods for HPV typing noted considerable differences in the type specific sensitivities as well as the ability to detect multiple infections between the individual test systems (Qu et al, 1997; van Doorn et al, 2002). Moreover, although more sensitive than cytology, HPV testing has modest specificity and positive predictive value (PPV) for detection of pre-cancerous lesions, and cannot distinguish infections that will resolve from those that will progress. Thus, an important question is how to triage HPV-positive women and further specific and sensitive biomarkers are necessary to answer.

Table 4- Most important currently available commercial assays for the multiple detection of α-HPV (Poljak & Kocjan, 2010).

HR-HPV DNA-based screening tests	**HPV DNA-based genotyping assays**
Hybrid Capture 2 HPV DNA (HC2) test (Qiagen)	INNO-LiPA HPV Genotyping (Innogenetics)
Cervista HPV HR test (Hologic)	Linear Array HPV Genotyping Test (Roche)
Amplicor HPV test (Roche)	EasyChip HPV Blot Kit
Care HPV test (Qiagen)	REBA-HPV-ID
HR-HPV-DNA-based screening assays with concurrent or reflex HPV 16 and HPV 18 genotyping	PapilloCheck HPV-Screening Test (GreinerBio)
	Clart HPV 2 – papillomavirus clinical arrays
	HPV GenoArray Test Kit
RealTi*me* High Risk HPV test (Abbott)	GeneTrack HPV DNA Chip
Cobas 4800 HPV Test (Roche)	GeneSQUARE HPV Microarray
Cervista HPV 16/18 Test (Hologic)	Infiniti HPV Assays
HR-HPV 16/18/45 Probe Set Test	PANArray HPV Genotyping Chip
***In situ* hybridization**	HPV DNAChip
INFORM HPV (Ventana Medical)	GG HPVCHIP
GenPoint HPV Biotinylated DNA Probe (Dako)	Multiplex HPV Genotyping Kit (xMAP, Luminex)
Zyto*Fast* HPV Probes (ZytoVision)	**HR-HPV E6/E7 mRNA-based screening assays**
HPV OncoTect Test Kit (InCellDx)	PreTect HPV-Proofer
	NucliSENS EasyQ HPV (bioMérieux)
	APTIMA HPV Assay (Roche)

1.3.3 The prophylactic vaccine

Antibody generally binds to conformational determinants on structural components of a microorganism, and assists with pathogen clearance or protects against reinfection by promoting phagocytosis and by neutralizing infectivity. Demonstration that the L1 protein of HPV was the most immunogenic viral protein and could self assemble into virus-like particles (VLPs) eliciting host protective neutralizing antibody, enabled development of prophylactic vaccines designed to prevent HPV associated disease. The commercially available vaccines are Gardasil® (Merck & Co.) and Cervarix® (GlaxoSmithKline, GSK). These vaccines are produced in yeast or insect cells and induce a polyspecific antibody response which recognizes a range of conformational determinants on the viral capsid that are generally genotype-specific. In fact, Gardasil® has been developed to protect against HPV 16, 18, 6 and 11 and Cervarix® against HPV 16 and 18. In several phase III clinical trials, vaccines have been shown effective at preventing infection with the HPV types in the vaccine and associated premalignant disease of the genital tract for periods of up to five years in previously uninfected women. Data on longer term protection, and on protection in men, are awaited from ongoing clinical trials (Frazer, 2009).

Although HPV vaccination provides an opportunity to diminish the global cervical cancer incidence and successful vaccination programs are expected to substantially reduce HPV-related diseases burden, screening programs based on cytology or HPV testing will continue as a secondary preventative measure.

1.4 HPV AND IMMUNE RESPONSE: ANTIGENS PRESENTATION, IMMUNOPROTEASOME AND THE ROLE OF INTERFERONS (IFNs)

Both cellular and humoral immune response are essential for the clearance of HPV in the infected epithelium. The adaptive immune response to HPV appears slower compared with other pathogenic virus infections and recognizes predominantly conformational determinants displayed only when the capsidic protein L1 is correctly configured into pentamers as in the native virus. Antibodies titres against L1 following natural infection are low, and although mucosal antibodies (secretory IgA and IgG) are detected in the previous 12 months of HPV detection and may protect against HPV infection, assays are difficult to standardize, limiting the utility of serology in HPV diagnosis (Sheu et al, 2007). Moreover, for most of the duration of the HPV infectious cycle, there is little or no release into the local milieu of pro-inflammatory cytokines that are important for dendritic cells (DC) activation and migration,

and the essential signals to kick start the immune response in squamous epithelia are absent. Together, these facts suggest that HPV may have developed strategies to evade host immune mechanisms and there are different possibilities.

The primary mechanism of viral immune evasion for HPV infection is avoidance of antigen presentation, which takes place via the MHC Class I pathway (Fig. 10A). Briefly, the endogenous antigentic peptides (8-11 amino acid products) generated by the intracellular proteolysis machinery (i.e. proteasome) are translocated by the transporter associated with antigen processing (TAP1/2 heterodimer) into the endoplasmatic reticulum (ER), where the chaperons-dependent assembly of MHC class I molecules occurs. Functional molecules are composed by a heavy chain (H), a light chain (β_2-microglobulin, β_2m) and the antigenic peptide. The chaperon protein involved in this step is Tapasin. Once the trimolecular complex is formed, it is delivered to the cell surface via an exocytic pathway, where cytotoxic T cells ($CD8^+$ CTLs) are responsible of the sensing of these presented antigens (Hwang et al, 2001). The proteasome is a cylindric-shaped protease complex arranged as four axially stacked heptameric rings. The subunits of the catalytic core are represented by two homologous gene products, α (two outer rings, highly conserved) and β (inner rings, divergent, with enzymatic activity). Protein degradation may be performed in ubiquitin- or ATP-dependent as well as -independent manner. Upon IFNs induction (especially IFN-γ), the β subunits LMP7, LMP2 and MECL-1 displace its homologues in the "constitutive" proteasome and assemble in the so-called "immunoproteasome" (Fig. 10B). This altered catalytic specificity of the proteasome is important for generating peptides that are optimal for binding to MHC class I molecules.

IFNs-induced MHC class I pathway activation can be mediated also by proteins belonging to the NLR family (nucleotide-binding domain, leucine-rich repeat) such as the recently characterized NLRC-5, which acts as nuclear transcriptional transactivator (CITA) (Meissner et al, 2012).

Absence of cell lysis and systemic viremia during HPV infection and production of immunogenic proteins in terminally differentiated layers of the epidermis minimize antigen availability for presentation, and also ensure that few pro-inflammatory signals are given to generate adaptive immune responses. Moreover, the genomic instability which characterizes HPV persistent-infected cells and cervical cancer may alter also the complex genomic HLA region affecting genes encoding HLA class I-II molecules (Sheu et al, 2007).

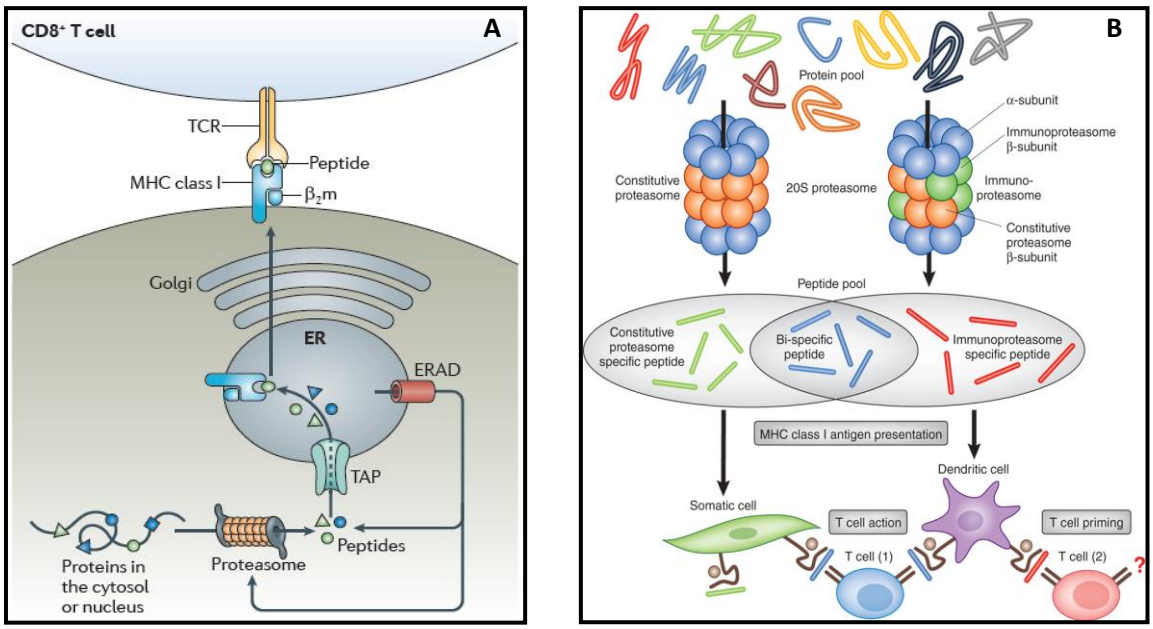

Figure 10 – MHC Class I antigen presentation pathway (A) and presenting immunoproteasome-derived peptides (B) (Neefjes et al, 2011; Spaapen & Neefjes, 2012).

HPV evolved anti-inflammatory and immune inhibitory mechanisms to suppress key steps of the type I IFNs pathway, impairing the antigen presentation and T-cells activation (Frazer, 2009).

Human type I IFNs (i.e. IFN-α, -β, -ω, and -κ) have antiviral, antiproliferative, antiangiogenic and immunostimulatory properties. Viral functional oncoproteins E6 and E7 interact directly with molecules involved in IFNs signalling (Tab. 5 and Fig. 11). For example, E7 inhibits IFN-*α*-mediated signal transduction by binding to IRF-9 (IFN regulatory factor-9), preventing its translocation to the nucleus, thereby inhibiting the formation of the ISGF-3 (IFN-stimulated gene factor 3) transcription complex that usually binds ISRE (IFN-specific response element) in the nucleus. Moreover, E7 physically interacts with IRF-1, inhibiting IFN-β promoter (Koromilas et al, 2001). On the other hand, E6 binds to IRF-3 homodimer and inhibits its transcript activation function, preventing transcription of IFN-β; binding to Tyk2, prevents binding to the cytoplasmic portion of the IFN receptor inhibiting phosphorylation of Tyk2, STAT (signal transducer and activator of transcription) 1 and STAT2, impairing JAK (*Janus* kinase)/STAT activation and therefore inhibiting specific IFN*α*-mediated signaling (Stanley et al, 2007).

Table 5- List of the proteins involved in MHC class I antigen presentation pathway and IFNs-mediated antiviral response which are considered in this study and relative functions (Génin et al, 2009; Hwang et al, 2001; Meissner et al, 2012).

Pathway	Protein	Functions and Interactions
MHC Class I Antigen presentation	HLA	Heavy chain family including HLA-A, -B and –C Highly polymorphic (250 alleles) The extracellular domain form a shape-specific peptide-binding pocket
	TAP	ATP binding cassette transporter Asymmetric transmembrane heterodimer TAP1/TAP2 in ER ATP-dependent transport of peptides in unidirectional manner across membranes Reversibly regulated via phosphorylation at several conserved residues in its cytoplasmatic domain Functional polymorphisms to change the peptide pool available for binding MHC class I alleles
	Tapasin	Chaperone protein Mediates antigen presentation by interacting with MHC class I complex and TAP complex Enhances peptide translocation activity of TAP altering the competitive advantage of certain antigenic petides
Interferon Responsive Factors (IRFs)	IRF-3	Constitutively expressed in all cell types Harbours DNA binding domain (specific ISREs recognition) Active in the phosphorylated homodimeric form and interacts with CBP/p300 in the nucleus (transcriptional regulation of Tipe I IFNs genes)
	IRF-7	Constitutive expressed in lymphoid cells and IFN-induced during viral infection; most cells express it at very low amount Harbours DNA binding domain (specific ISREs recognition) Active in the phosphorylated form Interacts with CBP/p300 in the nucleus (transcriptional regulation of Type I IFNs genes)
	IRF-9 (p48)	Interacts with STAT proteins forming a complex (ISGF-3) which translocates into the nucleus and stimulate transcription of ISG Harbours DNA binding domain (specific ISREs recognition)
Interferon Stimulated Genes (ISGs)	Mx1	IFN-induced GTPase with antiviral activity Accumulates in the cytoplasm of IFN-stimulated cells blocking viral replication soon after virus entry Targets viral capsid recognizing major capsidic protein
	PKR	IFN-induced protein kinase with antiviral and antiproliferative activity
	OAS1	IFN-induced 2'-5'-oligoadenylate synthetase 1 Inhibition of viral replication by recruiting RNASEL Different isoforms exist
Immunoproteasome	LMP7 LMP2	IFN-induced large multifunctional protease 7 and 2 (beta type) Related to antigen processing by MHC class I pathway
	MECL-1	IFN-induced proteasome subunit beta-10 Related to antigen processing by MHC class I pathway
CITA	NLRC5	NLR family, containing a N-term CARD domain and C-term leucine rich repeats (LRRs). No DNA-binding domain. Highly inducible by IFN-γ. Both cytoplasmatic and nuclear. Transcriptional activator of MHC class I genes.

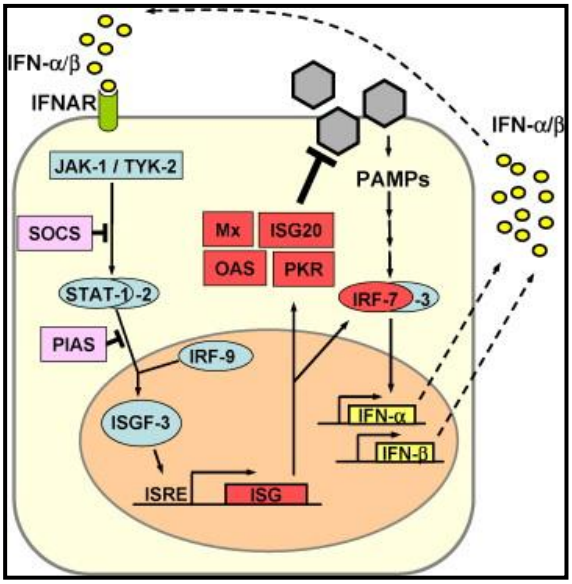

Figure 11 – Intracellular type I IFNs signalling (Haller et al, 2007). Briefly, type I IFN binds to the receptor (IFNR1 and 2) and transducers signals through the sequential activation of receptor-associated kinases Jak and Tyk-2 leading to tyrosine phosphorylation and activation of STAT proteins. They associate to IRF-9 in the nucleus, forming the ISGF-3 complex and activating IFN-stimulated genes (ISGs) transcription.

1.4.1 IFN-κ

IFN-κ is the last discovered type I IFN which showed constitutively expression in keratinocytes and inducible in monocytes and DCs (LaFleur et al, 2001). The gene encoding the protein is located in the chromosome 9, adjacent to the type I IFNs cluster and analysis of cDNA and genomic sequences from other species failed to identify an orthologous, suggesting it may evolved later to play a specific role in humans. Most type I IFNs are expressed only upon viral infection and the constitutive expression of IFN-κ in resting keratinocytes is an important different characteristic which may provide a new mechanism of host defence. During viral infection, IFN-κ is up-regulated in keratinocytes. Another distinct feature compared to other type I IFNs is that IFN-κ seems to have a cell surface expression, carrying out its signalling and functions in a cell-associated manner, rather than being completely secreted (autocrine and juxtacrine, not paracrine effect) (Buontempo et al, 2006).
Concerning HPV infected cells, it has been recently shown that IFN-κ expression is inhibited in HPV 16 or 18-positive cervical cancer cells by *de novo* promoter methylation and the viral oncoprotein E6, not E7, seems to be involved (Rincon-Orozco et al, 2009). Moreover, since its expression is decreased in precursor lesions and abolished in cancers, it has been concluded that IFN-κ repression may be an event occurring early in cervical carcinogenesis.

1.4.2 Type I IFNs in cervical cancer therapy

IFNs are used to treat a broad spectrum of diseases including multiple sclerosis, melanoma, some solid tumours, leukaemia and hepatitis. Unfortunately, for cervical cancer and pre-cancerous lesion treatment, controversial results have been observed in clinical trials (Beglin et al, 2009; Koromilas et al, 2001). Theoretically, IFN treatment should result in the clearance of HPV lesions and elimination of the virus, even in cases of latent infection. However, it is still far from widespread therapy. IFNs have been used successfully in treating patients with GW induced by LR-HPV types, but showed mixed results in treating low-grade lesions and cancers induced by HR-HPVs. A compilation of studies *in vivo* indicates that IFN-β is more effective than IFN-α and generally type II IFNs (i.e. IFN-γ) are more effective than type I. From later experiments it has been shown that treatment with IFNs can result in selecting cells with integrated copies of HPV DNA making it an ineffective methodology unless it can be combined with other therapeutic agents. Since it has been reported that the expression of viral oncoproteins, particularly E7, is significantly higher in non responsive patients, it is clear that the efficacy of IFNs is strictly dependent upon the level of viral oncogenes and the complex interactions between E6/E7 and cellular factors that affect both viral and host gene expression.

The discovering of the new IFN-κ with similarities, but also differences compared to other well known type I IFNs needs further investigation to better define its role in HPV infection and carcinogenesis and to assess its potential role as new treatment.

2. Aims of the thesis

The work presented in this thesis spaces between applied diagnostic and basic research on clinical samples and cell lines of cervical cancer and HPV-associated HNSCCs. The main aims are the following:

1) evaluate and improve diagnostic procedures for HPV-associated diseases by both assessing the performance of a new commercially available type-specific multiple-primer DNA sequencing method for HPV DNA genotyping on clinical samples from cervical lesions/cancers compared to a well known and diffuse reverse hybridization-based assay, in order to evaluate advantages and disadvantages in the clinical diagnostic practice, and determining the potential diagnostic value of virological markers, such as viral oncoprotein expression, viral load, physical state and DNA methylation, in HPV 16-positive cervical adenocarcinoma and HNSCCs in function of the available clinical and epidemiological data;

2) deep the role of HPV 16 in carcinogenesis by using data obtained from the analysis of virological markers (in particular viral DNA methylation) in clinical samples and analyzing the response to ectopic expression of IFN-κ in both cervical cancer and HPV-positive HNSCCs cell lines.

3. Materials and Methods

PART 1: COMPARISON OF HPV SIGN GENOTYPING TEST WITH INNO-LIPA HPV GENOTYPING EXTRA ASSAY ON HISTOLOGIC AND CYTOLOGIC CERVICAL SPECIMENS (Barbieri et al, 2012)

3.1 Clinical specimens

Eighty-seven human cervical samples, previously tested by the INNO-LiPA assay, were analyzed by the new HPV sign Genotyping Test. Among these, 34 were 10 μm thick paraffin-embedded biopsies belonging to patients with a histological diagnosis of cervical adenocarcinoma *in situ* (AIS) or invasive adenocarcinoma (invasive AdCa) and 53 cervical swabs, belonging to patients with a histological diagnosis of squamous cervical intraepithelial neoplasia of low (CIN1) or high grade (CIN2+), collected in PreservCyt® medium (Hologic, Marlborough, MA, USA). Histological diagnosis was confirmed based on pathology consensus review of tissue samples.

Clinical samples and data used in this study were obtained in the course of institutional diagnostic service, investigation described in this study could be carried out on residual specimens following diagnostic analysis, provided that all data would be kept anonymous.

3.2 DNA isolation

Total nucleic acids were extracted following different protocols. For biopsies, after heat deparaffinization at 95°C for 10 min and centrifugation at 12000 rpm for 10 min, tissue samples were digested with 20 μl of proteinase K in 200 μl of lyses solution at 56°C for 3 hours. DNA was extracted with QIAmp DNA Mini Kit (Qiagen, Hilden, Germany) following manufacturer's instructions and eluted in 100 μl. For cytological samples, 200 μl of each specimens was processed with NucliSENSE EasyMag system (bioMérieux, Marcy l'Etoile, France), following manufacturer's instructions, and eluted in 100 μl of Elution Buffer. Extracted DNA was stored at -80°C.

3.3 INNO-LiPA HPV Genotyping Extra assay (Innogenetics, Ghent, Belgium)

This assay detects 28 different HPV genotypes, including 18 high-risk HPV (16, 18, 26, 31, 33, 35, 39, 45, 51, 52, 53, 56, 58, 59, 66, 68, 73, 82), 6 low-risk HPV (6, 11, 40, 43, 44, 54,

70) and 3 other HPV (69, 71, 74), as well as the HLA-DPB1 gene as internal control for DNA quality, simultaneously in a single reaction. The addition of UNG to the amplification mixture is a contamination prevention measure. Briefly, 10 µl of the extracted DNA were used to carry out the PCR with biotinilated SPF10 primers (patent protected), targeting a 65 bp-fragment of the L1 ORF, in a final volume of 50 µl following manufacturer's instructions. Then, 10 µl of amplification product are denaturated and hybridized to a nitrocellulose strip, with different probes on its surface, specific for one of the possible amplicons using the automatic procedure in the *Auto-LiPA* machine. The hybrid is revealed with a colorimetric reaction involving a streptavidin-conjugated alkaline phosphatase and its substrate NBT/BCIP (Fig. 12). The obtained pattern of bands is analyzed with the LIRAS® software. Only samples positive for any HPV and/or for the internal control were included in the analysis. In case of multiple HPV infection and if at least one HR genotype was present, the sample was considered as HR. If only LR genotypes were present, the sample was considered as LR.

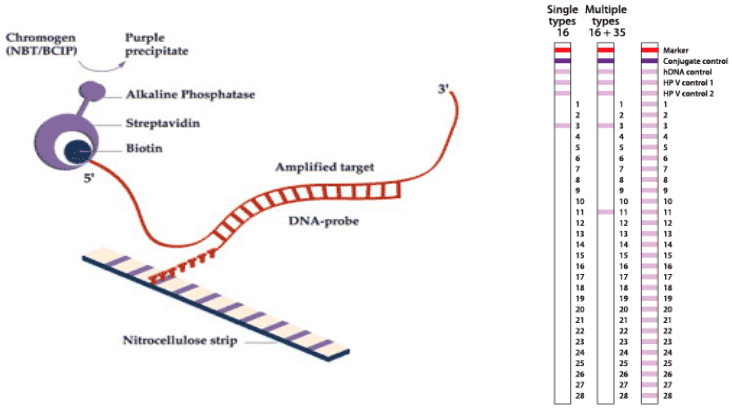

Figure 12 – Scheme of the hybridization step of the INNO-LiPA Genotyping extra assay (left) and examples of pattern of bands on the nitrocellulose strips (right).

3.4 HPV sign® Genotyping Test (Qiagen, Hilden, Germany)

This assay is based on a broad-spectrum HPV DNA amplification, using 10 µl of sample, in real time-PCR (EVA Green™ chemistry) on Rotor-Gene Q (Qiagen, Hilden, Germany). Mixed primers targeting an hypervariable region of the HPV L1 ORF and the betaglobin gene are used, followed by pyrosequencing with multiple sequencing primers (Fig.13). The melting curve analysis allows the semiquantitative determination for the presence/absence of HPV DNA. Only HPV positive samples are further analysed by pyrosequencing on the Pyromark Q24 system (Qiagen, Hilden, Germany), following manufacturer's instructions, using 4

specific sequencing primers to identify the viral genotypes, with the shortest possible sequence-read. The obtained programs are analyzed by the PyroMark Q24 software (SQA mode) and the specific pattern recognition software IdentiFire 1.0.5 (Biotage, Uppsala, Sweden) is used for library alignment and correct interpretation of the sequencing results as manufacturer recommends. For further information about the pyrosequencing principle see §3.11.3.

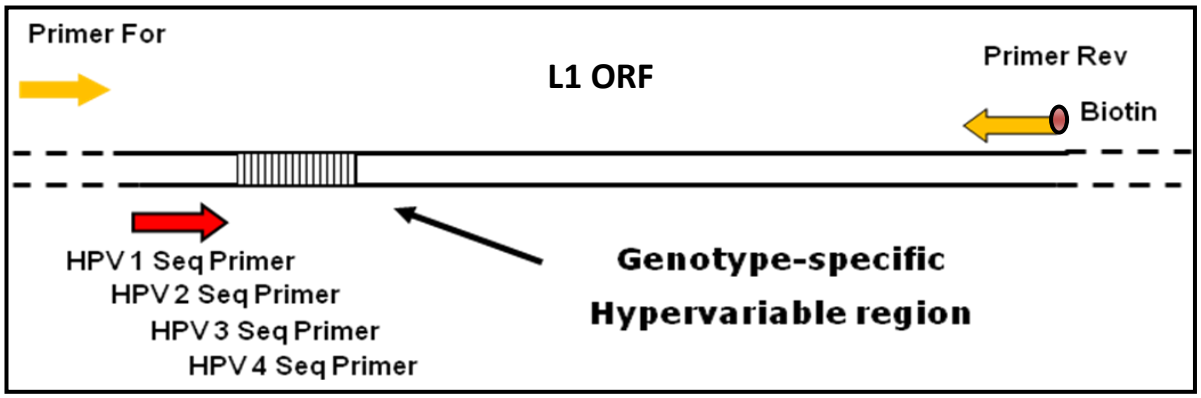

Figure 13 – Scheme representing how the HPV sign test works. Yellow arrows indicate primers used for the amplification step and the red arrow the position of the four primers used for the sequencing step.

3.5 Genotype specific quantitative real time-PCRs

Discordant samples for at least one genotype between the two assays were further analyzed by home-made genotype-specific quantitative real time-PCRs (Cricca et al, 2007) with Quantitect™ SYBR® Green (Qiagen, Hilden, Germany) to obtain a consensus result (2 out of 3 genotype-concordant results) and to detect the viral load (viral genome copies/reaction). We used 9 primer sets separately, designed using Clone Manager Professional Suite software 8.0, which amplify a fragment of the E6 ORF of HPV 16, 18, 31, 35, 45, 51, 52, 53 and 66 (Tab. 6). The choice to amplify these genotypes depended on their epidemiologic and clinical importance in our geographic region. Each reaction was carried out in a final volume of 20 µl with 1X SYBR® Green PCR Master Mix, 0.4 µM each primer and 5 µl of sample. The amplification program included an initial denaturation step at 95°C for 15 min, followed by 40 cycles of 15 s at 94°C, 20 s at 50°C and 20 s at 72°C. Data acquisition was performed at 72°C. Standard curves for E6 were obtained by amplification of 10-fold dilution series of 10^7 to 10^1 copies of plasmids containing the E6 ORF of each HPV genotype in a fixed amount of 300 ng of human fibroblast DNA. The standard curve for GAPDH was obtained by

amplification of 10-fold dilution series of 300 ng to 0.3 ng of human fibroblast DNA. The dilutions were tested in triplicate and in three different runs. GAPDH gene amplification was used to normalise viral load.

3.6 Statistical analysis

All the samples were merged and analyzed by 2-by-2 tables, dividing them in two different categories: biopsies and cervical swabs. Proportions were presented with 95% confidence intervals (95% CIs), estimated by standard methods. Agreement between two methods was measured by absolute agreement and Cohen's kappa statistics (*k*). For the analysis of each HPV genotype, proportion of positive agreement (*Ppos*), which was calculated as (twice the number of agreed positives)/(total number of specimens + number of agreed positive – number of agreed negatives), proportion of negative agreement (*Pneg*), which was calculated as (twice the number of agreed negatives)/(total number of specimens + number of agreed negatives – number of agreed positives) and *P* values by McNemar's test were calculated.

Table 6 - Primer sets used for discordant analysis by quantitative real time-PCRs targeting E6 ORFs of HPV 16, 18, 31, 35, 45, 51, 52, 53 and 66.

HPV genotype		Primers (5'-3')	Position
HPV 16	Forward	AAAGCCACTGTGTCCTGAAGA	424 bp
	Reverse	CTGGGTTTCTCTACGTGTTCT	553 bp
HPV 18	Forward	GCGGTGCCAGAAACCGTTGAA	422 bp
	Reverse	TGCTCGGTTGCAGCACGAATG	539 bp
HPV 31	Forward	ACGTGTCAAAGACCGTTGTG	420 bp
	Reverse	TGGGTTTCAGTACGAGGTCTTC	550 bp
HPV 35	Forward	AAACCGCTGTGTCCAGTTG	431 bp
	Reverse	CCTCGGTTTCTCTACGTGTTG	554 bp
HPV 45	Forward	CGGTGCCAGAAACCATTGAAC	420 bp
	Reverse	TTTCCCTACGTCTGCGAAGTC	567 bp
HPV 51	Forward	TAGCAGGTCTGTGTATGG	333 bp
	Reverse	AACGTCCCGCTATTTCATGG	490 bp
HPV 52	Forward	GTTTGAGGATCCAGCAACAC	104 bp
	Reverse	TTCTTCCAGCACCTCACAC	164 bp
HPV 53	Forward	GCACCAGCTATGTGAAGTTG	149 bp
	Reverse	TGCACACTCCATACGGATAC	303 bp
HPV 66	Forward	TGGCCATATGCAGTATGTAGGG	282 bp
	Reverse	ACGGACATTGACATCGGTAG	438 bp

PART 2: VIROLOGICAL MARKERS IN HPV-ASSOCIATED CERVICAL ADENOCARCINOMA AND OROPHARYNGEAL CARCINOMA

3.7 Populations

The investigation described in this study could be carried out on residual specimens following diagnostic analysis, provided that all data would be kept anonymous.

3.7.1 Cervical Adenocarcinoma (AdCa)

The study included 131 patients (age range 24-94 years, mean age 47.5 years, median age 43 years), afferent to different hospitals in the Emilia-Romagna region (i.e. Bologna, Modena, Imola and Cesena) between 1991 and 2011. Clinical and epidemiological data were collected and resumed in Table 7. According to the World Health Organization (WHO) classification of tumours of the uterine cervix, all the samples were classified for the correspondent histological types/subtypes of cervical AdCa. Among 84 invasive AdCa, tumour stage (T stage) was available for 51 (60.7%): 90.2% were T1, 7.8% T2 and 2.0% T4. Additional information on lymph node involvement (N stage) or metastasis (M stage) was not available.

Table 7 – Clinical and epidemiological characteristic of the cervical AdCa population.

		Cervical AdCa, n (%)
Overall		131 (100%)
Age (years)	Mean ± SD	47.5 ± 15.6
	Range	24 – 94
Histological Types	AIS	47 (35.9%)
	Invasive AdCa	84 (64.1%)
Histological Subtypes*	Mucinous	95
	Endocervical	4
	Intestinal	2
	Signet Ring	0
	Minimal Deviation	0
	Villoglandular	4
	Endometrioid	15
	Clear Cells	5
	Serous	2
	Mesonephric	1
	Adenosquamous	3
CIN-associated	Yes	27 (20.6%)
	No	104 (79.4%)

*WHO histological classification of the tumours of the uterine cervix (www.screening.iarc.fr)

3.7.2 Oral and Oropharyngeal Squamous Cell Carcinoma (OSCCs and OPSCCs)

The study included 81 patients (age range 26-88 years, mean age 63.8 years, median age 65.0 years; 55 males and 26 females), afferent to the Department of Otolaryngology at the S.Orsola-Malpighi Hospital in Bologna, between 2001 and 2012 (Tab. 8). Topographic locations included malignancies of the oropharynx and oral cavity, in particular tonsils, wall of the pharynx, base of the tongue, tongue, floor of mouth and gum.

Table 8 – Clinical and epidemiological characteristic of the OSCCs and OPSCCs population.

		OSCCs and OPSCCs n (%)
Overall population		**81 (100%)**
Age (years)	Mean ± SD	63.8 ± 12.0
	Range	26 - 88
Gender	Male	55(67.9%)
	Female	26 (32.1%)
Seat of the lesion	Oropharynx (OPSCCs)	**75 (92.6%)**
	Tonsil	55 (67.9%)
	Base of the tongue	16 (19.8%)
	Wall of the pharynx	4 (4.9%)
	Oral Cavity (OSCCs)	**6 (7.4%)**
Clinical stage	I/II	13 (16.1%)
	III/IV	68 (83.9%)
T stage	T1	9 (11.1%)
	T2	36 (44.4%)
	T3	29 (35.8%)
	T4	7 (8.6%)
N stage	N0	14 (17.3%)
	N+	67 (82.7%)
Risk factors	Smoke and/or alcohol	42 (51.9%)
	No	39 (48.1%)

3.8 Cell lines, samples and nucleic acids extraction

Cervical cancer cell lines CaSki (~500 integrated copies of HPV 16 genome), SiHa (1–2 integrated copies of HPV 16 genome) and HeLa (~400 integrated copies of HPV 18 genome) were obtained and grown as monolayers as recommended by the American Type Culture Collection, Rockville, MD (DMEM medium, 10% Fetal Calf Serum, 1% SP). These cell lines have been widely used as model systems to investigate HPV activity in terms of viral load, integration and methylation analysis.

For both the populations we collected 10 μm thick tumour histological-confirmed paraffin-embedded biopsies. After deparafinization at 95°C for 15 min and centrifugation for 10 min at 12000 rpm, the tissue samples were digested with 20 μl of proteinase K in 200 μl of lyses buffer at 56°C for 2/3 hours. DNA was extracted with QIAMP DNA Mini Kit (Qiagen, Hilden, Germany) following manufacturer's instructions, eluted in 200 μl (OSCCs and OPSCCs) or 100 μl (cervical AdCa) of elution buffer (AE buffer) and stored at -80°C.

3.9 HPV Genotyping and mRNA detection

In order to detect and genotype HPV in our clinical samples, we used the INNO-LiPA Genotyping Extra assay (Innogenetics, Ghent, Belgium), following the manufacturer's instructions as previously described (see §3.3).

Samples positive for DNA of HPV 16, 18, 31, 33 or 45 were considered eligible for HPV E6/E7 mRNA detection by real time multiplex nucleic acid sequence-based amplification (NASBA). Transcripts of HR-HPV types 16, 18, 31, 33, and 45 were detected by the NucliSens EasyQ HPV assay (bioMérieux), according to the manufacturer's instructions.

3.10 HPV 16 and 18 viral load and physical state

Samples positive for HPV 16 and/or 18 were further tested to assess the viral load and genome integration by real time-PCRs, performed with the Rotor-Gene 3000 analyzer (Corbett Research). Primers and TaqMan LNA-probes were designed with ProbeFinder software (UniversalProbe Library, Roche) available at the website www.universalprobelibrary.com, as previously described (Leo et al, 2009). We performed three different real time-PCRs: one targeting a fragment of the E6 ORF, one targeting the human betaglobin gene and one targeting the E2 ORF (Table 9). Each reaction was carried out in a final volume of 25 μl, with 1X Premix Ex Taq^{TM} (TaKaRa), 200 nM each primer, 100 nM of the specific probe and 5 μl of sample. The two-step amplification profile was holding at 95°C for 10 sec and cycling at 95°C for 5 sec and 60°C for 30 sec repeated 45 times.

The E2 ORF is often interrupted when viral genome is integrated in the host cell genome, whereas the E6 gene is always intact. Quantification for the copy number of E6 and E2 genes was carried out using two standard curves obtained with known concentration of a plasmid (pSL1180 vector) containing the HPV 16 full length genome processed in triplicate (Fig. 14). The E6/E2 ratio was used to define the physical state of the viral genome: totally (E2/E6=0)

or mainly (0<E2/E6<0.5) integrated and totally (E2/E6=1) or mainly (1>E2/E6≥0.5) episomal.

The standard curve for human betaglobin was obtained by amplification of 10-fold dilution series of 300 ng to 0.003 ng of Human Genomic DNA (Roche) processed in triplicate. Since clinical samples are not homogeneous and we do not know exactly how many tumour cells/HPV infected cells are contained, the viral load was expressed as HPV copies/300 ng of human genomic DNA (HGD, corresponding to about 50 000 cells). Values $>5 \cdot 10^6$ copies/300 ng HGD (i.e. ~100 copies/cell) were considered as high viral load.

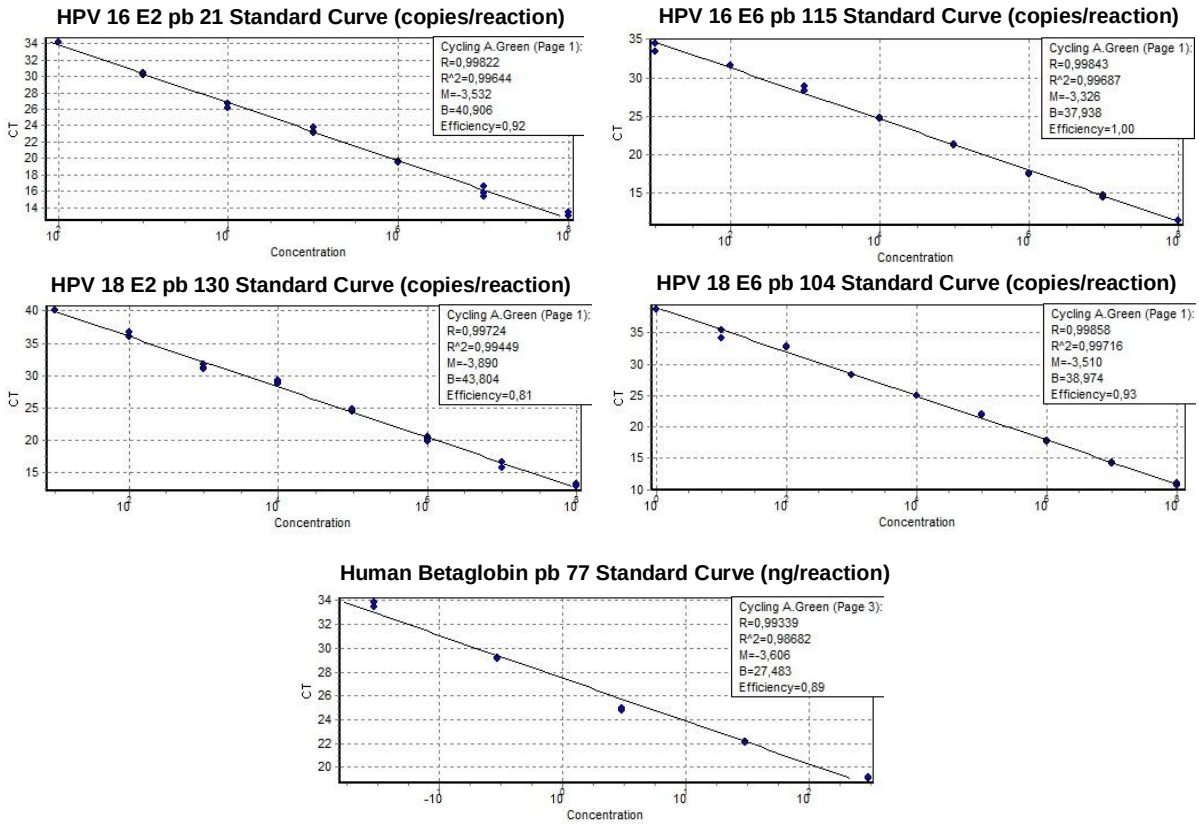

Figure 14 – Standard curves used to assess HPV 16 or 18 viral load and physical state.

Table 9 – Primer pairs and related probes used for the viral load and viral physical state analysis by real time-PCR.

Target		Primers (5'-3')	Probe
HPV 16 E2_hinge_right	PrL16_E2	CGACTATCCAGCGACCAAG	Pb#21
	PrU16_E2	TGAGTCTCTGTGCAACAACTTAGTG	(CAGAGCCA)
HPV 16 E6	PrL16_E6	TGTTTCAGGACCCACAGGA	Pb#115
	PrU16_E6	TTGTTTGCAGCTCTGTGCAT	(GACCCAGA)
HPV 18 E6	PrU18_E6	CTCGGTTGCAGCACGAAT	Pb#104
	PrL18_E6	GAAAAACGACGATTTCACAACA	(CTGGGCAC)
HPV 18 E2	PrU18_E2	GGTCCACAATGCTGCTTCTC	Pb#130
	PrL18_E2	AAAGACCTACGGCCAGACG	(CTGGACAC)
Betaglobin	PrU betaglo	AACTGAAGACAGCAGCAATCAA	Pb#77
	PrL betaglo	TGACATCAGGAAAGACTACACCA	(CCACCACC)

3.11 CpG methylation analysis of HPV 16 LCR and 3'L1 by pyrosequencing

3.11.1 Assay design

We designed the quantitative methylation analysis by pyrosequencing taking into account what was previously described by Rajeevan and colleagues (Rajeevan et al, 2006). This bisulfite-based assay was focused on the 19 CpG sites in nucleotide positions 6999-124 of HPV 16, a region encompassing the 3' region of L1 and LCR that includes the enhancer and E6 promoter sites (Fig. 15) and the E2 binding sites (E2BSs). Within the LCR, five sites (nucleotide positions 31, 37, 43, 52 and 58) are located in the E6 promoter, six sites (positions 7535, 7553, 7676, 7682 and 7694) are located in the enhancer, and six sites (positions 7233, 7270, 7428, 7434, 7455, 7461) are in the 5' region of the LCR. The remaining 4 sites (positions 7032, 7091, 7136 and 7145) are located in the 3' end of L1. CpG site at position 7434 is lost for Af2 variant due to a G to A change at position 7435. The LCR contains four E2BSs, with CpG dinucleotides located at nts 7455, 7461 (E2BS1; AC**CG**AATT**CG**GT), 7862 (E2BS2; AC**CG**TTTTGGGT; not considered in this study), 37, 43 (E2BS3; AC**CG**AAAT**CG**GT), 52 and 58 (E2BS4; AC**CG**AAAC**CG**GT) (Snellenberg et al, 2012).

Amplification and sequencing primers were designed for the sense strand sequence of the bisulfite converted DNA using Assay Design Software (Biotage, Inc., Charlottesville, VA). To take into account for DNA fragmentation introduced by bisulfite treatment, four different amplification reactions were designed to cover all CpG sites in four amplicons (A to D, Table 10). Since optimal read length of pyrosequencing per primer is limited to <50 nucleotides, more than one sequencing primer is needed to cover multiple CpG sites spread >50 nucleotides within certain amplicons. One primer in each amplification reaction was labelled with 5'-biotin. The choice of primer for 5'-biotinylation was based on the direction of pyrosequencing (reverse primer biotinylated for forward sequencing and forward primer biotinylated for reverse sequencing).

The dNTPs dispensation order during the pyrosequencing reaction was automatically generated by the software. The complete conversion of C to T in a non-CpG site was identified in order to ensure the successful modification, by adding a C in the dispensation order. If the bisulfite conversion has been completed successfully, there should not be a C incorporation in correspondence of this dispensation (i.e. no light signal).

Cervical carcinoma cell lines CaSki and SiHa with high and low methylation level in the LCR, respectively, were kept as models and controls.

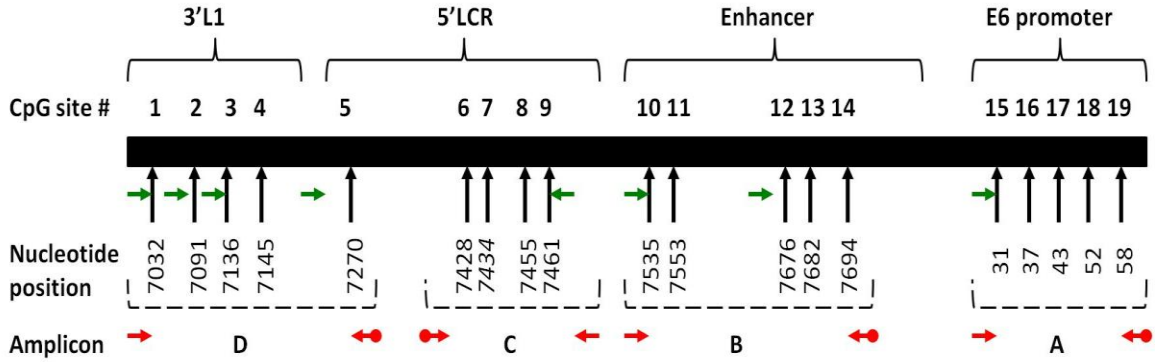

Figure 15 – Representative scheme of the CpG methylation analysis for the HPV 16 LCR and 3'L1 ORF. Red arrows represent the amplification primers and green arrows the sequencing primers and their directions (forward or reverse).

3.11.2 DNA conversion by bisulfite treatment

Sodium bisulfite deaminates cytosine residues (C) on single strand DNA molecules and converts them into uracils (U), while 5-methyl C (meC) remain protected from conversion (Fig. 16). When bisulfite-modified DNA is subjected to PCR amplification, the U are converted to thymidines (T) by DNA polymerase in the amplicon. In our study, 500 ng of total DNA underwent bisulfite conversion using the EZ DNA Methylation kit (Zymo Research, CA) following the manufacturer's instructions. The bisufite-modified DNA (3 aliquots of 10 µl for each sample) was stored at −80°C.

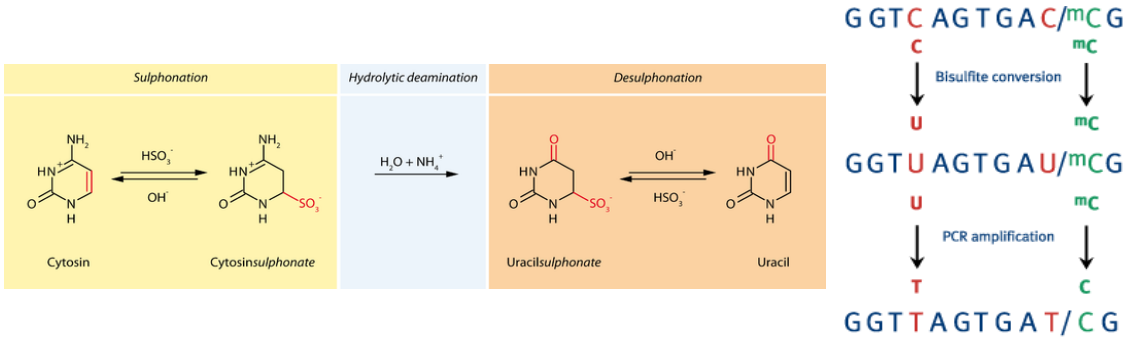

Figure 16 – Bisulfite-mediated conversion of non-methylated C in U (left) and the resulting C/T single nucleotide polymorphism (SNP) in the PCR product (right).

3.11.3 Amplification and pyrosequencing

PCR reactions were performed in a final volume of 50 µl with the following components: 200 mM dNTPs mix, 0.5 µM each of forward and reverse primers (Table 10), 2.5 mM $MgCl_2$, 0.62U of Hot Start GoTaq® DNA polymerase (Promega) and 5 µl of bisulfite-converted DNA. The conditions were the following: enzyme activation at 95°C for 2 min, 50 cycles of 95°C for 30 s, 55°C for 30 sec (51°C for amplicon A only), 72°C for 30 sec and final

extension at 72°C for 10 min (Tab. 11). Correct amplification was checked in 2% agarose gels stained with GelRed™ (Biotioum) using 2 μl of product.

Pyrosequencing provides a site-specific quantification of methylation at individual CpG sites in a reliable and rapid manner. The reaction involves four steps (Fig. 17A): 1) a sequencing primer is hybridized to a single-stranded PCR amplicon that serves as a template, and incubated with the enzymes, DNA Polymerase, ATP Sulfurylase, Luciferase, and apyrase as well as the substrates, adenosine 5' phosphosulfate (APS), and luciferin; 2) the first deoxribonucleotide triphosphate (dNTP) is added to the reaction. DNA polymerase catalyzes the incorporation of the deoxyribo-nucleotide triphosphate into the DNA strand, if it is complementary to the base in the template strand. Each incorporation event is accompanied by release of pyrophosphate (PPi) in a quantity equimolar to the amount of incorporated nucleotide; 3) the ATP Sulfurylase converts PPi to ATP in the presence of adenosine 5' phosphosulfate (APS). This ATP drives the Luciferase-mediated conversion of luciferin to oxyluciferin that generates visible light in amounts that are proportional to the amount of ATP. The light produced in the Luciferase-catalyzed reaction is detected by a charge coupled device (CCD) chip and seen as a peak in the raw data output (pyrogram). The height of each peak (light signal) is proportional to the number of incorporated nucleotides; 4) the enzyme Apyrase continuously degrades unincorporated nucleotides and ATP. When degradation is complete, another nucleotide is added. The addition of dNTPs is performed sequentially. It should be noted that deoxyadenosine alfa-thio triphosphate (dATP·S) is used as a substitute for the natural deoxyadenosine triphosphate (dATP) since it is efficiently used by the DNA polymerase, but not recognized by the Luciferase. As the process continues, the complementary DNA strand is built up and the nucleotide sequence is determined from the signal peaks in the pyrogram trace (Fig.17B).

In our study, the pyrosequencing analysis was performed using the PyroGold kit and the PyroMark™ Q24 system (both Qiagen, Hilden, Germany) as directed by the manufacturer. Briefly, 10 to 20 μl of each biotinylated PCR product was immobilized on streptavidin-coated Sepharose HP beads (AmershamBiosciences, Piscataway, NJ) and the non-biotinylated strand removed using the PyroMark™ Q24 Vacuum Workstation and the dedicated reagents. The biotinylated single stranded product was annealed to the appropriate sequencing primer (0.4 μM), and then subjected to sequencing using automatically generated nucleotide dispensation

order for "sequences to analyze" corresponding to each reaction and the sequencing primers listed in Table 10. The obtained pyrograms were analyzed using the allele quantification (AQ) mode in the PyroMark™ Q24 Software to determine the proportion of C/T or G/A and hence methylated and non-methylated cytosines at the targeted position(s). If the sequencing primer was forward, the targeted site C/T, on the other hand if the sequencing primer was reverse, the target site was G/A. The frequency of G in the antisense strand was equal to C in the sense strand. Methylation frequency was reported as the mean (± standard deviation, SD) of two to three separate sequencing reactions.

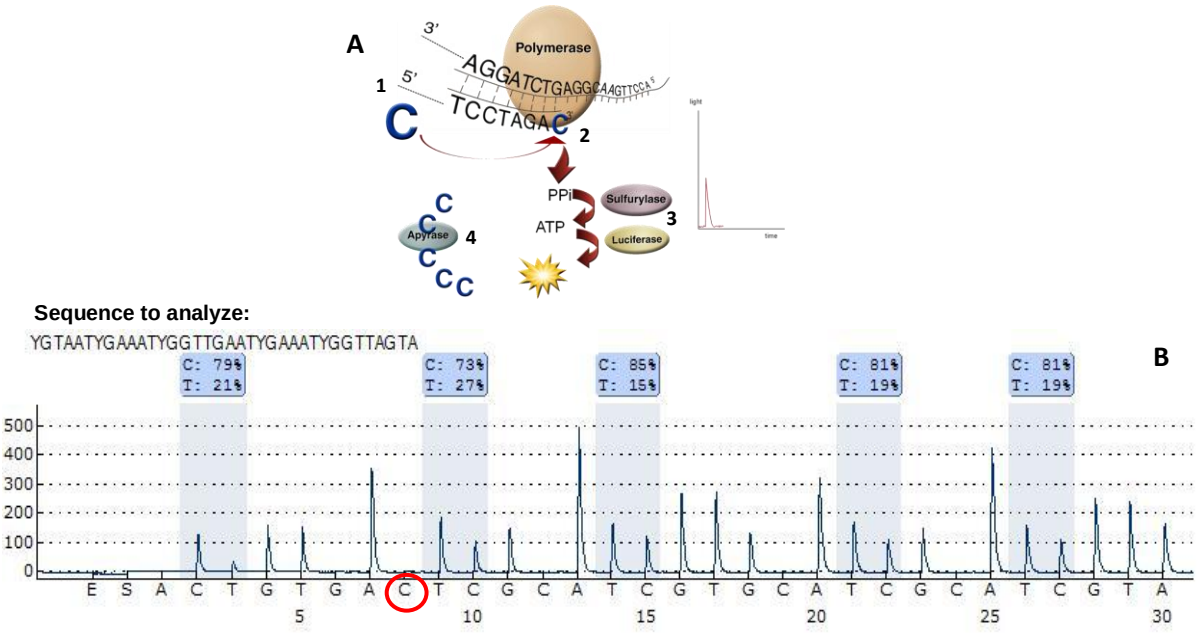

Figure 17 – Pyrosequencing. (A) Representative scheme of the reaction for a dCTP dispensation and incorporation. (B) Example of pyrogram resulted from the analysis of the 5 CpG sites in the HPV16 E6 promoter region. The red circle indicates the position of the complete bisulfite-conversion-control.

3.11.4 Specificity and sensitivity

The sensitivity of the methylation assay to HPV 16 copy number was evaluated by spiking HPV 16 positive CaSki or SiHa cells into HPV negative UT7 cells (leukemia cell lines) prior to DNA extraction. In a total cell count of 3×10^6 cells, dilutions were prepared representing one HPV 16 positive cell in the background of 3, 30, 3×10^2, 3×10^3, 3×10^4 and 3×10^5 negative cells (Rajeevan et al, 2006). Bisulfite treatment and pyrosequencing (Amplicon A) was performed as described above. Preliminary evaluation of the specificity of the reaction for HPV 16 sequences was conducted by analyzing extracts of CaSki, SiHa, HeLa and UT7 cell lines.

Table 10 – Primers used for the CpG methylation analysis. Primers in bold font are biotynilated at the 5'-end.

Amplicon	Primer	Sequence (5'-3')	Sequencing Primer, sequence (5'-3')	Target CpGs
A	16_E6prom_F	GGTGTGTGTAAATAGATTTTGGGTTATA	S1: AATAATTTATGTATAAAATTAAGGG	31, 37, 43, 52, 58
(178 bp)	**16_E6prom_R**	**ATAAATCCTAAAACATTACAATTCTCTT**		
B	16_Enhan_F	GGTTGTATGTTTTTTGGTATAAAATGTG	S2: TGTATATTGTGTTATATAAAATAAA	7676, 7682, 7694
(356 bp)	**16_Enhan_R**	**ACTAACCTTTACACAATTCATATATAAACT**	S3: GTTAGTAATTATGGTTTAAATTTG	7535, 7553
C	**16_5LCR1_F**	**ATTGTGTTGTGGTTATTTATTGTA**	S4: TTTTATACCAAAAAACATAC	7428, *7434*, 7455,
(146 bp)	16_5LCR1_R	AAAAACACATTTTATACCAAAAAA		7461
D	16_3L15LCR2_F	TTGGGAAGTAAATTTAAAGGAAA	S5: GTGTTTGTATGTATGGTATAAT	7270
			S6: ATTATTTTATTTATTTTTATAATTG	7136, 7145
(390 bp)	**16_3L15LCR2_R**	**AATAACCACAACACAATTAATAAA**	S7: ATTAAAATTTATATTAGGAA	7091
			S8: TTAGATTAGTTTTTTTTAGG	7032

Table 11 – PCR amplification profile ([a]Amplicon A only).

Step	Temperature (°C)	Time	Cycles
Enzyme Activation	95°C	2 min	1
Denaturation	95°C	20 sec	
Annealing	**51[a]/55°C**	30 sec	**50**
Extension	72°C	30 sec	
Final Extention	72°C	10 min	1

3.12 Statistical analysis

For statistical analysis, GraphPad Prism 5 software was used. Fisher's exact test was used to analyze 2x2 contingency tables. For the HPV 16 DNA methylation analysis we used non-parametric tests such as Mann-Whitney test to compare two groups or Kruskall-Wallis test for more than two groups to identify differentially methylated regions or individual CpG sites as suggested in Clarke et al, 2012. Differences in overall disease-free survival (DFS) were evaluated by using the Kaplan-Meier method and the log-rank test. The cut-off date for follow-up was 31st December, 2012.

Proportions were presented with 95% confidence intervals (95% CIs); *P* values <0.005 were considered statistically significant and all tests were two-tailed.

PART 3: ANALYSIS OF THE RESPONSE TO IFN-κ TRANSFECTION IN CERVICAL CANCER AND HPV-POSITIVE HNSCC CELL LINES

(experiments performed under the supervision of Dr. Bladimiro Rincon Orozco and Prof. Dr. Frank Rösl at the Division of Viral Transformation Mechanisms, Research Program in Infection and Cancer, German Cancer Research Center, Heidelberg, Germany)

3.13 Cell Lines

Cervical cancer cell lines CaSki (~500 copies of HPV 16 genome), SiHa (1–2 copies of HPV 16 genome), HeLa (~400 copies of HPV 18 genome) and HNSCC cell lines Cal27 (HPV 16 DNA positive/RNA negative), SCC25 (HPV 16 DNA positive/RNA negative), UDSCC2 (HPV 16 DNA positive/RNA positive) and 93V4 (HPV 16 DNA positive/RNA negative) were grown at 37°C (5% CO_2) in DMEM or RMPI 1640 medium, 10% Fetal Calf Serum, 1% Streptomycin-Penicillin.

3.14 IFN-κ plasmid

The complete IFN-κ ORF was previously cloned in the pSecTagA vector (Invitrogen), under the control of Cytomegalovirus (CMV) promoter, in order to have an additional Igκ leader sequence at the N-term of the molecule to improve its secretion, a *myc* epitope and a $(His)_6$ tail at the C-term for its purification (Fig. 18). The recombinant protein has a final molecular weight of about 35 kDa.

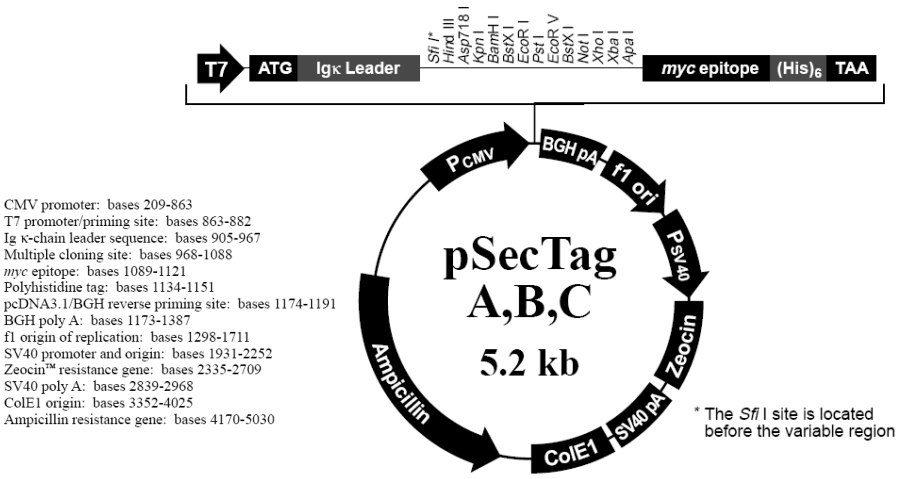

Figure 18 – The Invitrogen pSecTagA vector map and its characteristics.

3.15 IFN-κ transfections and IFN-β/IFN-γ treatments

Transient transfections were performed in 10 cm petri dishes using 2×10^6 cells in a final volume of 12 ml. Twelve micrograms of plasmid with IFN-κ or empty vector (mock) were diluted in 1200 µl of Opti-MEM® (Gibco) and 16 µl of Turbofect (Fermentas), following manufacturer's instructions for reverse transfection. Twenty-four hours post-transfection, cells were recovered for mRNA and proteins analysis. The respective supernatants were also collected by centrifugation at 4°C, 1500 rpm for 10 min and stored at -80°C.

In order to have a control for the response to IFN-κ, cells were also treated for 24 h with 1000 units of commercially available (NIH) IFN-β and IFN-γ and recovered for mRNA analysis.

3.16 mRNA extraction and RT-qPCR analysis

Total RNA was extracted using the RNeasy kit (Qiagen) with an in-column DNAse digestion step, following manufacturer's instructions. cDNA synthesis was performed following the RevertAid™ Reverse Transcriptase protocol (Thermo Scientific). Briefly, 1 µg of extracted RNA was incubated at 65°C for 5 min with 100 pmol Oligo $(dT)_{18}$ primer and DEPC-treated water up to 12.5 µl. Then, 1X Reaction buffer, 20 U RiboLock RNase Inhibitor (Thermo Scientific), 1 mM dNTPs mix and 200 U RevertAid enzyme mix were added in a final volume of 20 µl and the mix incubated at 42°C for 1h. The reaction was terminated by heating at 70°C for 10 min. Each sample was tested in a mix with or without reverse transcriptase (RT+ or RT-) which underwent hGAPDH amplification by classic PCR (Fw 5'-GCTCTTGCTGGGGCTGGTGG-3' and Rv 5'-GCCTTCCGTGTCCCCACTGC-3', 345 bp) to check for the presence of DNA contamination and the good quality of the cDNA.

One microliter of cDNA (1:5 dilution of RT+ mix in RNase-free water) was used to carry out the qPCR analysis, in a final volume of 20 µl, with 1X SYBR Green mix (BioRad) and 200 nM each primer using the CFX96 Touch™ Real Time PCR Detection System (BioRad) (Tab. 12). The two-step amplification program was 50°C for 5 min, 95°C for 10 min, 40 cycles 95°C for 15 sec and 60°C for 1 min. Melting curve analysis with default parameters was used to check product specificity.

The hTBP1 (human TATA box protein 1) expression was used as reference gene (housekeeping) to normalize data obtained for the genes of interest (GOI) and, for each cell line, results from transfected/treated cells were compared to those from untransfected/untreated cells (naïve). The ΔΔCt analysis was performed to obtain the fold-change value (Fc, mean ± SEM of two different transfections analyzed in triplicate).

Table 12 – Primers designed using the Primer-BLAST tool (www.ncbi.nlm.nih.gov/tools/primer-blast/) and used for the qPCR analysis.

Target	Primer	Sequence (5´-3´)	Position (bp)	Amplicon size (bp)
hTBP1 (housekeeping)	Forward	GAGTCGCCCTCCGACAAAG	16-119	103
	Reverse	GTTTCCTCTGGGATTCCATCG		
hLMP7	Forward	GCTGGCGGTCATGGCGCTAC	19-125	107
	Reverse	AGTCAGGACGGTCCGAGCGA		
hLMP2	Forward	CTGGGACCAACGTGAAGGAG	435-506	72
	Reverse	ATGGCAAAAGGCTGTCGAGT		
hMECL-1	Forward	CACTGAGCTCACCCACAGAG	680-786	107
	Reverse	TAGCTCCAGGGTTAGTGGCT		
hTAP1	Forward	CCCTGCCGGGACTTGCCTTG	652-861	210
	Reverse	GCCGACGCACAGGGTTTCCA		
hTAP2	Forward	CCTGCTCATAAGGAGGGTGC	1250-1473	224
	Reverse	GCTGTCGGTCCATGTAGGAG		
hHLA-B	Forward	CTACCCTGCGGACATCA	750-988	255
	Reverse	ACAGCCAGGCCAGCAAC		
hOAS1	Forward	GGTCAGTTGACTGGCAGCTA	575-731	157
	Reverse	TGAGGCTCTTGAGCTTGGTG		
hPKR	Forward	CCCAGATTTGACCTTCCTGA	97-206	110
	Reverse	ACTTGGCCAAATCCACCTG		
hIRF7	Forward	GGCTGGAAAACCAACTTCCG	638-708	71
	Reverse	CCCGAGTTATCTCGCAGCAT		
hIRF9	Forward	AGCTCTTCAGAACCGCCTAC	44-176	108
	Reverse	CATGGCTCTCTTCCCAGAAA		
hMX1	Forward	CCCCGGTTAACCACACTCTG	2190-2328	139
	Reverse	CGGCTAACGGATAAGCAGGA		
hCyclin E1	Forward	ATACTTGCTGCTTCGGCCTT	1075-1222	148
	Reverse	TCAGTTTTGAGCTCCCCGTC		
hCDK2	Forward	TCCTGAAATCCTCCTGGGCT	747-897	151
	Reverse	CCCCAGAGTCCGAAAGATCC		

Table 12 – Continue.

Target	Primer	Sequence (5´-3´)	Position (bp)	Amplicon size (bp)
hCyclin D1	Forward	CGGACTACAGGGGAGTTTTGTT	5-70	84
	Reverse	ACTCTGCTGCTCGCTGCTA		
hIFNR1	Forward	GGCCCATGGGTGTTGTCC	196-315	120
	Reverse	GACAGACTCATCGCTCCTGT		
hIFNR2	Forward	GGCCATTTCCTAACCTGCCA	1191-1243	152
	Reverse	GGTATAGCCACCGCCACTTG		
hIFN-κ	Forward	CTGGGAGATTGTCCGAGTGG	569-705	137
	Reverse	TTTGGTGCATTTGCGTAGCC		
hIFN-β	Forward	CCTTTGCTCTGGCACAACAG	26-125	100
	Reverse	GTGGAGAAGCACAACAGGAGA		
hNLRC5	Forward	CTCCTCACCTCCAGCTTCAC	5402-5629	228
	Reverse	GTTATTCCAGAGGCGGATGA		

3.17 Proteins extraction and Western-blot analysis

For proteins analysis, cells were washed 2 times in DPBS to remove residual media and resuspended in 80-100 μl of RIPA buffer (10 mM Tris pH 8.0, 150 mM NaCl, 1 mM EDTA, 1% NP-40, 0.1% SDS) in ice. The lysate was centrifuged 30 min at 14,000 rpm in a cold microfuge (4°C). The supernatant was recovered for the quantification by Bradford assay and cooked at 95°C for 10 min with 1X SDS-loading buffer blue (300 mM Tris-HCl pH 6.8, 12.5% β-mercaptoethanol, 5mM EDTA-2Na pH 6.8, 86% Glycerin, 10% SDS). Eighty micrograms of proteins were used to run a 15% SDS-PAGE. Semi dry protein transfer was performed with the Trans-Blot® Turbo system (BioRad) with buffer Anode I (300 mM Tris, 10% MeOH, pH 10.4), Anode II (2.5 mM Tris, 10% MeOH) and Cathode (25 mM Tris, 90 mM Glycerin, 10% MeOH, pH 9.4).

Membranes were blocked for 1 h with 5% milk in 1X TBS-T buffer (100 mM NaCl, 10 mM Tris pH 7.5, 0.1% Tween 20), washed with 1X TBS-T and probed with the following antibodies (1:1000 dilution): IFN-κ (Abnova), Mx1 (kindly obtained from Otto Haller, University Freiburg), CyclinD1 (Santa Cruz) and Tubulin (Santa Cruz).

3.18 Antiviral activity assay (cytopathic effect reduction assay)

The antiviral assay of human IFNs is based on the induction of a cellular response in human cells, which prevents or reduces the cytopathic effect of an infectious virus. The potency of tested IFNs is estimated by comparing its protective effect against a viral cytopathic effect with the same effect of the appropriate reference preparation.

In this study, Encefalomyocarditis virus (EMCV) has been used in combination with the A549 human epithelial lung carcinoma cell line. In a 96 wells plate, A549 cells were seeded in a final volume of 100 µl of medium (DMEM, 5% FCS) and incubated at 37°C, 5% CO_2. After 48 h, cells were treated in triplicate with serial 2-fold dilutions (8 dilutions from 1:2 to 1:256) of supernatant from cells transfected with pSecTagA_IFN-κ or empty vector, or of IFN-β reference dilution (NIH). After 24h, the medium was removed and 100 µl of the properly diluted suspension of EMCV (DMEM, 1% FCS) was dispensed to all wells including virus control line, but excluding cell control line. After 44 h, plates were microscopically examined to check that the EMCV had caused a cytopathic effect in the virus control line. If yes, 1X MTT solution was added to each well and after 4 h cells were lysed with lysis buffer. Absorbance at 570 nm was read after at least 12 h of incubation, considering as blank the virus control line. Cell viability was expressed considering the cell control line as reference (100%).

3.19 Cell proliferation assay

Cells were collected 24 h post-transfection with IFN-k/mock pSecTagA vector, counted and seeded in three 96 wells plates (about 5 000 cells/well in triplicate, medium up to 100 µl, one plate for each measurement). The plates were followed for 1, 2 and 4 days after seeding (i.e. 2,3 and 5 days after transfection). At each time point, the medium was replaced with 100 µl of 3-(4,5-Dimethylthiazol-2-yl)-2,5-diphenyltetrazolium bromide (MTT) 1X solution in medium without red phenol. After 4 h at 37°C, 5% CO_2, cells were lysed with 100 µl of lysis buffer. The OD at 570 nm (blue) was measured after 12 h incubation and the proliferation index (PI) was calculated as follows:

$$PI = \frac{\text{Average } OD_{570nm} \text{ day X}}{\text{Average } OD_{570nm} \text{ day 1}}$$

Results are shown as PI ± SEM at each time point of two separate experiments.

3.20 Statistical analysis

For data elaboration and statistical analysis, GraphPad Prism 5 software was used. The two-tailed t-Student test was used to calculate the *P* values, which were considered statistically significant when <0.05 (*), <0.01 (**) or <0.001 (***).

4. Results

PART 1: COMPARISON OF HPV SIGN GENOTYPING TEST WITH INNO-LIPA HPV GENOTYPING EXTRA ASSAY ON HISTOLOGIC AND CYTOLOGIC CERVICAL SPECIMENS (Barbieri et al, 2012)

4.1 HPV-detection concordance between HPV sign and INNO-LiPA tests.

Sixty out of 87 archival samples tested with INNO-LiPA assay were HPV positive (69.0%) and 27 were HPV negative (31.0%). Among positive samples there were 34 single infections (56.7%) and 26 multiple infections (43.3%).

After the analysis of the 87 samples by the amplification step of the HPV sign, 53 (60.9%) resulted positive and 21 (24.1%) negative for both the assays, with an overall agreement of 85.1% (*k* 0.66). On the other hand, there were 13 discordant samples: 7 INNO-LiPA HPV positive samples (8.0%) resulted negative with the HPV sign and 6 INNO-LiPA negative samples (6.9%) resulted positive. The seven INNO-LiPA-positive cytological samples which were negative by HPV sign were 2 CIN2+ and 5 CIN1. On the other hand, the six INNO-LiPA-negative samples (4 biopsies and 2 swabs) which resulted positive by HPV sign were high-grade lesions or tumours (4 AdCa and 2 CIN2+).

Considering biopsies and cytological swabs separately, we observed more agreement rate for biopsies than for cytological specimens (30/34=88.2%, *k* 0.76 *vs* 44/53=83.0%, *k* 0.54, respectively).

4.2 HPV genotyping concordance between HPV sign and INNO-LiPA tests.

For the 53 agreed positive samples, we assessed the concordance for single/multiple infections genotyping and results are resumed in Table 13. Twenty-nine samples (54.7%) resulted single infections and 3 (5.7%) multiple for both the techniques, with an overall agreement of 60.4% (*k* 0.08). On the other hand, there were 21 discordant samples (39.6%): 2 INNO-LiPA HPV single infections (3.8%) resulted multiple with the HPV sign and 19 INNO-LiPA multiple infections (35.8%) resulted single. Splitting our samples in biopsies and cytological swabs, we observed that there was less agreement rate for biopsies than for cytological specimens (52.9%, *k* 0.03 *vs* 63.9%, *k* 0.09, respectively).

Table 14 compares the genotyping results by HPV sign and INNO-LiPA tests considering one by one the HPV types detected in all histological and cytological samples. The overall agreement rate between HPV sign and INNO-LiPA tests is 95.7%.

For biopsies, the agreement rate between the HPV sign and the INNO-LiPA tests ranged from 88.2% for HPV 16 to 97.1% for HPV 18, 35 and 51, with an overall agreement rate of 94.1% (*k* 0.72). There was no statistical evidence of an imbalance in the samples between the two assays for each HPV genotyping, as determined by the McNemar's test. The proportion of positive agreements ranged from 0 for HPV 51 to 0.889 for HPV 18. For HPV 16 we observed a small *P* value (0.617), but the concordance resulted substantial (*k* 0.73).

For cytological samples, the agreement rate between the two assays ranged from 88.7% for HPV 16 and 18 and 100 % for HPV 33, 54 and 59 with an overall agreement rate of 96.0% (*k* 0.49). There was no statistical evidence of an imbalance in the samples between the two assays for each HPV genotyping. The proportion of positive agreements ranged from 0 for many genotypes (40, 45, 52, 53, 66, 73 and 74) to 1.000 for HPV 33, 54 and 59. For HPV 16 we observed a small *P* value (0.683), but the concordance resulted substantial (*k* 0.73).

Table 13 - Concordance between HPV sign and INNO-LiPA assay for single/multiple infections.

		HPV Sign/INNO-LiPA					
	Total	**S/S**	**S/M**	**M/S**	**M/M**	**Agreement rate**	***k***
Biopsies	17	7	6	2	2	9	0.03
%	100	41.2	35.3	11.8	11.8	52.9	
Cytolocgical swabs	36	22	13	0	1	23	0.09
%	100	61.1	36.1	0.0	2.8	63.9	
Overall	53	29	19	2	3	32	0.08
%	100	54.7	35.8	3.8	5.7	60.4	

S= single infection, M= multiple infections

4.3 Analysis of discordant samples.

The analysis with qRT PCRs of 30 discordant samples, 9 biopsies and 21 cytological samples, revealed the presence false positive (FP) genotypes (n. 20: 4 biopsies and 16 cytological swabs) only for the INNO-LiPA assay (Table 15). Among these we found HPV 35 once, HPV 16, 53 and 66 twice, HPV 18, 31 and 51 three times and HPV 52 four times.

The 10 false negative genotypes (FN) for the INNO-LiPA assay (4 biopsies and 6 cytological swabs) were HPV 31 once, HPV 18 and 45 twice and HPV 16 five times. Interesting, 2 out of 5 HPV 16 FN samples were defined HPV 16 African variant type 2 by HPV sign. Considering the 14 FN genotypes for the HPV sign test (4 biopsies and 10 cytological swabs),

they were HPV 18, 31, 45 and 53 twice and HPV 16 and 66 three times. The viral load of all FN HPV types with one of two methods, quantified by qRT PCRs, ranged from $5 \cdot 10^1$ to $8 \cdot 10^2$ copies/reaction, as reported in Table 4.

Table 14 - Genotype-specific concordance HPV sign and INNO-LiPA assay.

Sample	HPV genotype	HPV sign/INNO-LiPA +/+	+/-	-/+	-/-	Agreement rate (%)	*Ppos*	*Pneg*	Exact *P* value[a]	*k*
Biopsies	16	9	3	1	21	88.2	0.818	0.913	0.617	0.73
	18	4	0	1	29	97.1	0.889	0.983	1	0.87
	31	1	0	2	31	94.1	0.500	0.969	0.480	0.48
	35	1	0	1	32	97.1	0.667	0.985	1	0.65
	45	3	1	2	28	91.2	0.667	0.949	1	0.61
	51	0	0	1	33	97.1	0.000	0.985	n.a.[b]	n.a.[b]
	Overall	18	4	8	174	94.1	0.750	0.967	/	/
Cytological swabs	16	13	2	4	34	88.7	0.813	0.919	0.683	0.73
	18	2	2	4	45	88.7	0.400	0.938	0.683	0.34
	31	1	1	3	48	92.5	0.333	0.960	0.617	0.30
	33, 59	1	0	0	52	100.0	1.000	1.000	1	1
	40, 82	0	0	1	52	98.1	0.000	0.990	n.a.[b]	n.a.[b]
	45	0	1	0	52	98.1	0.000	0.990	n.a.[b]	n.a.[b]
	51	1	0	2	50	96.2	0.500	0.980	0.479	0.48
	52, 53	0	0	4	49	92.5	0.000	0.961	n.a.[b]	n.a.[b]
	54	2	0	0	51	100.0	1.000	1.000	1	1
	56	1	0	3	49	94.3	0.400	0.970	0.248	0.38
	66	0	0	5	48	90.6	0.000	0.950	n.a.[b]	n.a.[b]
	70	1	0	1	51	98.1	0.667	0.990	1	0.67
	73	0	3	0	50	94.3	0.000	0.971	n.a.[b]	n.a.[b]
	74	0	0	3	50	94.3	0.000	0.971	n.a.[b]	n.a.[b]
	Overall	23	9	35	1046	96.0	0.511	0.979	/	/
Biopsies + Swabs Overall		41	13	43	1220	95.7%	0.594	0.978	/	/

[a] *P* value determined by McNemar's test. *P* values <0.05 were considered statistically significant;
[b] n.a. not applicable;
- negative; + positive.

After resolution of discrepant results, HPV sign showed an overall genotype specificity of 100% and a sensitivity of 76.3% [CI 0.65-0.87] and INNO-LiPA showed an overall genotype specificity of 97.1% [CI 0.96-0.98] and a sensitivity of 84.5% [CI 0.75-0.94]. However, HPV sign revealed a higher sensitivity respect to INNO-LiPA for HPV 16 (90.0%, CI 0.79-1.01 *vs* 83.3%, CI 0.70-0.97). The lower sensitivity of HPV sign concerned genotypes 31, 53 and 66. In fact, considering genotypes 16, 18, 35, 45, 51 and 52 the sensitivity is 85.0% [CI 0.76-0.96] for HPV sign respect to 83.3% [CI 0.73-0.94] for INNO-LiPA.

Table 15 - Analysis of 30 specimens with discordant results for HPV genotyping between INNO-LiPA and HPV sign assays, retested with real time-PCRs with primer sets specific for HPV 16/18/31/35/45/51/52/53/66.

Samples		Histological definition	INNO-LiPA genotype[a]	HPV sign genotype[a]	SYBR Green Genotype (viral load[c])	FP/FN INNO-LiPA	FP/FN HPV sign
Biopsies	1	AIS	16 18	18	18	FP 16	
	2	invasive AdCa	Neg	16[b]	16 ($4.5\cdot10^2$)	FN 16	
	3	AIS	Neg	16	16 ($8.4\cdot10^2$)	FN 16	
	4	invasive AdCa	31 35	16	16 ($2.4\cdot10^2$)	FP 31 35 FN 16	
	5	AIS	18 35 51	35	18 ($6.2\cdot10^1$) 35	FP 51	FN 18
	6	AIS	16 31	16	16 31 ($1.1\cdot10^2$)		FN 31
	7	invasive AdCa	16 45	16	16 45 ($1.6\cdot10^2$)		FN 45
	8	AIS	16 45	16	16 45 ($9.8\cdot10^1$)		FN 45
	9	invasive AdCa	Neg	45	45 ($5.4\cdot10^2$)	FN 45	
Cytological swabs	10	CIN1	16 (54)	(54)	Neg	FP 16	
	11	CIN2+	16 18	Neg	16 ($1.5\cdot10^2$) 18 ($7.2\cdot10^1$)		FN 16 18
	12	CIN2+	16 51 (68)	Neg	16 ($2.3\cdot10^2$)	FP 51	FN 16
	13	CIN1	16	Neg	16 ($1.5\cdot10^2$)		FN 16
	14	CIN1	66	16	16 ($7.2\cdot10^2$)	FN 16 FP 66	
	15	CIN2+	Neg	16[b]	16 ($3.4\cdot10^2$)	FN 16	
	16	CIN2+	(82)	18	18 ($8.9\cdot10^1$)	FN 18	
	17	CIN1	18 31 53	(73)	53 ($9.2\cdot10^1$)	FP 18 31	FN 53
	18	CIN1	18	Neg	Neg	FP 18	
	19	CIN2+	51 52 66	18	18 ($6.1\cdot10^1$) 66 ($1.1\cdot10^2$)	FP 51 52 FN 18	FN 66
	20	CIN1	31	Neg	31 ($1.3\cdot10^2$)		FN 31
	21	CIN2+	31	45	45 ($1.4\cdot10^2$)	FP 31/FN45	
	22	CIN2+	52	31	31 ($1.8\cdot10^2$)	FP 52/FN 31	
	23	CIN1	52	(91)	Neg	FP 52	
	24	CIN2+	16 52	16	16	FP 52	
	25	CIN1	66 (70)	(70)	66 ($5.4\cdot10^1$)		FN 66
	26	CIN1	66 (70)	Neg	Neg	FP 66	
	27	CIN1	16 18 53	16 (42)	16	FP 18 53	
	28	CIN2+	53 (56)	(73)	53 ($1.6\cdot10^2$)		FN 53
	29	CIN1	53	Neg	Neg	FP 53	
	30	CIN2+	16 66	16	16 66 ($7.2\cdot10^1$)		FN 66

[a]HPV genotypes in round brackets were not tested by real time-PCR.

[b]HPV 16 African variant type 2 for HPV sign.

[c]Viral load is expressed in copies/reaction and reported only for FN discrepant results.

PART 2: VIROLOGICAL MARKERS IN HPV-ASSOCIATED CERVICAL ADENOCARCINOMA AND OROPHARYNGEAL CARCINOMA

4.4 HPV prevalence and mRNA in cervical AdCa

According to the INNO-LiPA assay, the overall HPV prevalence in our population was 92.4% (121/131), with 22.3% (27/121) multiple infections. Among positive samples, HPV 16 was the most prevalent genotype (81/121, 66.9%; 72.8% single and 27.2% multiple infections), followed by HPV 18 (42/121, 34.7%; 71.4% single and 28.6% multiple infections), HPV 45 (10/121, 8.3%; 40.0% single and 60.0% multiple infections), HPV 31 (6/121, 5.0%; 33.3% single and 66.7% multiple infections), HPV 35, 51, 52, 53 and 66 (1/121, 0.8% each; 100% multiple infections) (Fig. 19). LR-HPV 11 was also detected in 3 samples (2.5%), but always involved in multiple infections with other HR-HPVs. HPV 16 and/or 18 alone resulted involved in 81.8% (99/121) of the infections. Moreover, all the eligible samples resulted positive also for the correspondent mRNA and, in case of multiple infections, the transcript belonged to at least one of the HPV genotypes involved.

Considering the relation between age and infecting genotype, the median age of patients infected by HPV was 43 years. Those infected by HPV 16 or 18 alone showed a median age of 45 and 39 years, respectively (P=0.07).

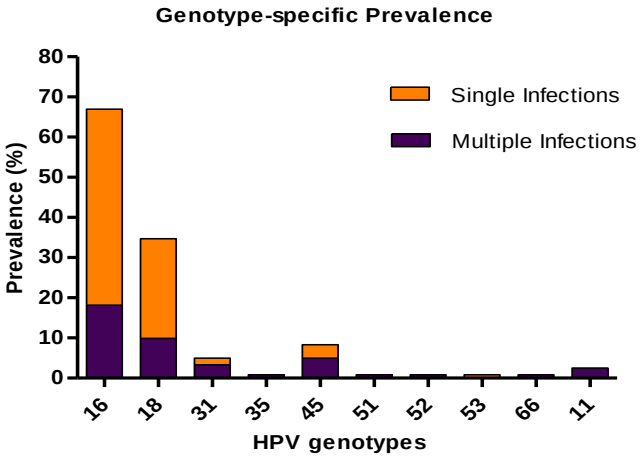

Figure 19- Genotype-specific prevalence among the 121 HPV-positive AdCa.

Concerning the histological classification of cervical AdCa, our population was composed by 65.7% (86/131) invasive AdCa (median age 48 years) with an overall HPV prevalence of 89.5% (77/86) and by 34.4% (45/131) AIS (median age 40 years) with an overall HPV prevalence of 97.8% (44/45) (P<0.0001 for the age). HPV 16 remains the most prevalent genotype in both invasive AdCa and AIS (75.3% and 52.3%, respectively) followed by HPV

18 (32.5% and 38.6%, respectively), HPV 45 (7.8% and 9.1%, respectively), HPV 31 (3.9% and 6.8%, respectively). HPV 35 and 53 were detected only in AIS (2.3% each) and HPV 51, 52 and 66 only in invasive AdCa (1.3% each).

Among patients with cervical AdCa with an associated CIN, 55.5% resulted HPV 16 infected, 37% HPV 18, 11.1% HPV 31 and 3.7% HPV 45. Most of them are single infections (81.5%).

4.5 HPV 16 and 18 viral load and physical state in cervical AdCa

Out of 81, 72 HPV 16 (88.9%) and 40/42 (97.6%) HPV 18 positive samples were analyzed for both viral load and physical state of the viral genome.

Concerning the viral load, for HPV 16 positive samples we observed values ranging from $1.61 \cdot 10^2$ to $7.09 \cdot 10^8$ copies of viral genome/300 ng HGD and 61.1% of the samples showed values $>5 \cdot 10^6$ copies/300 ng HGD. On the other hand, in HPV 18 positive samples we observed values ranging from $1.76 \cdot 10^1$ to $6.55 \cdot 10^7$ copies of viral genome/300 ng HGD, but 31.7% of the samples showed values $>5 \cdot 10^6$ copies/300 ng HGD.

For the physical state, we found that 13.9% of the HPV 16 positive patients harboured totally integrated viral DNA, 16.6% mainly integrated, 34.7% mainly episomal and 34.7% totally episomal. Among HPV 18 positive samples, we could observe that 15.0% harboured totally integrated viral DNA, 2.5% mainly integrated, 17.5% mainly episomal and 65.0% totally episomal.

Considering the histological classification in AIS and invasive AdCa, we observed that HPV 16 DNA was totally integrated/mainly integrated in 28.6% and 34.0% (P=0.79) of the cases, respectively, and HPV 18 DNA was in the same status in 17.65% and 17.39% (P=1.00) of the cases.

4.6 HPV 16 DNA methylation

4.6.1 Specificity and sensitivity of the HPV 16 DNA methylation analysis

The specificity of the primers was tested. As it was expected, we could observe the specific amplicons A, B, C and D for CaSki and SiHa, but not for HeLa or UT7 cell lines (Fig. 20). Concerning sensitivity and reproducibly, pyrosequencing assessed methylation levels in samples with one CaSki cell per 300 000 HPV negative cells (Fig. 21) and one SiHa cell per 3 000 HPV negative cells (data not shown for SiHa cells). This limit of detection, corresponding to 2–6 copies of HPV 16 DNA per/3 000 cells, is sufficient to evaluate methylation in most clinical samples.

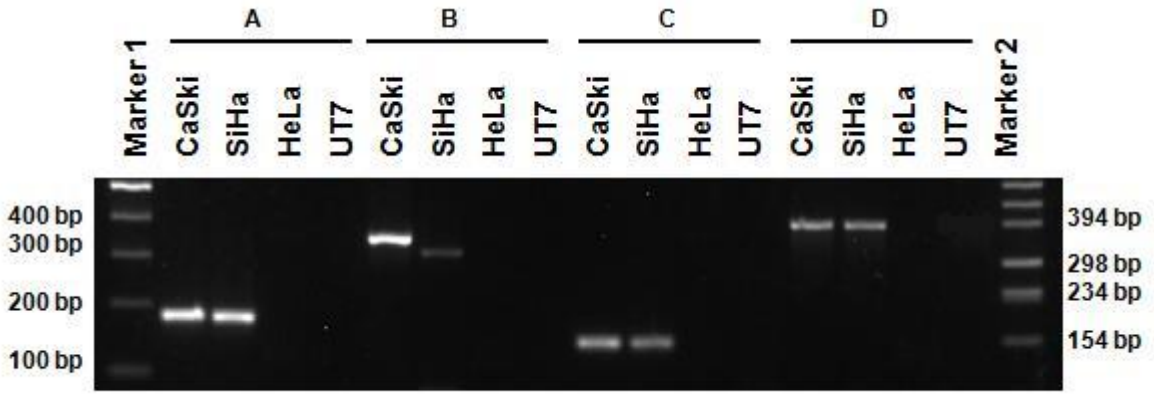

Figure 20 - Specificity for HPV 16 DNA amplification of each primer sets used for the methylation analysis and respective amplicons in a 2% agarose gel.

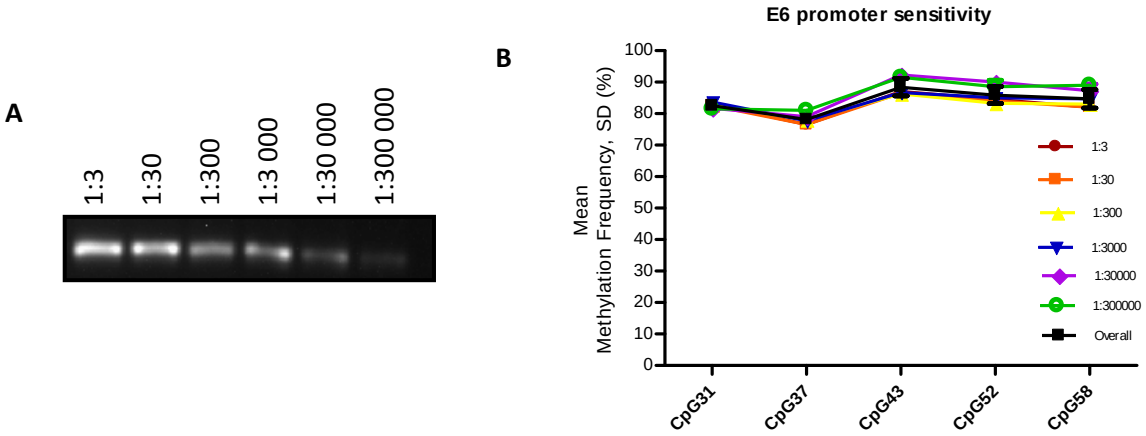

Figure 21 - Sensitivity of PCR and Pyrosequencing to quantify methylation in CaSki HPV 16 DNA. (A) Serial dilutions were made as described in materials and methods and used to generate amplicon A by PCR. (B) Amplicons from each dilution were sequenced using the correspondent primer that detects methylation frequency at positions 31, 37, 43, 52 and 58 in the E6 promoter region. Methylation frequency (%) are mean (±SD) of 3 sequencing reactions. Overall mean indicates the mean of all dilutions for each CpG site.

4.6.2 HPV 16 DNA methylation pattern in cervical AdCa: a general overview

Out of 81 HPV 16 positive samples, CpG DNA methylation analysis for the viral LCR and 3'L1 was possible in 64 (79.0%) (Table 16). The overall methylation frequency in cervical AdCa (17.2% ± 19.9% and 28.7% ± 28.0%) is lower than for CaSki cell line in both the regions (61.1% ± 23.5% and 42.6% ± 17.5%) and higher than SiHa cells only in the LCR (6.3% ± 6.6% and 78.0% ± 3.4%). Focusing the attention on the subregions in LCR, cervical AdCa showed a higher mean methylation frequency in the E6 promoter compared to SiHa

cells (17.0% ± 23.5% *vs* 1.6% ± 0.6%, respectively), but we observed high SD, as well as in the terminal part of the gene L1.

Table 16 - Methylation frequency of the HPV 16 LCR and 3'L1 in cell lines and cervical AdCa.

Region	CpG site (nt)	Methylation Frequency (%) ± SD		
		CaSki	SiHa	AdCa
Overall LCR		61.1 ± 23.5	6.3 ± 6.6	17.2 ± 19.9
E6 promoter	31, 37, 43, 52, 58	83.3 ± 4.3	1.6 ± 0.6	17.0 ± 23.5
Enhancer	7535, 7553, 7676, 7682, 7694	49.0 ± 18.3	8.6 ± 6.1	12.7 ± 7.9
5'LCR	7270, 7428, *7434*, 7455, 7461	47.7 ± 21.8	9.0 ± 7.4	18.7 ± 16.4
3'L1	7032, 7091, 7136, 7145	42.6 ± 17.5	78.0 ± 3.4	28.7 ± 28.0

The mean methylation frequency ± SD for each CpG site was plotted as histogram to better observe the methylation pattern and possible differences between individual sites (Fig. 22).

In the E6 promoter region, there are no differences between CpG sites for cervical AdCa which have similar values and SD ranging from 16.2% ± 23.5% in CpG 37 to 17.9% ± 23.8% in CpG 31. The same homogeneous pattern was observed also SiHa (ranging from 1.4% ± 0.5% in CpG 37 and 1.8% ± 0.8% in CpG 58), but in CaSki the CpG 37 showed a lower methylation frequency than the others (76.9% ± 2.1% *vs* >82.0%, respectively).

Considering the enhancer region, the three groups showed again similar patterns with CpGs 7535 and 7553 (6.5% ± 6.0% and 8.1% ± 5.9% in AdCa; 27.2% ± 2.0% and 31.7% ± 1.9% in CaSki; 3.5% ± 0.7% and 4.5% ± 2.1% in SiHa, respectively) lower in mean methylation frequency than CpG 7686, 7682 and 7694 (18.7% ± 8.1%, 13.8% ± 5.3% and 17.2% ± 6.3% in AdCa; 68.6% ± 2.6%, 55.9% ± 2.7% and 69.1% ± 1.9% in CaSki; 12.0% ± 7.2%, 8.7% ± 5.5% and 11.3% ± 8.5% in SiHa, respectively).

On the other hand, in the 5'LCR and 3'L1 we could observe more differences in methylation patterns. CaSki, SiHa and cervical AdCa seems to have the same pattern in the 5'LCR (i.e. increasing methylation from CpG 7270 to 7461), but CpG 7455 showed the tendency to be less methylated than the others in both SiHa and AdCa. Also in the terminal part of the gene L1, SiHa and AdCa had the same pattern with CpG 7091 more methylated than the others (37.1% ± 28.1% *vs* 25.8% ± 30.0%, 25.3% ± 26.4% and 26.6% ± 27.3% in AdCa; 89.0% ± 2.0% *vs* 78.2% ± 3.1%, 72.7% ± 4.4% and 72.3% ± 3.1% in SiHa). In CaSki, the same position is less methylated than the others (15.8% ± 1.6% *vs* 40.4% ± 1.7%, 58.2% ± 2.9% and 55.9% ± 3.0%).

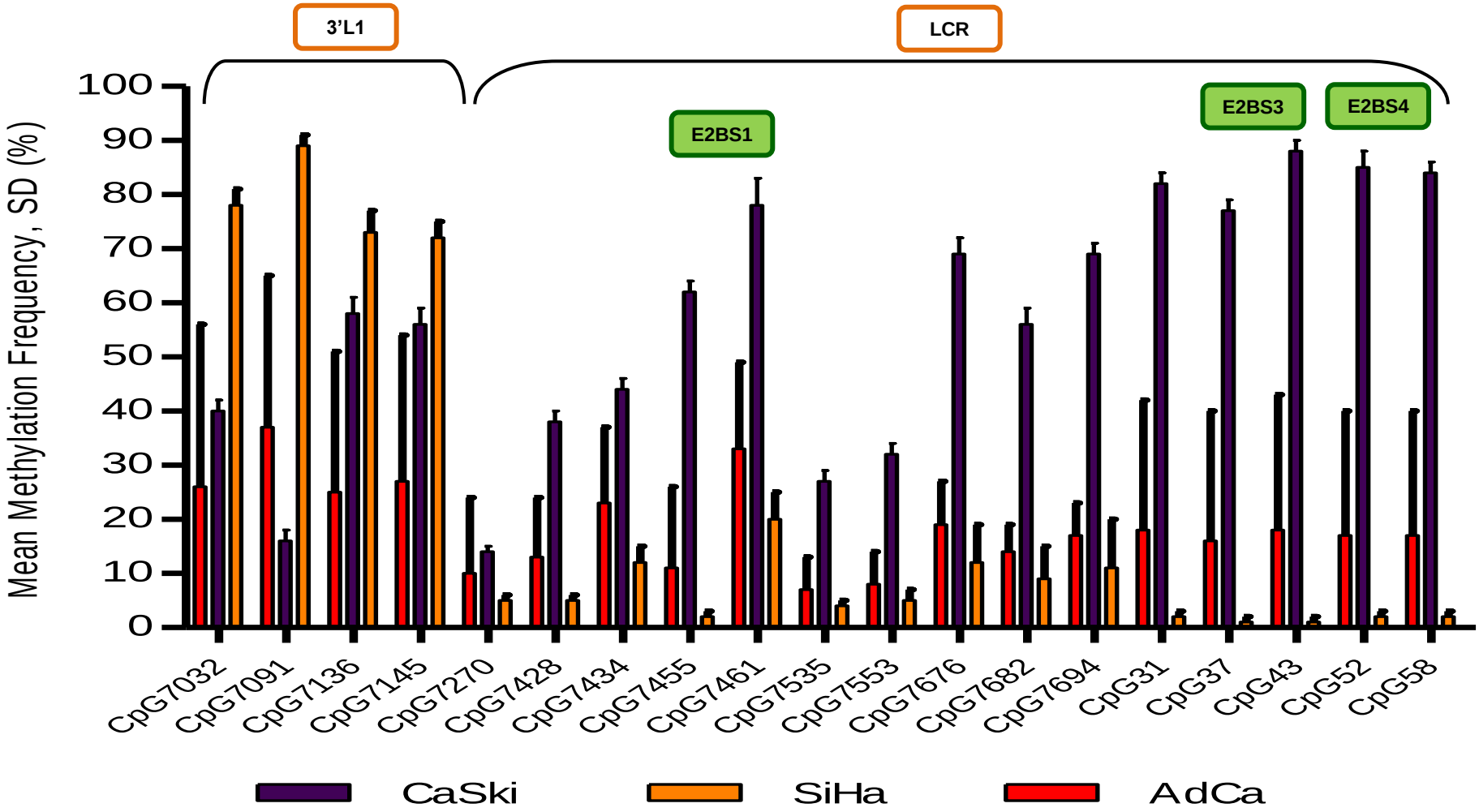

Figure 22- Methylation pattern in HPV 16 LCR and 3'L1 in clinical samples of cervical AdCa, CaSki and SiHa cells.

4.6.3 Methylation frequency of E2BSs in cervical AdCa

In order to deepen the role of viral DNA methylation, we first analyzed the methylation frequency in the E2BSs (Fig. 23). The median methylation frequency in the EBS1 resulted 12.5%, significantly higher than E2BS3 (2.3%, *P*=0.002) and E2BS4 (4.0%, *P*=0.02). There was no difference between E2BS3 and E2BS4 (*P*=0.27).

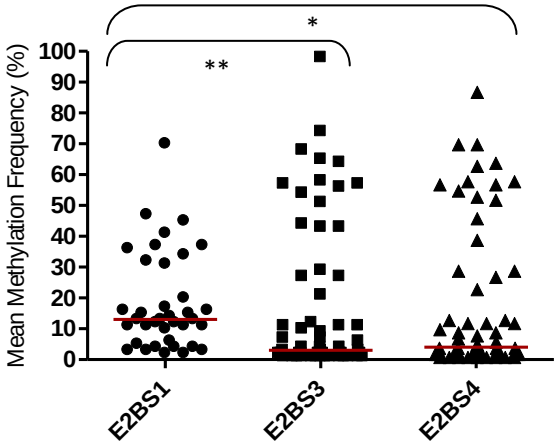

Figure 23 - Overall methylation frequency in the E2BSs in cervical AdCa. Red lines indicate the median value for each group (*=*P*<0.05 and **=P<0.01, Mann-Whitney test).

4.6.4 HPV 16 E6 promoter methylation and clinical/virological data in cervical AdCa

Focusing the attention on the overall methylation frequency in the E6 promoter region, we tried to find a correlation with available clinical and virological data.

As we noted in the previous paragraph, invasive AdCa showed the tendency to have a higher median overall methylation frequency in the E6 promoter compared to AIS (2.8% *vs* 5.0%, respectively; *P*=0.24).

Taking into account the viral physical state, patients with totally integrated viral DNA showed a median methylation frequency equal to 1.0%, mainly integrated 3.0%, mainly episomal 8.0% and totally episomal 5.0% (*P*=0.06; Fig. 24).

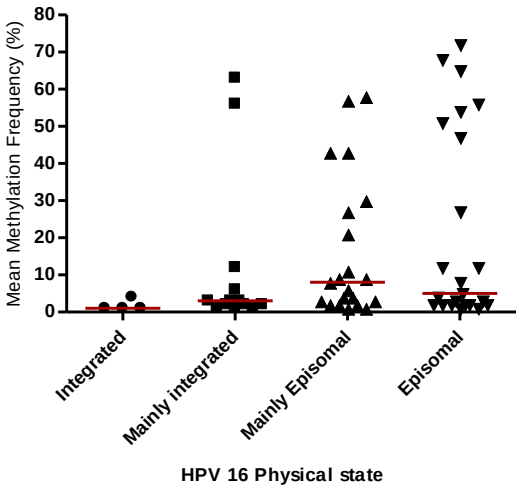

Figure 24 - Relationship between E6 promoter methylation frequency and viral physical state in the E6 promoter region in AdCa. Red lines indicate the median value for each group (*P*=0.06 One-way ANOVA, Kruskall-Wallis test).

Analyzing our samples one-by-one, we could observe a group of patients (18/64, 28.1%) with a methylation frequency ≥20% (Fig. 25). Among these, 2 were AIS and 16 invasive AdCa (*P*=0.06); 12 mucinous and 6 non-mucinous AdCa (*P*=0.03); 6 showed low and 12 high viral load (*P*=0.05); 2 harboured integrated or mainly integrated HPV genome and 15 episomal or mainly episomal viral DNA (*P*=0.02) (Fig. 26).

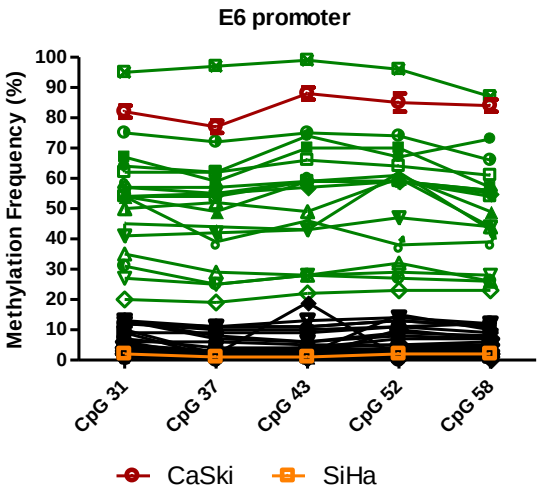

Figure 25 - Methylation frequency in the E6 promoter region: one-by-one analysis of each AdCa patient. Green lines indicate patients with mean frequency>20%; black lines indicate patients with mean frequency<20%.

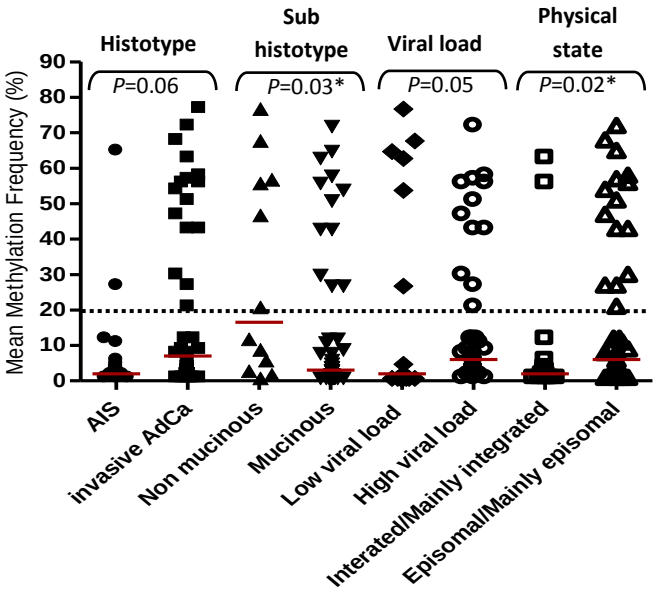

Figure 26 - Methylation frequency in the E6 promoter region in function of the clinical and virological data in cervical AdCa. Red lines indicate the median value for each group and the black dashed line indicates the cut-off value (*=*P*<0.05, Mann-Whitney test).

Considering the 3'L1 region, the patients with higher methyleted E6 promoter showed also a high methylation in the 3'L1 region, but they were not the only ones. In addition, there were 8 patients with a methylation frequency >20% in the terminal part of the gene L1, which were not methylated in the E6 promoter (2 AIS and 6 invasive AdCa).

4.7 HPV prevalence in OPSCCs and OSCCs.

Seventy-five of the 81 patients enrolled for this study (92.6%) were OPSCCs and 6 (7.4%) were OSCCs (Table 17). Most of the OPSCCs were carcinomas of the tonsils (55/75, 73.3%). Twenty-seven patients (33.3%) resulted HPV negative, whereas 54 patients (66.7%) were HPV positive (63.0% HR-HPV and 3.7% LR-HPV). HPV positive patients showed the tendency to be younger than negative ones (median age 64.5 years and 70.0 years, respectively), but, considering the genders, there are no differences between the two groups.

Focusing on genotype-specific prevalence among positive samples, HPV 16 was detected in 44 positive patients (81.5%) and other HR-HPV (HPV 33, 35 and 52) in 9 (16.7%). LR-HPV 6 was found in 3/54 cases (5.6%) and LR-HPV 11 in 2/54 cases (3.7%). Most of the HPV positive samples were characterized by a single infection (50/54, 92.6%) and just 4 were multiple infections (7.4%). HPV 16 infections were single in 40/44 of the cases (90.9%) and multiple in 4 (9.1%). HPV 6, 33 and 35 were involved only in single infections (each 5.6%),

HPV 52 in one single infection (1.8%) and in two multiple infections with HPV 16 (3.7%), whereas HPV 11 only in two multiple infections with HPV 16 (3.7%) (Fig. 27).
Considering the different seats of the lesions, tonsils had a higher percentage of HPV positive samples (39/55, 70.9%) than other sites (15/26, 57.7%). Interesting, this difference increased looking at only HR-HPV infection (69.1% *vs* 50.0%, respectively). LR-HPV 6 single infections were detected once in tumours of the tonsils and twice in the base of the tongue.
For what concerns clinical stage, T stage and N stage, we observed a trend showing that HPV positive tumours are high-grade tumours (i.e. clinical stage III/IV or N+ samples). Moreover, we could analyze the lymph node metastasis for two patients and these samples resulted positive for the same viral type detected in the seat of the primary tumour (i.e. HPV 16). According to tobacco and alcohol intake, HPV positive tumours seems to belong mainly to patients without other typical risk factor for HNSCC development rather than to those with (54.4% *vs* 29.6%, respectively; *P*=0.02).

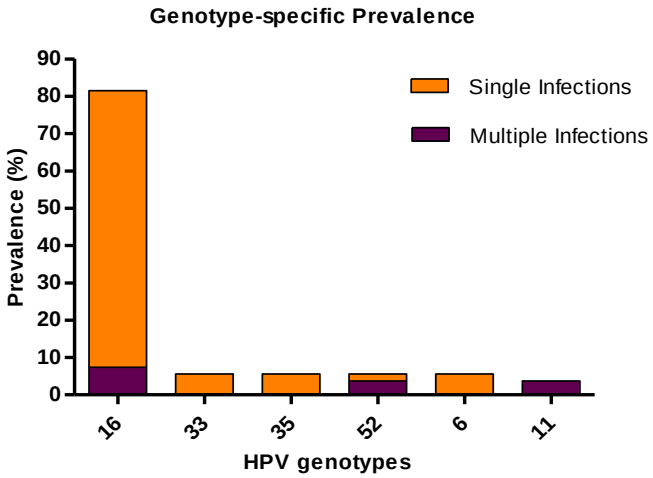

Figure 27 - Genotype-specific prevalence among the 54 HPV positive OPSCC/OSCC.

Eligible samples were tested by NASBA assay for the presence of viral E6/E7 mRNA and all were positive for the correspondent genotype.

Samples belonging to the oral cavity will not be considered for further analysis since they were underrepresented in our population and we could detect HPV 16 only in one case.

Table 17 – Clinical and epidemiological data for HPV positive and negative patients.

		HPV pos		HPV neg		Statistical analysis[a]
	total n	**n**	**%**	**n**	**%**	
Overall population	**81**	**54**	**66.7%**	**27**	**33.3%**	
Age, years						
Median (range)		64.5 (26-88)		70.0 (45-80)		*P* 0.20
Gender						
Male	55	37	68.5%	18	66.7%	M *vs* F *P* 1.00
Famale	26	17	31.5%	9	33.3%	
Seat of the lesion						OPSCCs *vs* OSCCs
Oropharynx (OPSCCs)	**75**	52	96.3%	23	85.2%	*P* 0.09
Tonsil	55	39	72.2%	16	59.2%	Tonsils *vs* Other
Base of the tongue	16	11	20.4%	5	18.6%	*P* 0.31
Wall of the pharynx	4	2	3.7%	2	7.4%	HR-HPV Tonsils *vs* Other
Oral Cavity (OSCCs)	**6**	2	3.7%	4	14.8%	*P* 0.14
Clinical stage						
I/II	13	7	13.0%	6	22.2%	I/II *vs* III/IV
III/IV	68	47	87.0%	21	77.8%	*P* 0.34
T stage						
T1	9	6	11.1%	3	11.1%	T1/2 *vs* T3/4
T2	36	23	42.6 %	13	48.1%	*P* 0.81
T3	29	20	37.0%	9	33.3%	
T4	7	5	9.4%	2	7.5%	
N stage						
N0	14	7	13.0%	7	25.9%	N0 *vs* N+
N+	67	47	87.0%	20	74.1%	*P* 0.21
Risk factors						
Smoke and/or alchool	42	23	42.6%	19	70.4%	Risk factors *vs* No
No	39	31	54.4%	8	29.6%	***P* 0.02**

[a]Fisher's exact test or Mann-Whitney test (two-tailed).

4.8 HPV 16 viral load and physical state in OPSCCs

Out of 44, 33 HPV 16 positive samples (75.0%) were analyzed to assess both the viral load and the physical state of the viral genome. Concerning the viral load, we observed values ranging from $4.32 \cdot 10^1$ to $1.30 \cdot 10^8$ copies /300 ng HG, but most of the samples showed values $>5 \cdot 10^6$ copies/300 ng HGD. Furthermore, we found that 15.1% of the them harboured totally integrated viral DNA, 36.4% mainly integrated, 36.6% mainly episomal and 3.0% totally episomal.

4.9 HPV 16 DNA methylation pattern in OPSCCs

Out of 44 HPV 16 positive samples, CpG DNA methylation analysis for the viral LCR and 3'L1 was possible in 34 (77.3%) (Tab. 18). The overall methylation frequency in OPSCCs was lower than for CaSki cell line in both the regions (9.9% ± 11.8% and 30.9% ± 27.8% *vs* 61.1% ± 23.5% and 42.6% ± 17.5%, respectively) and higher than SiHa cells only in the LCR (6.3% ± 6.6% and 78.0% ± 3.4%). Focusing the attention on the subregions of the LCR, OPSCCs showed a higher mean methylation frequency in the E6 promoter compared to SiHa cells (9.6% ± 15.1% *vs* 1.6% ± 0.6%, respectively), but we observed high SD, as well as in the terminal part of the gene L1.

Table 18 - Methylation frequency of the HPV 16 LCR and 3'L1 in cell lines and OPSCCs.

Region	CpG site (nt)	Methylation Frequency (%) ± SD		
		CaSki	SiHa	OPSCCs
Overall LCR		61.1 ± 23.5	6.3 ± 6.6	9.8 ± 11.8
E6 promoter	31, 37, 43, 52, 58	83.3 ± 4.3	1.6 ± 0.6	9.3 ± 14.9
Enhancer	7535, 7553, 7676, 7682, 7694	49.0 ± 18.3	8.6 ± 6.1	7.8 ± 5.0
5'LCR	7270, 7428, *7434*, 7455, 7461	47.7 ± 21.8	9.0 ± 7.4	11.5 ± 10.7
3'L1	7032, 7091, 7136, 7145	42.6 ± 17.5	78.0 ± 3.4	29.5 ± 27.5

The mean methylation frequency for each CpG site was plotted as histogram to better observe the methylation pattern and possible differences between individual sites (Fig. 28).

In the E6 promoter region, there are no differences between CpG sites for OPSCCs which have similar values and SD ranging from 8.9% ± 15.1% in CpG 37 to 10.1% ± 15.7% in CpG 31. Considering the enhancer region, OPSCCs showed again the CpGs 7535 and 7553 (3.6% ± 2.3% and 4.9% ± 2.9%) lower in mean methylation frequency than CpG 7686, 7682 and 7694 (11.7% ± 4.9%, 8.1% ± 3.4% and 11.0% ± 4.6%).

For the 5'LCR and 3'L1, also OPSCCs showed similar methylation pattern to SiHa: the same pattern in the 5'LCR (i.e. increasing methylation from CpG 7270 to 7461), but CpG 7455 showed the tendency to be less methylated than the others. Also in the terminal part of the gene L1, SiHa and OPSCCs had the same pattern with CpG 7091 more methylated than the others (38.5% ± 27.3% *vs* 30.1% ± 29.7% for 7032, 24.5% ± 25.5% for 7136 and 25.7% ± 26.9% for 7145 in OPSCCs).

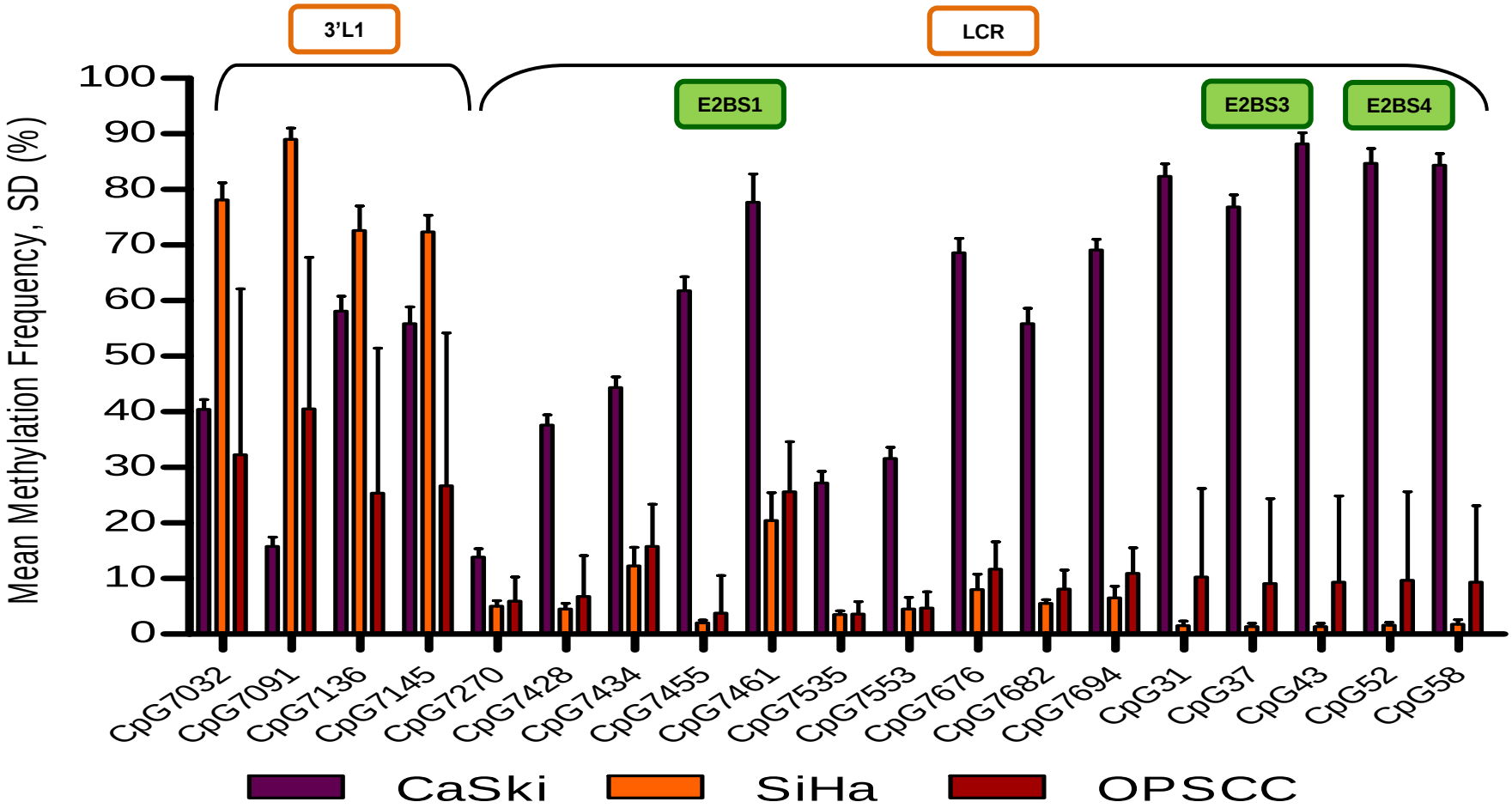

Figure 28 - Methylation pattern in HPV 16 LCR and 3'L1 in clinical samples of OPSCCs, CaSki and SiHa cell lines (cervical cancer). Green boxes indicate the E2BSs.

4.10 HPV 16 methylation frequency in the E2BSs in OPSCCs

Analyzing the methylation in the E2BSs, E2BS1 showed a median methylation frequency equal to 12.0% which was significantly higher than E2BS3 (2.0%, $P<0.0001$) and EBS4 (2.5%, $P<0.0001$) (Fig. 29). There was no difference between E2BS3 and E2BS4 ($P=0.44$).

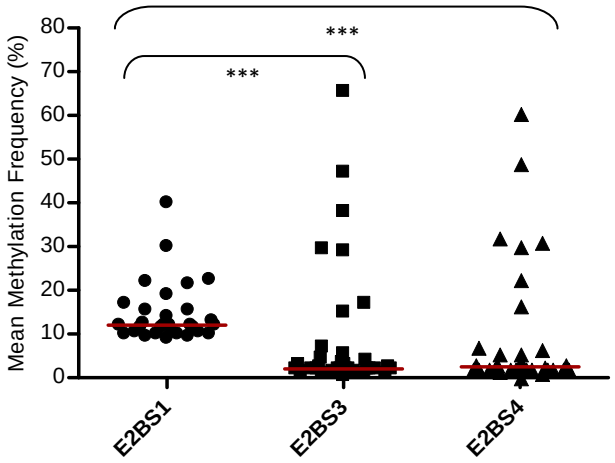

Figure 29 - Methylation frequency in the E2BSs in OPSCCs. Red lines indicate the median value for each group (*=*P*<0.0001, Mann-Whitney test).**

4.11 HPV 16 E6 promoter methylation frequency and clinical/virological data in OPSCC

As we have previously done, we focused the attention again on the E6 promoter region in OPSCCs and we tried to find a correlation with available clinical and virological data.

Concerning the viral physical state, patients with totally integrated viral DNA showed a median methylation frequency equal to 3.0%, mainly integrated 3.0%, mainly episomal 2.0% and totally episomal 2.0% ($P=0.42$; Fig. 30).

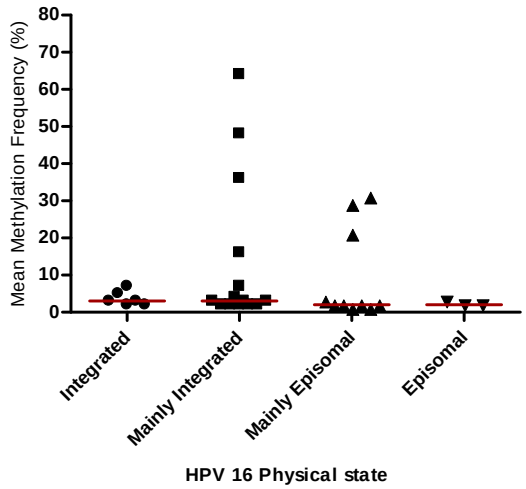

Figure 30 - Relationship between E6 promoter methylation frequency and viral physical state in the E6 promoter region in OPSCCs. Red lines indicate the median value for each group (*P*=0.42 One-way ANOVA, Kruskall-Wallis test).

Analyzing our samples one-by-one, we could observe a group of patients (n 7, 21.2%) with a mean methylation frequency in the E6 promoter ≥10% (Fig. 31). Among these, 4 were T1/2 and 3 T3/4 (*P*=0.47), 1 was at clinical stage 1/2 and 6 clinical stage 3/4 (*P*=1.0), all with high viral load (*P*=0.88); 4 harboured integrated or mainly integrated HPV genome and 3 episomal or mainly episomal viral DNA (*P*=0.14), 5 had a history of tobacco/alcohol use (*P*=0.53) (Fig. 32).

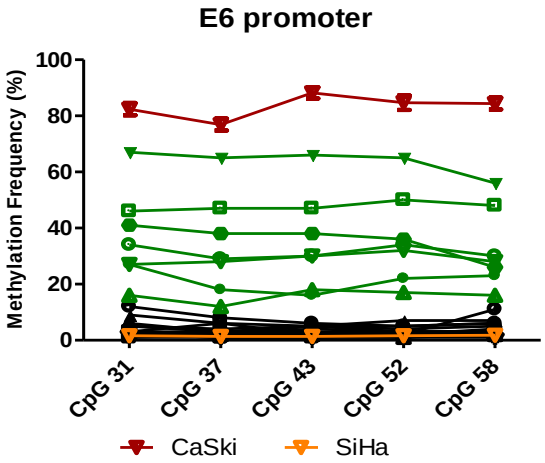

Figure 31 - Methylation frequency in the E6 promoter region: one-by-one analysis of each OPSCCs patient. Green lines indicate patients with mean frequency>10%; black lines indicate patients with mean frequency<10%.

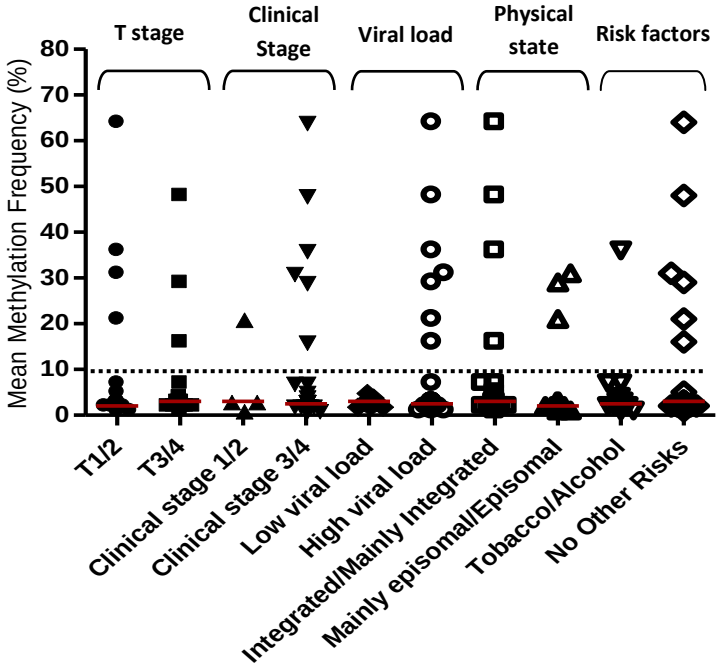

Figure 32 - Methylation frequency in the E6 promoter region in function of clinical and virological data in OPSCCs. Red lines indicate the median value for each group and the black dashed line indicates the cut-off value.

4.12 Viral physical state and methylation as potential prognostic markers for OPSCCs

Since for our patients we could recover data about the follow up, virological data such as HPV DNA presence/absence, viral integration and E6 promoter methylation were analyzed also in function of the disease-free survival (DFS). The median follow-up time for this study was 33 months (2.75 years). As shown by the Kaplan-Meier curves, the DFS% of HPV positive patient was very similar to those HPV negative, even if in the long-term period (at least 5 years) the former group showed a higher proportion (85.66% *vs* 76.09%, log-rank *P* 0.49; Fig. 33A). Stratifying HPV 16 positive patients by viral physical state or viral DNA methylation frequency in the E6 promoter region, the DFS proportion revealed larger differences. Patients harbouring integrated/mainly integrated viral DNA showed the tendency to have a similar prognosis compared to those HPV negative, but worse compared to those harbouring episomal/mainly episomal viral DNA (Fig. 33B). Patients with mean methylation frequency in the E6 promoter region >10% showed the tendency to have a worse prognosis compared to patients with lower methylation frequency or negative for HPV DNA (5-years 68.6% *vs* 82.0% and 76.1%, respectively) (Fig. 33C).

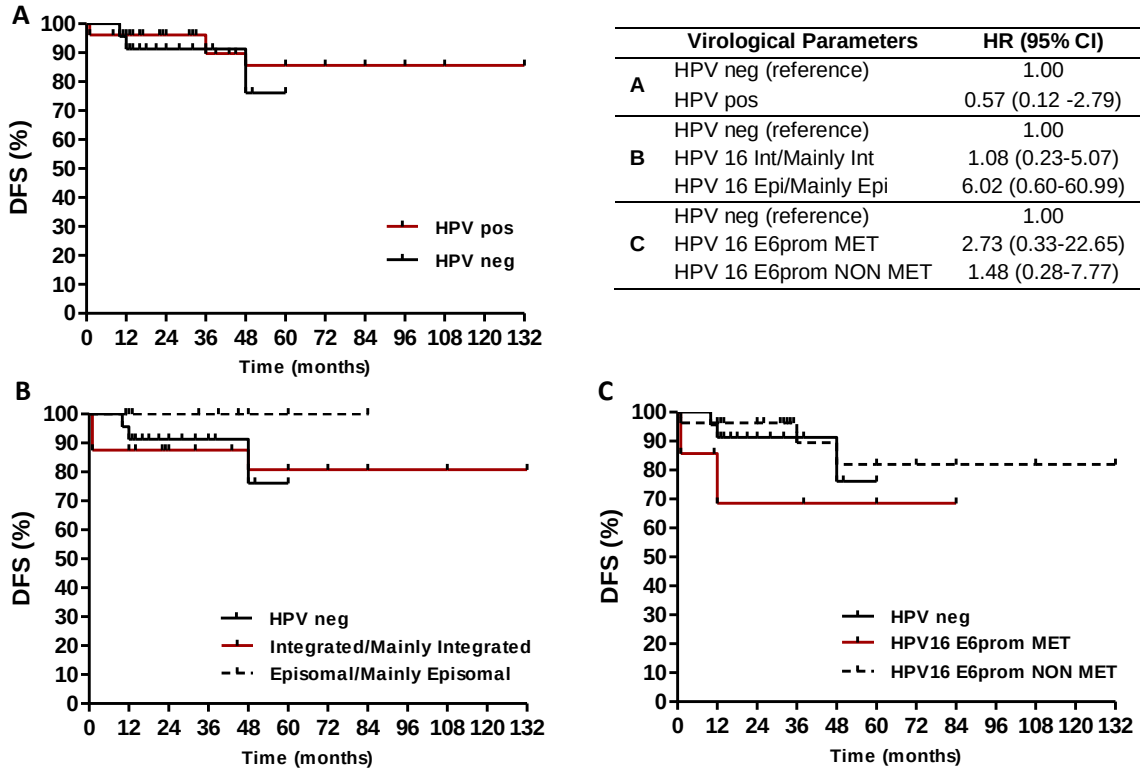

	Virological Parameters	HR (95% CI)	*P*
A	HPV neg (reference)	1.00	
	HPV pos	0.57 (0.12 -2.79)	0.49
B	HPV neg (reference)	1.00	
	HPV 16 Int/Mainly Int	1.08 (0.23-5.07)	0.91
	HPV 16 Epi/Mainly Epi	6.02 (0.60-60.99)	0.13
C	HPV neg (reference)	1.00	
	HPV 16 E6prom MET	2.73 (0.33-22.65)	0.35
	HPV 16 E6prom NON MET	1.48 (0.28-7.77)	0.64

Figure 33 – Kaplan-Meier curves used to evaluate virological parameters as prognostic markers for DFS in OPSCCs. Hazard ratio (HR) and log-rank *P* value (Cox model) for each graph are listed in the table. (A) HPV presence/absence. (B) HPV 16 DNA integration. (C) HPV 16 DNA mean methylation frequency in the E6 promoter region.

<u>PART 3:</u> ANALYSIS OF THE RESPONSE TO IFN-κ TRANSFECTION IN CERVICAL CANCER AND HPV 16-POSITIVE HNSCC

(experiments performed under the supervision of Dr. Bladimiro Rincon Orozco and Prof. Dr. Frank Rösl at the Division of Viral Transformation Mechanisms, Research Program in Infection and Cancer, German Cancer Research Center, Heidelberg, Germany)

4.13 Basal IFN-κ and type I IFNRs expression

First of all, we checked the basal expression level of IFN-κ in our target cells. As we can see in Figure 34A, in cervical cancer cell lines, we could detect IFN-κ mRNA only in CaSki (reference cell line in this analysis), but not in SiHa and HeLa. Among HNSCCs, SCC25 and UDSCC2 cells showed a significantly lower level compared to CaSki (Fc 0.13 ± 0.07, P=0.0007; Fc 0.05 ± 0.01, P<0.0001, respectively), but Cal27 and 93V4 cells were negative. On the other hand, immortalized keratinocytes expressing only the viral oncoprotein E7 showed the highest IFN-κ basal expression level (Fc 311.6 ± 40.5, P<0.002).

Concerning type I IFNRs expression, SiHa cells were taken as reference (Fig. 34B). Cal27 cells showed similar expression of IFNR1 (Fc 1.11 ± 0.34), followed by CaSki (0.80 ± 0.01, P=0.009), 93V4 (0.56 ± 0.003, P=0.0005), SCC25 (0.48 ± 0.06, P=0.002), HeLa (0.40 ±0.03, P=0.0003) and UDSCC2 (0.30 ± 0.003, P<0.0001) having lower levels. For IFNR2, SCC25 showed significantly higher levels than SiHa (1.72 ± 0.005, P=0.002), in contrast to CaSki (0.31 ±0.08, P=0.002), HeLa (0.45 ±0.04, P=0.001), 93V4 (0.93 ±0.06), UDSCC2 (0.22 ±0.05, P=0.002) and Cal27 (0.20 ±0.06, P=0.002) which showed lower levels.

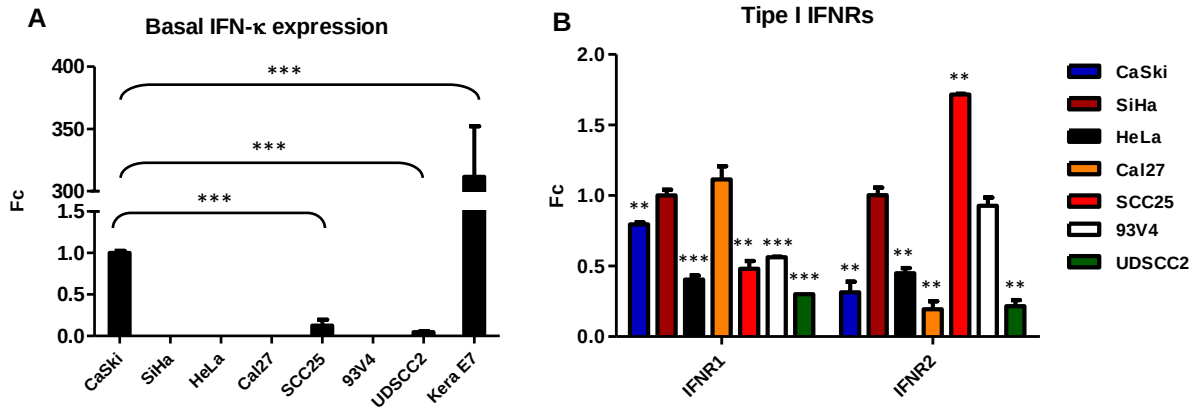

Figure 34 – Characterization of target cell lines for IFN-κ (A, CaSki cells were taken as reference) and type I IFNRs (B, SiHa cells were taken as reference) expression.

4.14 Effects of recombinant IFN-κ transfection and IFN-β/ IFN-γ treatment

In order to check the correct transfection of our recombinant IFN-κ, we tested cells for mRNA expression after 24h by classic RT-PCR. As we can see in Figure 35A, all the cells

transfected with the empty vector (mock) retained the basal IFN-κ expression level; on the other hand, cells transfected with the recombinant molecule showed an increase of expression. These results have been confirmed also at the protein level (Fig. 35B).

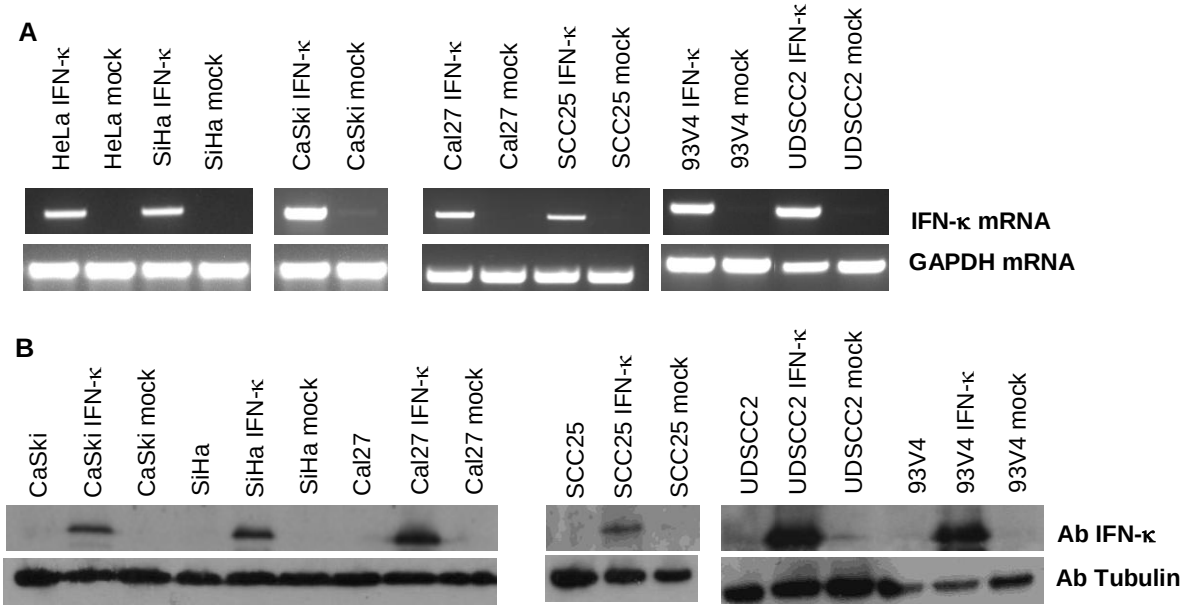

Figure 35 – Checking IFN-κ transfections in cervical cancer and HNSCCs cell lines by mRNA analysis (A) and Western Blot (B).

4.14.1 MHC class I proteins and immunoproteasome

In order to determine whether IFN-κ transfection influences the expression level of genes involved in MHC class I pathway and immunoproteasome, the same samples were analyzed by qPCR. We could observe a general increase in transcription of proteins involved in immunoproteasome and class I antigen presentation pathway in CaSki and SiHa, but not in HeLa (Fig. 36). In particular, the Fc for LMP7 was significantly higher in SiHa IFN-κ compared to the mock (3.31 ± 0.74 *vs* 0.78 ± 0.11, P=0.007); for LMP2 and MECL-1 the increase was significant in both CaSki IFN-κ (5.07 ± 0.83 *vs* 2.33 ± 0.40, P=0.01; 2.55 ± 0.01 *vs* 2.04 ± 0.07, P=0.01) and SiHa IFN-κ (3.09 ± 0.57 *vs* 0.58 ± 0.70, P=0.002; 7.05 ± 0.16 *vs* 3.16 ± 0.67, P<0.0001). Considering the MHC class I genes, the Fc for TAP1 and TAP2 was significantly higher only in SiHa IFN-κ compared to the mock (2.95 ± 0.49 *vs* 0.48 ± 0.11, P=0.0005 and 5.19 ± 0.25 *vs* 0.34 ± 0.01, P<0.0001, respectively); on the other hands, transcription of HLA genes was higher in both CaSki IFN-κ (HLA-A 2.88 ± 0.07 *vs* 1.49 ± 0.01, P<0.0001; HLA-B 3.06 ± 0.37 *vs* 1.34 ± 0.07, P=0.001; HLA-C 3.01 ± 0.07 vs 1.37 ±

0.01, *P*<0.0001) and SiHa IFN-κ (HLA-A 2.50 ± 0.23 *vs* 0.98 ± 0.02, *P*=0.003; HLA-B 2.17 ± 0.40 *vs* 0.85 ± 0.05, *P*=0.009; HLA-C 3.32 ± 0.23 *vs* 1.16 ± 0.03, *P*=0.0007) (Fig. 37). Under IFN-β or IFN-γ treatment we could observe the same tendency for CaSki and SiHa, but we detected a response also in HeLa, even if weaker compared to the other cells. For example, in SiHa IFN-β or SiHa IFN-γ, immunoproteasome proteins were up-regulated up to 8-times or 18-times, TAP heterodimer up to 10-times or 36-times and HLA genes up to 6-times or 8-times, respectively.

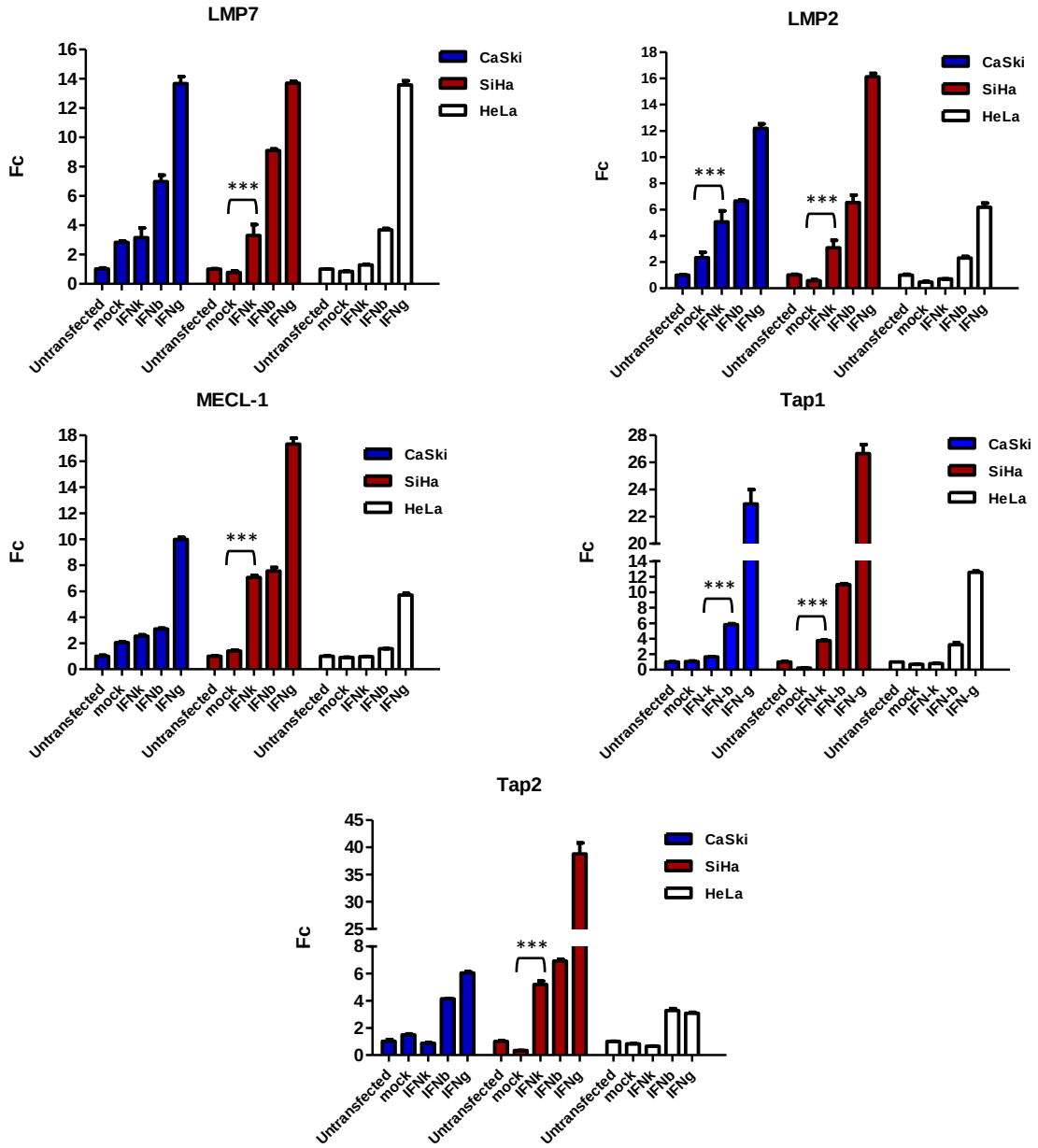

Figure 36 – RT-qPCR analysis for genes involved in immunoproteasome and TAP complex in cervical cancer cell lines transfected with IFN-κ/mock or treated with 1000 units of IFN-β or IFN-γ.

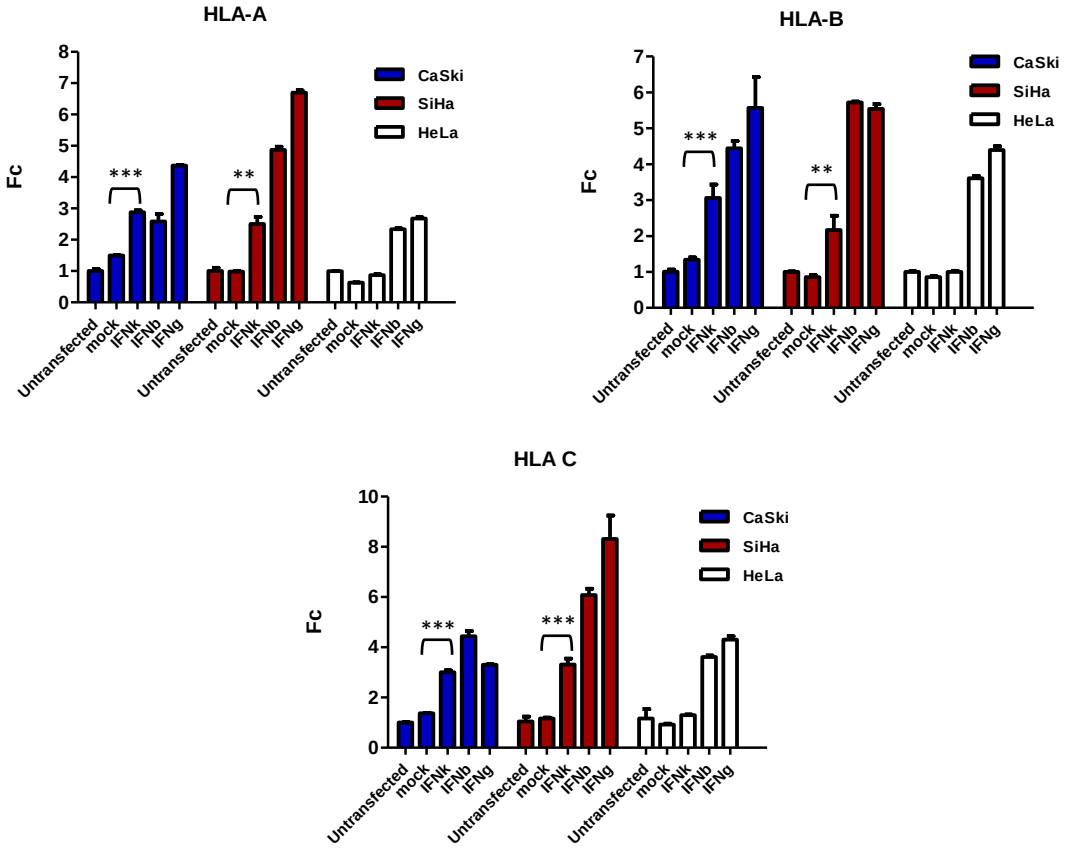

Figure 37 – RT-qPCR analysis for genes involved in MHC class I antigen presentation pathway in cervical cancer cell lines transfected with IFN-κ/mock or treated with 1000 units of IFN-β or IFN-γ.

Considering HPV 16-positive HNSCCs, after IFN-κ transfection in Cal27 and SCC25 we observed a significant increase in expression of LMP7 (3.39 ± 0.33 *vs* 1.40 ± 0.14, *P*=0.005; 2.69 ± 0.16 *vs* 1.67 ± 0.10, *P*=0.006, respectively) and LMP2 (3.59± 0.03 *vs* 1.87 ± 0.05, *P*<0.0001; 3.08 ± 0.10 *vs* 1.35 ± 0.03, *P*<0.0001, respectively), compared to the mock transfected or naive cells, but we could not observe the same effect in 93V4 (LMP7 1.52 ± 0.10 *vs* 1.58 ± 0.21; LMP2 1.00 ± 0.01 *vs* 0.89 ± 0.05) or UDSCC2 (LMP7 0.99 ± 0.03 *vs* 0.82 ± 0.01; LMP2 0.45 ± 0.01 *vs* 0.56 ± 0.01) cells (Fig. 38). The Fc was higher only in Cal27 and SCC25 also for TAP1 (3.25 ± 0.08 *vs* 1.5 ± 0.13, *P*=0.0003; 5.75 ± 0.45 *vs* 1.27 ± 0.18, *P*=0.003, respectively). HLA-B was up regulated only in SCC25 (2.28 ± 0.30 *vs* 1.10 ± 0.11, *P*=0.021).

On the other hands, after IFN-β or IFN-γ treatment, all the four cell lines responded with a significant increase in immunoproteasome, TAP1 and HLA-B expression.

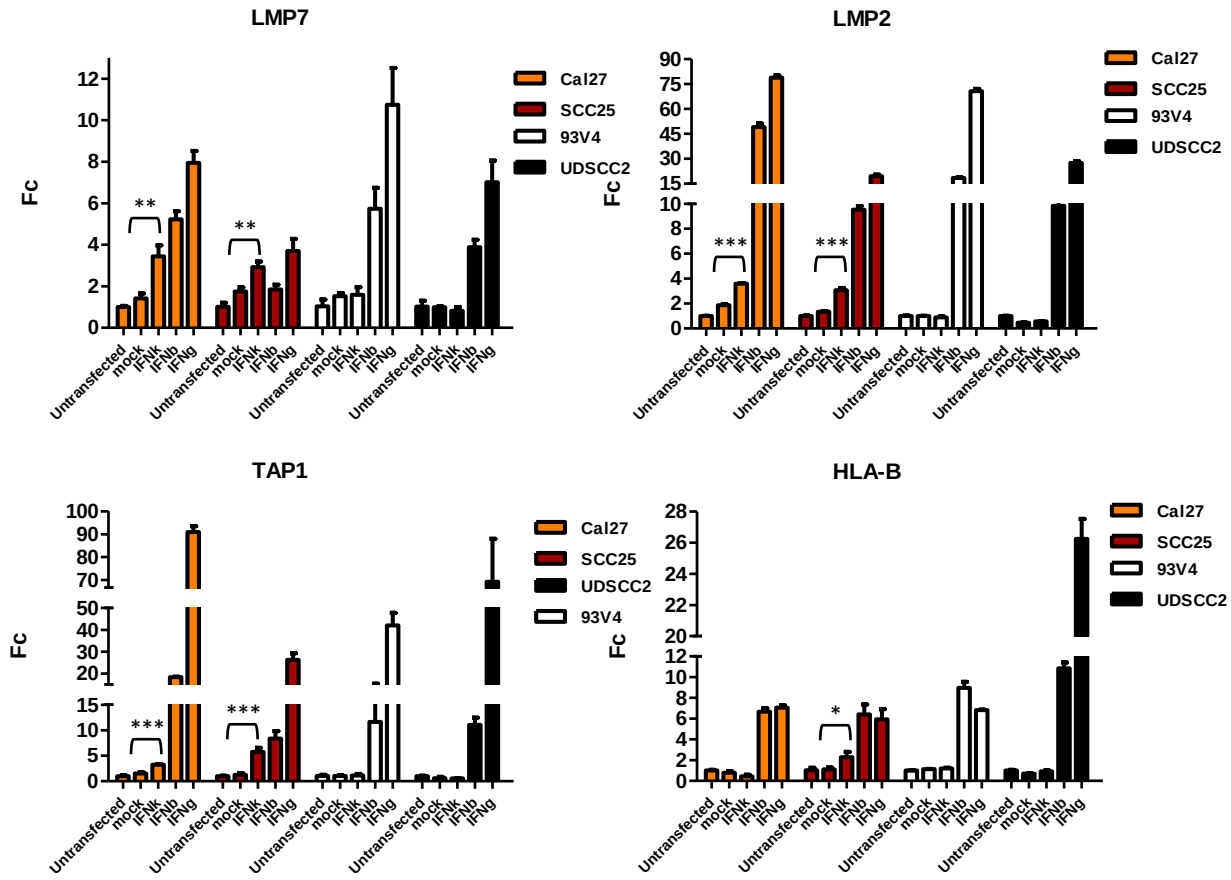

Figure 38 – RT-qPCR analysis for genes involved in immunoproteasome and MCH class I antigen presentation pathway in HPV-positive HNSCCs transfected with IFN-κ/mock or treated with 1000 units of IFN-β or IFN-γ.

4.14.2 Antiviral Response

The same analysis described in §4.14.1 was performed targeting ISGs (Fig. 39A). In particular, the Fc for OAS1, MX1, IRF7 and PKR was significantly higher in both CaSki IFN-κ (126.3 ± 7.2 *vs* 12.22 ± 3.1, *P*<0.0001; 293.0 ± 9.97 *vs* 5.12 ± 0.68, *P*<0.0001; 12.63 ± 0.91 *vs* 2.96 ± 0.78, *P*=0.0007; 4.10 ± 0.17 *vs* 1.27 ± 0.09, *P*=0.0001, respectively) and SiHa IFN-κ (27.18 ± 7.42 *vs* 1.13 ± 0.15, *P*=0.006; 61.56 ± 5.62 *vs* 2.15 ± 0.23, *P*<0.005; 5.42 ± 0.39 *vs* 0.55 ± 0.14, *P*<0.0001; 6.46 ± 0.33 *vs* 1.92 ± 0.05, *P*=0.0002, respectively) compared to the mock. The results concerning MX1 expression were confirmed also at the protein level for both CaSki and SiHa (Fig. 39B). Also IRF9 showed an increase in transcription level in both CaSki IFN-κ (5.33 ± 0.22 *vs* 1.80 ± 0.36, *P*<0.0001) and SiHa IFN-κ (1.76 ± 0.20 *vs* 0.60 ± 0.03, *P*=0.0002). Once again, we could not observe an increase in antiviral response in HeLa cells transfected with IFN-κ.

After treatment with other IFNs, the highest response was observed under IFN-β treatment rather than IFN-γ. Briefly, OAS1 and MX1 transcription was increased between 200- and 450-times in CaSki IFN-β and between 10- and 20-times in CaSki IFN-γ. Considering IRF7 and PKR, transcription was increased between 18- and 9-times in CaSki IFN-β and between 3- and 4-times in CaSki IFN-γ.

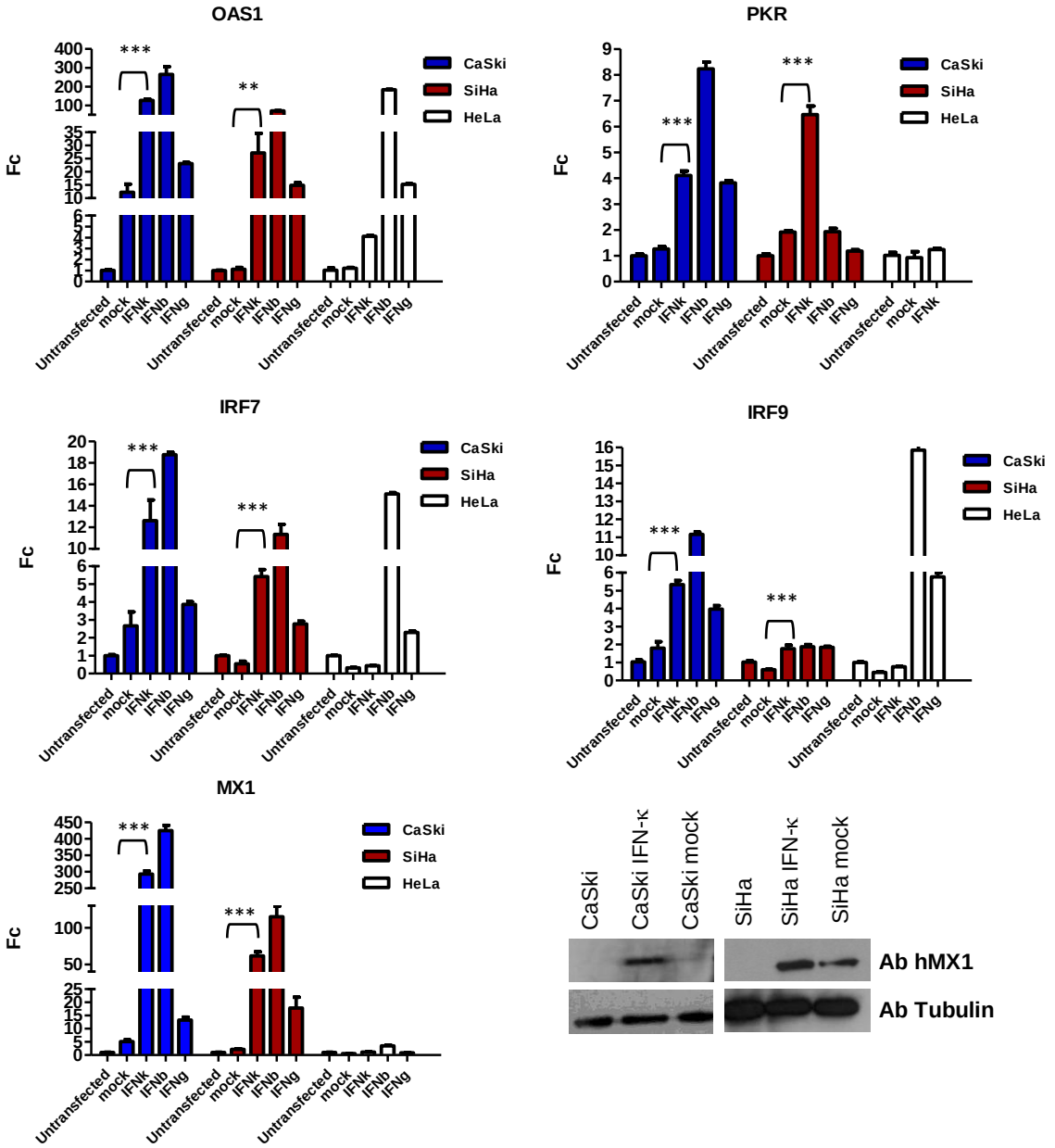

Figure 39 – RT-qPCR analysis for ISGs in cervical cancer cell lines transfected with IFN-κ/mock or treated with 1000 units of IFN-β or IFN-γ (A). Western blot for hMX1 in CaSki and SiHa (B).

Considering HPV 16-positive HNSCCs, after IFN-κ transfection we observed a significant increase in OAS1 expression in all the four cell lines (Cal27 11.38 ± 0.40 *vs* 2.03 ± 0.20, *P*=0.002; SCC25 26.81 ± 1.98 *vs* 2.83 ± 0.11, *P*=0.0003; 93V4 1.80 ± 0.08 *vs* 0.89 ± 0.01, *P*=0.0004; UDSCC2 2.40 ± 0.12 *vs* 1.26 ± 0.05, *P*=0.0009) (Fig. 40). On the other hand, IRF7 expression was increased only in Cal27 (2.44 ± 0.05 *vs* 0.46 ± 0.02, *P*<0.0001) and SCC25 (13.47 ± 0.77 *vs* 1.61 ± 0.07, *P*=0.0001). Once again, under IFN-β or IFN-γ treatment, all the four cell lines responded with a significant increase in genes involved in the antiviral response, with a higher effect after IFN-β treatment.

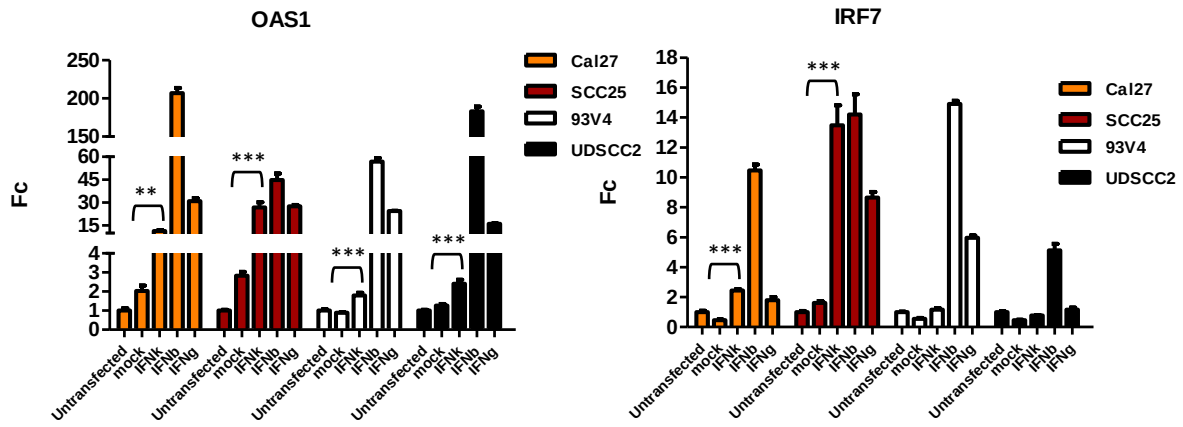

Figure 40 – RT-qPCR analysis for some ISGs in HPV-positive HNSCCs transfected with IFN-κ/mock or treated with 1000 units of IFN-β or IFN-γ.

4.14.3 IFN-β expression

Since most of these genes are induced also upon IFN-β stimulation, we decided to check IFN-β expression level in IFN-κ/mock transfected cells. As reported in Figure 41, IFN-β expression was increased in all the IFN-κ transfected cell lines analyzed in this study, but in HeLa. In particular, CaSki IFN-κ showed the highest up regulation (342.9 ± 11.49 *vs* 14.58 ± 1.53, *P*<0.0001) followed by SiHa IFN-κ (53.39 ± 0.62 *vs* 1.29 ± 0.29, *P*<0.0001), SCC25 IFN-κ (25.91 ± 3.53 *vs* 1.13 ± 0.09 *P*=0.002), Cal27 IFN-κ (7.95 ± 0.80 *vs* 0.87 ± 0.03, *P*=0.0009), UDSCC2 IFN-κ (4.99 ± 0.91 *vs* 3.13 ± 0.29) and 93V4 IFN-κ (2.43 ± 0.10 *vs* 0.64 ± 0.13, *P*=0.0005).

These results were also confirmed in cervical cancer by the antiviral activity assay performed using the supernatants collected from the same transfected cells (Fig. 42). Both the supernatants belonging to CaSki and SiHa transfected with IFN-κ showed a significantly higher protection against EMCV infection in A459 cells up to 1/16 dilution compared to

supernatants from mock transfected cells. On the other hands, supernatant from HeLa transfected with IFN-κ did not show any antiviral activity.

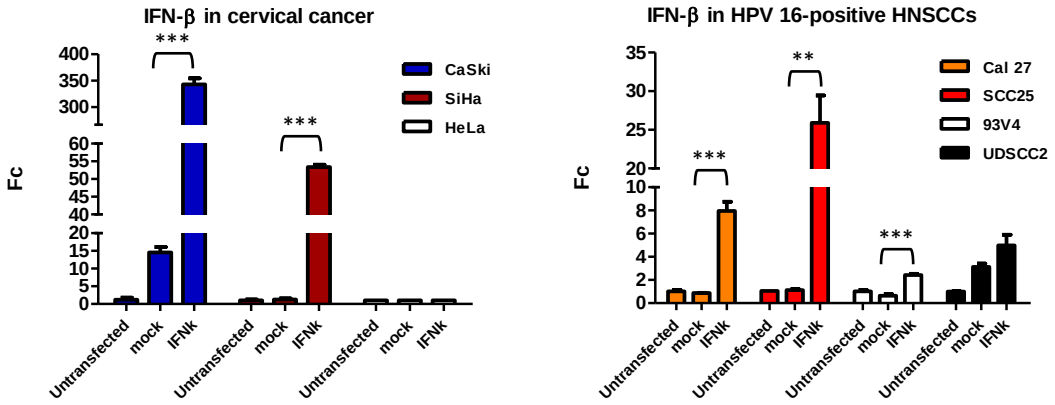

Figure 41 – IFN-β expression in cells transfected with IFN-κ or empty vector.

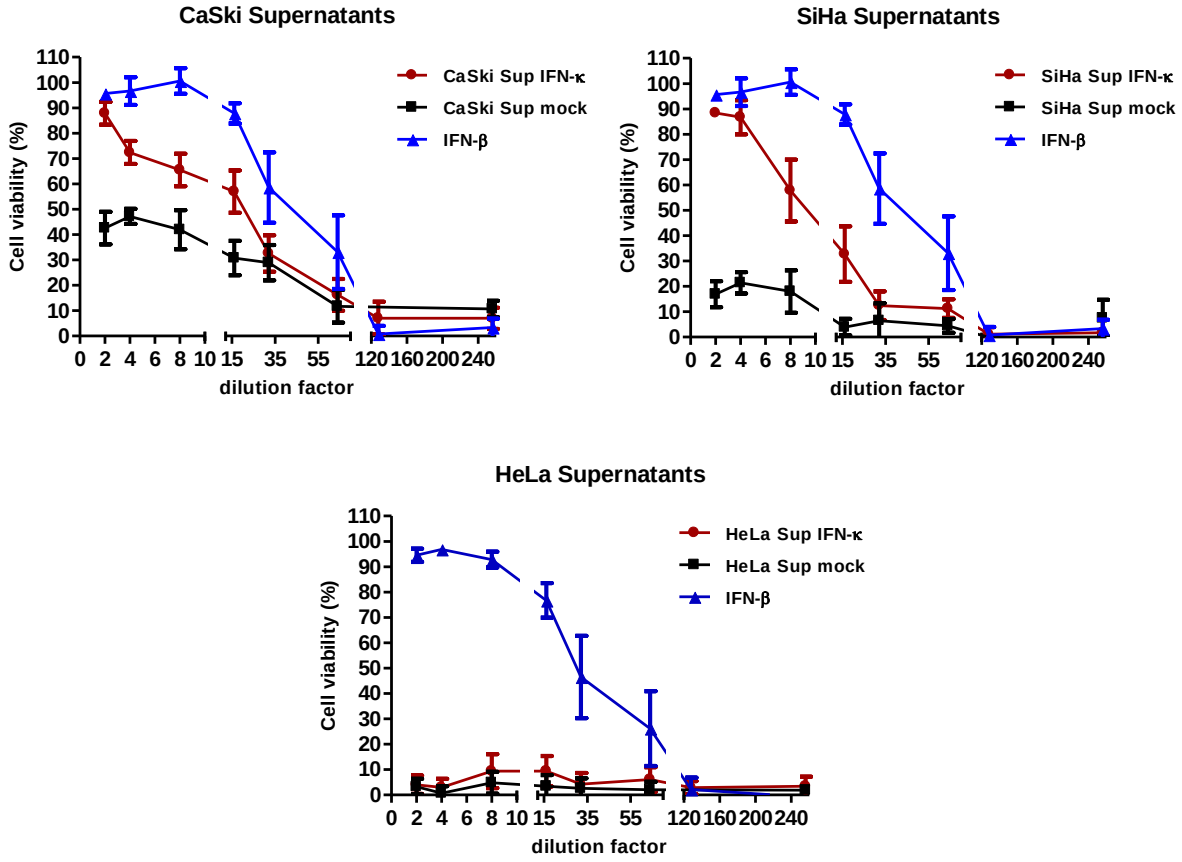

Figure 42 – Antiviral activity assay performed with supernatants collected from cells transfected with IFN-κ or empty vector.

4.14.4 NLRC5 expression

Concerning NLRC5 expression, which is a transactivator of MHC class I genes, we observed the higest increase after IFN-κ transfection compared to untransfected cells in CaSki (4.92 ± 0.12 *vs* 1.00 ± 0.03, *P*<0.0001) followed by SCC25 (2.59 ± 0.04 *vs* 1.00 ± 0.02, *P*<0.0001) and Cal27 (1.34 ± 0.05 *vs* 1.00 ± 0.05, *P*=0.0085), but we could not observe an increase in SiHa, 93V4 and UDSCC2 (Fig. 43).

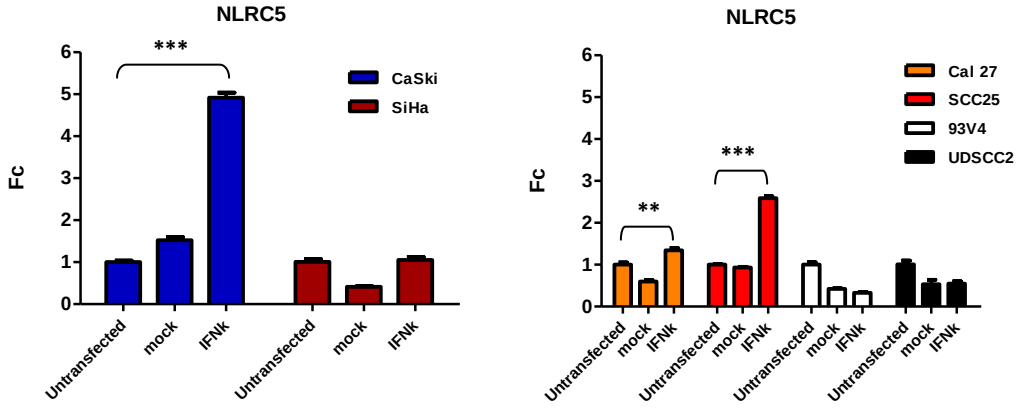

Figure 43 – NLRC5 expression in cells transfected with IFN-κ or empty vector.

4.15 Effects of long-term IFN-κ transfection: proliferation and IFN-β expression

In order to check the effect of IFN-κ transfection on cell cycle regulation, we first performed, for each cell line, the proliferation assay as previously described. We could observe a decrease in cells proliferation for SiHa IFN-κ compared to the mock (PI 3.07 ± 0.09 *vs* 3.78 ± 0.25, *P*=0.02, respectively) and CaSki IFN-κ, even if not significant (PI 3.62 ± 0.04 *vs* 3.90 ± 0.22, respectively) (Fig. 44A). Moreover, analyzing the expression level of some proteins involved in cell cycle regulation such as Cyclin E1, CDK2 and Cyclin D1, after 1 or 6 days IFN-κ transfection in SiHa cells we observed a progressive decrease in all the proteins even if with some differences (Fig. 44B). In particular, CDK2 and Cyclin D1 decreased after 6 days compared to 1 day in both IFN-κ and mock transfected, but the decrease is more pronounced in the presence of IFN-κ (0.19 ± 0.01 *vs* 0.23 ± 0.01, *P*=0.014; 0.30 ± 0.04 *vs* 0.68 ± 0.07, *P*=0.009, respectively). Results were confirmed at the protein level for Cyclin D1 (Fig. 44C). Moreover, SiHa cells also showed a significant decrease in IFN-β expression after 6 days from IFN-κ transfection compared to 1 day (4.33 ± 0.10 *vs* 53.39 ± 0.62, *P*<0.0001) (Fig. 45D). This result matches with expression levels of proteins involved in immunoproteasome,

antiviral response and MHC class I antigen presentation after 6 days IFN-κ transfection which were not as high as after 1 day (data not shown).

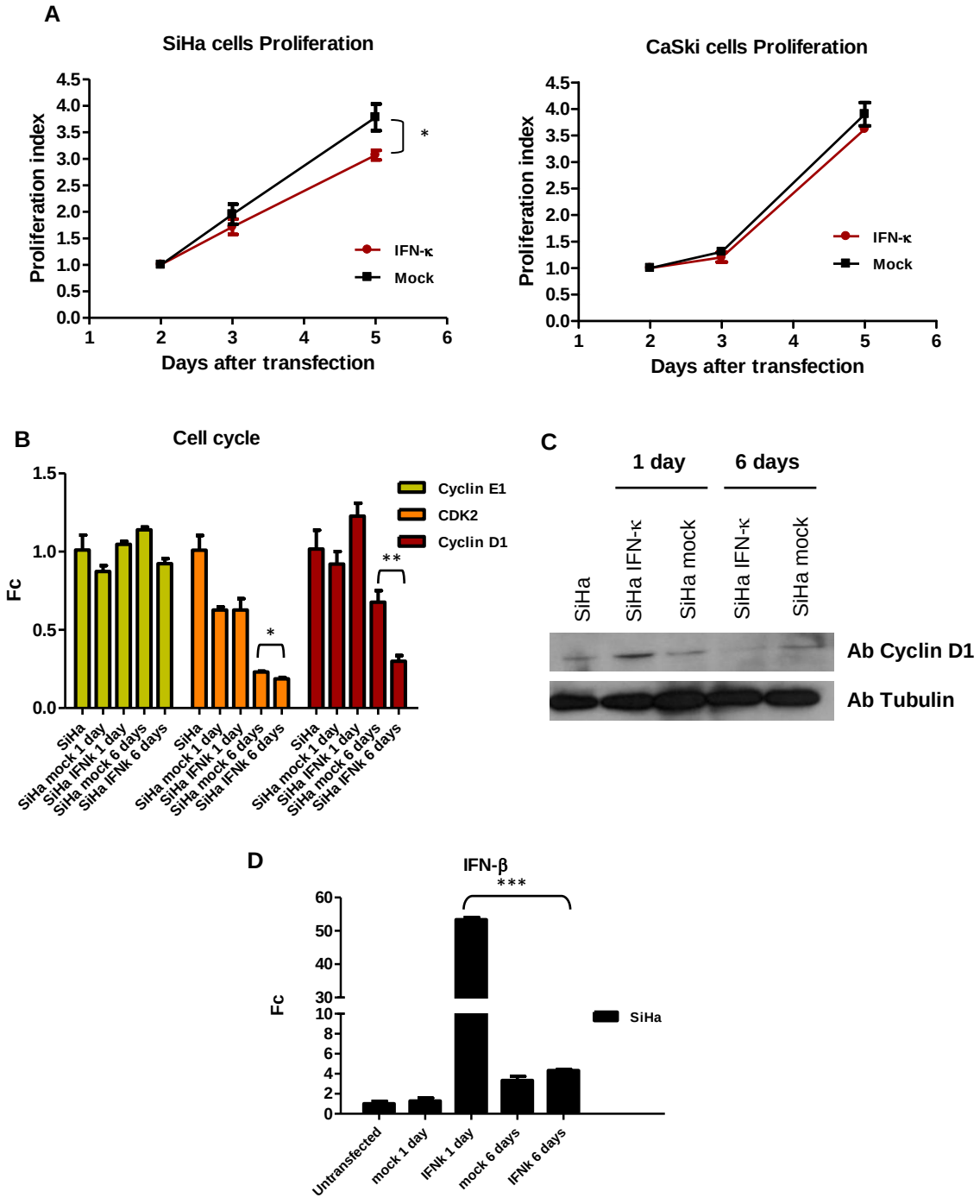

Figure 44 – Effect of the long-term IFN-κ/mock transfection (6 days) in cervical cancer cell lines on cell cycle. (A) Proliferation assay for SiHa and CaSki. (B) RT-qPCR analysis of proteins involved in cell cycle regulation in SiHa. (C) Western blot for Cyclin D1 expression in SiHa. (D) IFN-β expression in SiHa.

5. Discussion

PART 1: COMPARISON OF HPV SIGN GENOTYPING TEST WITH INNO-LIPA HPV GENOTYPING EXTRA ASSAY ON HISTOLOGIC AND CYTOLOGIC CERVICAL SPECIMENS (Barbieri et al, 2012)

An accurate tool for HPV typing is important for management of patients with HPV infection and studies which analyze benefits and limitations of different commercially available methods are very useful. In this study we compared for the first time the new HPV sign® Genotyping Test and the INNO-LiPA HPV Genotyping Extra assay.

We found a substantial agreement between the assays (85.1%, *k* 0.66) for HPV detection in clinical samples, even if it became moderate considering only cytological swabs rather than biopsies (83.0%, *k* 0.54 and 88.2%, *k* 0.76, respectively). The overall concordance for single/multiple infection detection was poor (60.4%, *k* 0.07), but this is a problem which other groups have handled yet working with sequencing methods (Barzon et al, 2012; Didelot-Rousseau et al, 2006; Gharizadeh et al, 2003; Gharizadeh et al, 2001; Gharizadeh et al, 2005; Zubach et al, 2012). For this reason, Gharizadeh developed a multiple-primer DNA-sequencing method, which helped to improve HPV co-infection detection by sequencing-based techniques (Gharizadeh et al, 2003). Moreover, many authors have reported that the INNO-LiPA system detects more multiple infections than other PCR based assays (Perrons et al, 2005; van Doorn et al, 2002). However, 14 (73.6%) of 19 INNO-LiPA multiple infections which were found as single infections by HPV sign agreed for the most clinically relevant genotype. Consequently, clinical decisions for the management of these patients, based on precancer and cancer risk, are in complete agreement.

The overall genotype-specific agreement was good for both biopsies (94.1%) and cytologic swabs (96.0%). The agreement levels for individual HPV genotypes targeted by both methods ranged from 88.2% to 97.1% for biopsies and from 88.7% to 100% for cytologic samples. Although overall agreement rates for the detection of 28 HPV types are >90%, it is clear that this is driven by the agreement of HPV-negative specimens, as shown through the high proportion of negative agreement rates (*Pneg* > 0.913 for all genotypes and sample types).

The observed lower proportion of positive agreement rates for both cytologic samples (*Ppos* 0.511) and biopsies (*Ppos* 0.750) indicate that there are discrepancies in the 2 assays' abilities to detect type-specific HPV positives, suggesting differences in assay sensitivity in different samples. It is important to note that HPV 40, 52, 53, 66, 74, and 82, detected by INNO-LiPA in 20.7% of all samples, were never detected by HPV sign. On the other hand, one HPV 73 was detected only by HPV sign.

In order to resolve these relevant discrepancies, to further analyze the performance of each genotyping assay and to define the sensitivity and specificity of each assay, a consensus genotype was defined for each discordant sample after resolution with 9 type-specific qRT PCRs. Interestingly, after the analysis of 30 discrepant samples, we assessed that INNO-LiPA was concordant with genotype-specific qRT PCRs in 30.0% of the cases and HPV sign in 56.6%.

The overall specificity of HPV sign was excellent (100%), and the INNO-LiPA overall specificity was good (97.1%). Two INNO-LiPA negative samples were positive for the HPV 16 African type 2 variant by HPV sign, suggesting a difficulty of the INNO-LiPA assay to detect viral intratype variants, which sometimes have an increased oncogenicity when compared to the main type (Lichtig et al, 2006; Sichero et al, 2012). Another problem that affects hybridization-based techniques is the cross-reactivity between assay probes and intratype variants or non-detectable genotypes. For example, in 1 sample, INNO-LiPA detected HPV 52 as a single infection, which was not confirmed by genotype-specific qRT-PCR, and HPV sign detected HPV 91, with a sequence match of 100%. It is well established that the SPF10 primer set is much more sensitive for HPV 52 detection than the GP5+/GP6+ primer set (van Doorn et al, 2002); in our case, all 4 HPV 52 infections detected by INNO-LiPA were negative by HPV sign and, surprisingly, genotype-specific real-time PCR confirmed the absence of HPV 52 DNA. Furthermore, the 50% (2/4) of the HPV 53 and the 40% (2/5) of HPV 66 infections revealed by the INNO-LiPA test were not detected by the specific qRT PCRs. On the other hand, the overall sensitivity was better for INNO-LiPA than for HPV sign (84.5% versus 76.3%), but HPV 16 infections, associated with higher absolute risks for progression to high-grade cervical lesions, were better detected by HPV sign (HPV sign sensitivity 90.0% [CI 0.79–1.01] versus INNO-LiPA sensitivity 83.3% [CI 0.70–0.97]). Furthermore, we observed that INNO-LiPA missed HPV 16 in precancerous lesions (n 3) and cervical carcinoma (n 2), but HPV sign missed it only in precancerous lesions (n 3).

The inability to detect some HPV genotypes by HPV sign may be due to the different DNA extraction protocols for cytologic samples, as recommended by the manufacturers: an initial sample volume of 4 mL of PreservCyt medium is needed for HPV sign compared to only 200 μL for INNO-LiPA, as was done in our work protocol. Because of the extraction method utilized, it may not be possible to obtain, in some samples, the number of copies of viral DNA for the optimal execution of the HPV sign test. Moreover, the current study performed the assay comparison by testing archival DNA extracted from biopsies and swabs stored at −80°C. Nevertheless, the storage of extracted DNA can degrade the viral nucleic acid and then reduce HPV detection by HPV sign.

To confirm this hypothesis with experimental evidence, we analyzed the viral load of HPV sign false-negative samples and we observed viral load values very close to or lower than 200 copies/reaction, which is the value correspondent to the limit of detection of the technique. Probably, using an initial sample volume of 4 ml of PreservCyt medium and fresh DNA extract by biopsies and swabs should improve the sensitivity of HPV sign.

In conclusion, HPV sign was similar in performance to the INNO-LiPA HPV Genotyping assay and it can be used for the detection of clinically relevant HPV genotypes. On the other hand, HPV sign has potential advantages in detecting subtypes and variants, the high specificity of a sequencing method, and a broad spectrum of detectable HPV types.

PART 2: VIROLOGICAL MARKERS IN HPV-ASSOCIATED CERVICAL ADENOCARCINOMA AND OROPHARYNGEAL CARCINOMA

5.1 Cervical AdCa

5.1.1 HPV genotyping as primary virological marker for risk of cervical AdCa development

As it has been previously described, cervical AdCa are rare compared to classic SCC, but less studied, more aggressive and frequent in young women who want to preserve their fertility. Moreover, their incidence increased during the last 20 years and it has been shown that the HPV DNA-test is more significant than Pap-test for assessing disease progression during the follow up of women conservatively treated for cervical AdCa (Costa et al., 2012).

In our population, HPV prevalence was 92.4% (77.7% single infections), in line with data published in literature (Castellsague et al, 2006; Li et al, 2011; Seoud et al, 2011). In fact, when 8 case-control studies from different countries worldwide (167 cases) were analyzed by Castellsagué and colleagues, the overall HPV prevalence was 93.0% (89.0% single infections). Concordance was found also for the genotype-specific prevalence, since HPV 16 was confirmed the most prevalent genotype (66.9%) (de Sanjose et al, 2010; Tornesello et al, 2011). However, HPV 18 and 45 showed a higher prevalence in cervical AdCa compared to SCC (34.7% *vs* 13.2% and 8.3% *vs* 4.4%, respectively), confirming these genotypes being more associated to AdCa development (data on SCC from (Li et al, 2011). Interestingly, we also noted a tendency for HPV 18-infected patients (single infection) to be younger than the overall median age or those infected by HPV 16 alone. This is consistent with results published by de Sanjose and colleagues and highlights the shorter time-for-progression to AdCa of HPV 18 cervical infections.

Considering the two major histological types, we could observe a significant association between HPV 16 and invasive AdCa rather than AIS (75.3% *vs* 52.3%, respectively, P=0.01). On the other hands, HPV 18 and 45 showed only a tendency to be more associated to AIS than invasive AdCa (38.6% *vs* 32.5% and 9.1% *vs* 7.8%, respectively). Our data are in contrast with those obtained by Tawfik El-Mansi and colleagues in Scottish patients, who did not note a significant relation between infecting HPV types and tumour invasion (Tawfik El-Mansi et al, 2006). However, it is well known that geographic variations can influence genotype-specific prevalence and associations.

Taken together, these results confirm the key role of HPV also in cervical AdCa development, with some little differences in genotype-specific prevalence compared to SCC and age-at-diagnosis which have to be considered by clinicians when the HPV DNA test is performed on women with positive Pap-test smear. Moreover, since in our population most of the infections were caused by HPV 16 and/or 18 alone (81.8%), the current HPV vaccination campaign implemented by the Italian National Health Service from 2008 in the Emilia-Romagna region can strongly contribute to the decrease not only of SCC but also of cervical AdCa.

The presence of HPV DNA or genotyping alone can inform the gynaecologist about the risk of cervical cancer development, but cannot distinguish between transient/productive and persistent/transforming infection or predict tumour grade, clinical stage, volume, invasion, lymph node involvement or prognosis when cancer has developed yet. For this reason, we decided to study other virological parameters, such as viral oncoprotein expression, viral load, physical state and DNA methylation, to improve the diagnosis of cervical AdCa.

5.1.2 Viral load and physical state seems not to be suitable as diagnostic marker

The presence of E6/E7 mRNA, that we could detect in all our HPV-positive samples, confirms viral activity and capability to produce its oncoproteins, but the association between viral load or integration and the different phases of the disease is still debated. Several authors have shown that high HPV16 viral load is associated with HSIL and increased risk of cancer development (Cricca et al, 2007; Gravitt et al, 2007). However, a longitudinal study published in 2010 showed that a single measurement of viral load made at an indeterminate point during the natural history of HPV infection, does not reliably predict the risk of acquiring cervical neoplasia (Constandinou-Williams et al, 2010). In our study we could detect not only high viral loads but also values $<10^6$ copies/300 ng HGD in 38.9% of HPV 16- and 68.3% of HPV 18-positive samples. Since we did not consider precancerous lesions but only cancers, our results agreed with Cricca and colleagues, who found viral loads lower in SCC than CIN3 lesions.

Concerning the viral physical state, during the last 30 years viral genome integration in cellular genome was considered the fundamental event for E6/E7 overexpression and cancer development. However, many studies reported HPV DNA in totally episomal form not only in precancerous lesions, but also in *in situ* or invasive carcinomas (Arias-Pulido et al, 2006). Our analysis agreed with data published in the mentioned article, confirming the presence of totally episomal DNA also in glandular cancerous lesions (about 34.0%). Moreover, the

percentage of samples harbouring totally or mainly integrated HPV 16 DNA was found to be higher in invasive AdCa compared to AIS (34.0% *vs* 28.6%). However, the same result was not observed for HPV 18 DNA.

Observing these results, we may consider HPV 16 integration as marker of cervical cancer progression in SCC as well as in AdCa and support the hypothesis that viral integration is an important but secondary event in carcinogenesis, being rather a consequence of the genomic instability due to viral oncoprotein overexpression (Matovina et al, 2009). However, since it is very difficult to know how many effectively infected cells are present in a clinical samples (contrary to established cell lines) and techniques available to assess both viral load and viral physical state are difficult to standardize, we may say that these virological parameters are not so suitable in clinical practice as diagnostic marker for early disease/prognosis of cervical SCC and AdCa.

5.1.3 Methylation frequency of the early promoter as suitable marker of invasion in cervical AdCa

The key mechanism involved in E6/E7 transcriptional deregulation and HPV-mediated carcinogenesis in SCC seems to be CpG methylation, in particular at sites encompassing the LCR. In fact, a differential methylation of the HPV 16 LCR during epithelial differentiation and neoplastic transformation has been previously reported, suggesting that a shift in viral methylome may be the switch from a permissive to a transforming infection (Vinokurova & von Knebel Doeberitz, 2011). Moreover, for clinical purposes, evaluating the methylation status at specific sites, as opposed to a more global genomic assessment, may yield more valuable and predictive information regarding cancer progression.

Many studies have been performed dealing with HPV 16 DNA methylation in cell lines and clinical samples, but most of them are focused on SCC with small size populations and not-quantitative methods, leading to conflicting and difficult to interpret results (Badal et al, 2003; Brandsma et al, 2009; Chaiwongkot et al, 2012; Clarke et al, 2012; Ding et al, 2009; Hong et al, 2008; Kalantari et al, 2004; Kim et al, 2010; Mirabello et al, 2012; Snellenberg et al, 2012; Sun et al, 2011). For all this reasons, we decided to analyze DNA methylation of the HPV 16 LCR also in cervical AdCa, using a quantitative method.

From our analysis, the overall mean methylation frequency in the LCR seems to be higher in cervical AdCa compared to previous results obtained by Sun and colleagues using the same technique in CIN3+/SCC (~17% *vs* <5%, respectively) (Sun et al, 2011). Focusing the

attention on the E2BSs, we also observed a significant tendency for E2BS1 to be more methylated than E2BS3 and 4, which is in contrast with data obtained by Sun, but in agreement with those published by other groups (Chaiwongkot et al, 2012; Snellenberg et al, 2012). Although methylation at the E2BSs interferes with binding of E2, preventing transcriptional regulation of viral oncoproteins, it has has little or no effect on binding of other transcription factors such as Sp1 (CpG31, near E2BS3) and YY1 (near E2BS1), allowing E6/E7 to be efficiently transcribed (Höller et al, 1988; Thain et al, 1996). However, we observed wide standard deviations for the methylation frequency, in particular in the early promoter, suggesting a heterogeneous methylation in this region among samples and a possible relation with clinical/virological parameters. We found a tendency for invasive AdCa or non mucinous AdCa to be more methylated in the P_{97} promoter than AIS or mucinous AdCa, leading us to suppose that high methylation frequency in this zone may serve as marker of tumour invasion.

On the other hand, regarding the viral physical state and viral load, we observed a tendency for tumours harbouring totally episomal/mainly episomal viral DNA to have higher methylation frequency in the E6 promoter and no correlation was found with the viral load. These results seems to be in contrast with those showing in CaSki cell lines that integrated-multi copy viral DNA are silenced by *de novo* self-methylation to control gene dosage, starting from the enhancer and spreading towards the early promoter (De-Castro Arce et al, 2012). However, if CaSki are established cell lines for which the number of integrated copies of viral genome is known, it is not the same for clinical samples. So, methylation of both episomal and integrated DNA may have different functions/consequences depending on the stage of viral life cycle and cellular conditions.

5.2 Oral and Oropharyngeal SCCs

5.2.1 HPV 16 is confirmed the most prevalent genotype in OPSCCs

HPV infection is the necessary cause for cervical cancer development, but it is also associated to a well defined subgroup of HNSCCs, in particular OPSCCs, with many unresolved issues that have been studied in translational and clinical research during the last 30 years. An HPV-induced oral/oropharyngeal precancerous lesion has not been identified yet and the presence of HPV infection remains the only currently available indicator of future OPSCCs risk. However, current guidelines have not incorporated specific treatment modalities for HPV-related tumours.

Actually, many studies have analyzed HPV prevalence in HNSCCs. In our population, HPV prevalence was 66.7% which is higher than the overall prevalence published in two meta-analysis. In fact, Kreimer and colleagues, resuming data obtained in 60 studies from 26 countries worldwide, presented an HPV prevalence of 35.6% (Kreimer et al, 2005) and Mehanna, selecting 269 studies and 19 368 patients, reported 47.7% HPV positive OPSCCs (Mehanna et al, 2012). Our result may have been influenced by the high number of tonsillar tumours (55/81, 67.9%), known to have the strongest association with HPV (Syrjanen, 2004). However, our result agreed with the range of overall prevalence reported in studies performed after 2000 (range from 52.9% to 85.7%), highlighting the increased HPV prevalence over time, probably due also to an improvement of the sensitivity of the techniques used.

Agreement was also found concerning the genotype-specific prevalence, since HPV 16 as single infection was confirmed the most prevalent genotype among HPV-positive samples (81.5%). We did not detect HPV 18, but in three cases HPV 6 as single infections (5.6%). LR-HPV single infections in HNSCCs has been previously reported yet by Rautava (HPV 6 8.8% and HPV 11 2.9%) suggesting a different oncogenic potential of these genotypes compared to the cervical region (Rautava et al, 2012). However, this hypothesis has to be deepen with further experiments.

As we mentioned above, tonsillar carcinoma showed the highest association to HPV also in our population (69.3%), confirming this anatomical site as the preferential site for HPV infection in the oropharynx, maybe due to its histological similarity to the squamous-columnar junction of the cervical mucosal epithelium.

5.2.2 Preferentially high viral load and mixture of episomal and integrated forms of the virus is present in OPSCCs

There are few and variable data concerning the physical state or copy number of HPV in OPSCCs and its significance in these tumours.

In a descriptive update on the role of HPV in HNSCCs, Goon resumed results obtained by five previous studies, reporting that tonsillar carcinoma have higher viral load than non tonsillar and higher copy number of episomal viral DNA may be able to induce more rapid growth (Peter KC Goon, 2012). On the other hand, he also reported data from a study suggesting that a higher viral load (>190 copies/betactin) could be a favourable prognostic indicator. In our study, we observed high viral loads (>100 copies/cell) in most of the

samples, maybe due to the overrepresented tonsillar carcinoma, without significant association with clinical parameters.

Tonsillar carcinomas have been also reported to have the highest prevalence rate of episomal HPV DNA among HPV-positive HNSCCs. We detected prevalently a mixture of both integrated and episomal viral DNA and totally episomal genome only in 3 cases, suggesting a high heterogeneity and variation in the oncogenic pathways among these tumours.

5.2.3 There are differences in methylation frequency of the LCR among HPV-driven OPSCCs

Actually, in literature there are only two studies dealing with HPV 16 DNA methylation in HNSCCs (Balderas-Loaeza et al, 2007; Park et al, 2011). Balderas-Loeza analyzed 12 HPV 16-positive oral carcinoma with cloning followed by sequencing, finding hypermethylation of the LCR in 10 cases. On the other hand, Park, analyzing methylation through the entire viral genome in 22 patients with stage III/IV HPV-associated OPSCCs by bisulfite-sequencing method, observed a preferential hypomethylation of the LCR, in particular in the enhancer and inhibitory E2BSs. Moreover, he found a trend between viral methylation and E6/E7 expression or viral load, speculating that tumours with high viral loads could have significant silencing of the redundant copies through methylation and correspondingly low viral oncoproteins expression levels, which may account for improved survival rates. However, E6/E7 expression can be influenced by other factors than integration, such as (random) sites of integration of the viral genome in the host genome, which may be permissive or not for gene expression.

Results obtained in our study partially agree with those reported above. First of all, we confirmed the tendency of high-grade OPSCCs to be unmethylated in >50% of the CpG sites in the LCR, in particular in the enhancer and early promoter (Tab. 8, Fig. 29 and 30). However, we could observe significantly higher methylation frequency of the E2BS1 compared to E2BS3 and E2BS4 and seven patients harbouring viral DNA methylation frequency in the E6 promoter ranging from 20% to 65%, significantly higher than the overall mean (10%). We could not find a statistically significant correlation between mean methylation frequency in this 5 CpGs and tumour stage, clinical stage, viral load or physical state, highlighting the complexity of HPV-transforming pathway in OPSCCs.

5.2.4 Methylation frequency of the early promoter as suitable prognostic marker in OPSCCs

Treatment options for patients with HNSCCs are multimodal, involving a combination of surgery, radiotherapy, and chemotherapy (Peter KC Goon, 2012). The advantage of exclusive chemoradiotherapy (CRT) is its potential to preserve speech and swallowing function. It has been previously shown that HNSCCs positive for both HPV DNA and RNA have a better prognosis or response to CRT compared to completely negative tumours, suggesting an important role of the virus in cancer development and opening new horizons in the diagnostic field (Holzinger et al, 2012; Worden et al, 2008). Finding virological markers complementary to HPV DNA, which might help clinicians to decide for exclusive CRT or surgery as primary treatment or predict the good or bad prognosis, would be very useful and might improve both survival and quality of life, in particular in presence of young patients (Sharma et al, 2012).

Recently, it has been proposed that a triple panel p16-IHC/consensus PCR/HR-HPV ISH could improve HPV-driven OPSCCs detection in clinical samples (Pannone et al, 2012). On the other hand, Holzinger and colleagues tried to find biomarkers useful to reliably determine truly HPV-driven OPSCCs in 199 cases, finding viral RNA expression in only 20% of HPV 16-positive patients and observing that viral load or RNA pattern analysis is better suited than p16 expression for prognostic purposes (Holzinger et al, 2012). Although we could detect viral transcription in all the HPV 16-positive patients, making them all HPV-driven tumours, taking into account the DFS and viral parameters such as viral integration and methylation, we noted interesting trends and differences among them. In fact, when DFS was analyzed in function of the HPV presence/absence, patients with HPV-driven tumours had the tendency to have better 5 years-prognosis compared to HPV-negative ones. However, the Kaplan-Meier curves were quite overlapping. For this reason, we further analyzed the DFS dividing the HPV 16-driven patients in four groups: patients harbouring a) integrated/mainly integrated DNA, b) episomal/mainly episomal DNA, c) early promoter methylation frequency >10% and d) early promoter methylation frequency <10%. Concerning viral physical state, integration seems to be associated to a bad 5-years prognosis, similar to HPV-negative patients, and high methylation frequency in the E6 promoter region even worse. Interestingly, patients belonging to this group have not history of alcohol/tobacco use, making HPV infection the only risk factor for OPSCCs development. Even if the statistically significant difference was not obtained as well, the same trend regarding the association between early promoter

hypermethylation and worse prognosis compared to hypomethylation was previously observed also by Ding and colleagues in cervical SCCs (Ding et al, 2009).
From a technical point of view, however, since the methods to analyze the viral physical state (frequently real time-PCRs) are difficult to standardize, the analysis of viral DNA methylation by PCR followed by pyrosequencing seems to be more suitable for the development of a new diagnostic assay.

5.3 A mechanistic suggestion for HPV-mediated carcinogenesis alternative/synergistic to integration

The virus-mediated pathogenesis in both cervical cancer and HNSCCs is less than clear and the existence of multiple pathways to carcinogenesis is highly likely. Taken together, our results support the hypothesis that high methylation frequency in the LCR influences cervical cancer progression. Even if CpG methylation may be performed by both virus and cell, having distinct functional consequences and making a simple mechanistic interpretations difficult, we may speculate that during a normal productive infection, in basal cell lines, HPV uses the cellular machinery to methylate its episomal genome (preferentially the LCR), controlling gene expression. For unclear reasons (host factors may be involved), the balance between low and excessive methylation frequency may be shifted in favour of the latter, leading to cellular transformation (Fig. 45). In particular, in asymptomatic/normal infected cells, methylation frequency of the gene L1 and E2BS1 may progressively increase, causing L1 silencing, P_{97} upregulation, E6/E7 overexpression (first step for cellular transformation) and genomic instability (favouring viral integration). Then, methylation may spread towards the early promoter increasing its frequency also in correspondence of the E2BS3 and E2BS4, favouring more and more viral oncoproteins expression even in the presence of intact E2 (episomal viral genome). So, an excess of methylation frequency in viral genome, combined to methylation of other cellular genes (such as *hCADM1*, *hMAL*, *hTERT* in cervical cancer, see Overmeer et al, 2011), may start the "short-circuit" during viral productive infection leading to cellular breakdown. Once the virus becomes integrated into the host genome, methylation patterns may be altered due to complex epigenetic changes in integrated viral genomes.
According to this mechanistic suggestion and our results, methylation frequency at the E2BS1 may serve as diagnostic marker for pre-cancerous lesions and the same analysis at the E2BS3

and 4 (early promoter) as diagnostic marker (invasion or not) for cancerous lesions, at least in cervical AdCa or prognostic marker (DFS) in HPV 16-driven OPSCCs.

There are some limitations of these studies that should be discussed. Most importantly, we did not analyzed E2BS2 for HPV 16 DNA methylation. This is due mainly to technical reasons, but since this is the site with the lowest affinity for E2 binding and it is not involved in viral oncoproteins expression, we considered it not so important for our clinical purpose. Then, we analyzed only cancerous lesions. It would have been interesting to analyze also precancerous lesions, but, unfortunately, for cervical AdCa they are very difficult to obtain and for OPSCCs they have not been recognized yet. The number of HPV 16-positive OPSCCs analyzed for methylation *vs* clinical outcome and the time of follow-up which was less than 3 years for most of our patients: further studies should include additional centers to increase the size of population, longer time of follow-up (at least 5 years) and different types of treatments in order to assess the reproducibility of our results. Another limitation is the retrospective design; but it is important to note that the treatment regime during the study period was standardized and that the majority of the patients during the period were included.
However, we think that our findings may be a step toward the establishment of individualized therapy for patients with both cervical AdCa and HPV-driven OPSCCs.

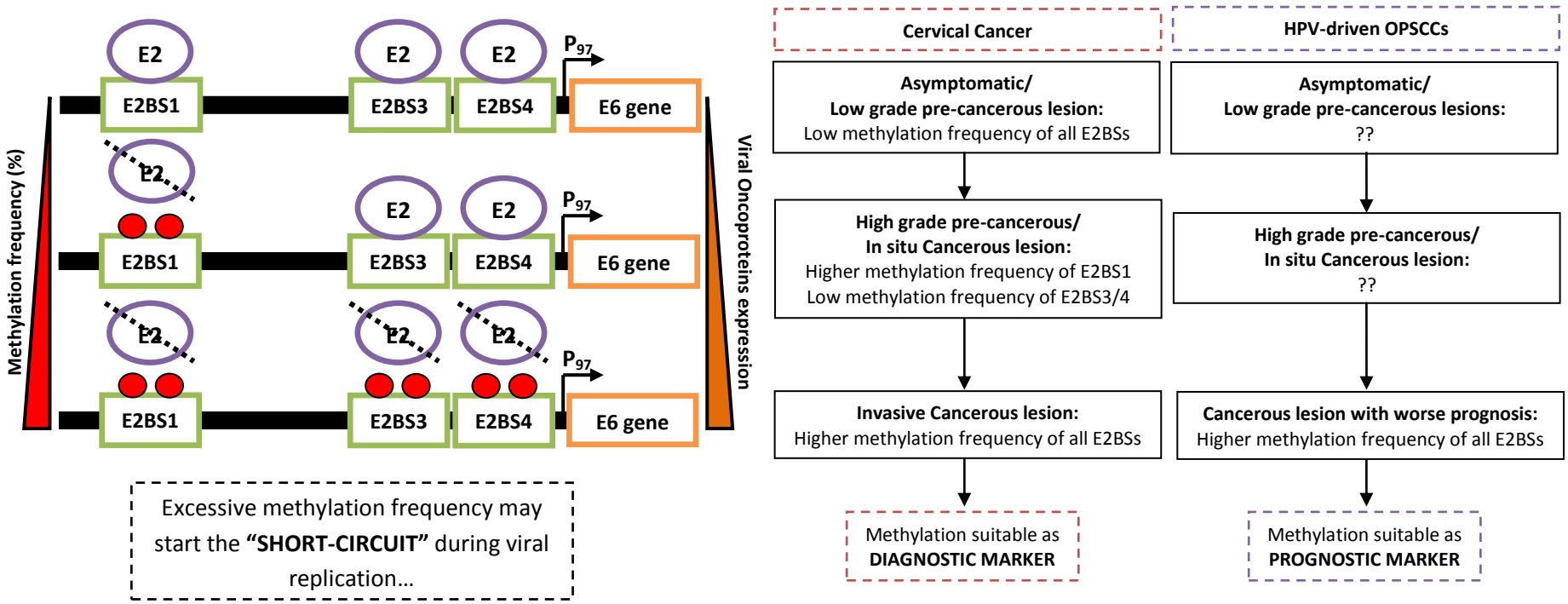

Figure 45 – Scheme summarising the suggested mechanism for HPV-mediated carcinogenesis, alternative/synergistic to viral integration, taking into account data previously published in literature (Clarke et al., 2012 and Chaiwongkot et al., 2012) and results obtained in the present study (left). Red circles correspond to meCpG sites. We also indicate the possible implications of HPV 16 methylation frequency in the E2BSs as diagnostic or prognostic marker in cervical cancer (in particular cervical AdCa) and HPV-associated OPSCCs (right).

<u>PART 3:</u> ANALYSIS OF THE RESPONSE TO IFN-κ TRANSFECTION IN CERVICAL CANCER AND HPV 16-POSITIVE HNSCCs

(experiments performed under the supervision of Dr. Bladimiro Rincon Orozco and Prof. Dr. Frank Rösl at the Division of Viral Transformation Mechanisms, Research Program in Infection and Cancer, German Cancer Research Center, Heidelberg, Germany)

IFNs are a family of structurally related cytokines successfully applied as biological therapy for many human cancers due to its antitumor activity. Since they also have antiviral and immunomodulatory effects, IFNs are particularly suitable as additional therapy for malignancies having infectious causes, such as cervical cancer or other HPV-associated diseases. However, existing IFNs-based therapies showed undesirable side effects (such as fever, fatigue and flu-like symptoms) which stimulate researchers to find alternative or complementary treatments.

In 2001, a new type I IFN expressed constitutively in epidermal keratinocytes and, after stimulation, in monocytes and DCs has been discovered. It was called IFN-κ and showed autocrine/juxtacrine activity. The few studies carried out to deepen its function in HPV-infected cells suggested an important role of this molecule in virus-mediated carcinogenesis, in particular because of its epigenetic silencing in HPV 16-positive cervical cancer cell lines, CaSki and SiHa, as well as clinical specimens (Rincon Orozco et al., 2009).

In this study, we transiently transfected both cervical cancer and HPV 16-positive HNSCCs cell lines with a recombinant form of IFN-κ (cloned into the pSecTagA vector) to analyze the effects on the expression of proteins involved in antigens presentation (MHC class I pathway), immunoproteasome and antiviral response. Even if weaker than IFN-β or IFN-γ treatment, 24 hours post-IFN-κ transfection, we could observe a significant increase in transcription levels of the genes involved in the mentioned pathways, for all the HPV 16-positive cell lines, compared to both the naïve and mock-transfected, but not for HPV 18-positive HeLa cells. These effects on ISGs and class I molecules can be attributed to the relevant increase of respectively IFN-β and NLRC5 expression and, since it has been reported that HeLa cells are not able to produce the former molecule, the absence of response is not surprising. Moreover, differences in the intensity of the response to IFN-κ transfection among tested cells may be due to differences in the amount of type I IFNR expressed, in particular the subunit IFNR1. In fact, CaSki, SiHa and Cal27 cells, which showed higher response to

both IFN-κ transfection and IFN-β treatment, showed higher levels of IFNR1 as well. This is the subunit mainly involved in starting type I IFNs signalling, since some phosphorilated Tyrosines within it serve as docking sites for the recruitment of downstream STAT proteins.
The antitumor activity of type I IFNs is exerted through different mechanisms and, among these, there are senescence induction and antiproliferative properties (Bekisz et al, 2010; Chiantore et al, 2012). For this reason, we decided to monitor also the effects of IFN-κ transfection on cell cycle. In cervical cancer, we observed a decrease in proliferation of transfected cells after 5 days, which was more evident and statistically significant in SiHa, rather than CaSki. This result was confirmed at both mRNA and protein level, since we did not detected significant down-regulation of proteins involved in cell cycle progression, such as Cyclin D1, CDK2 and Cyclin E1, after short-term transfection (1 day), but after longer time (6 days) in SiHa. Interestingly, we observed significantly lower IFN-β expression levels as well.

Taken together, these results suggest that IFN-κ has a role in antigens presentation by stimulating immunoproteasome formation and, even if less, HLA molecules production in HPV 16-infected cells, with more appreciable effects on cervical cancer cell lines rather than HPV-associated HNSCCs. This may have important implications, since it has been previously reported that the defect for presenting HPV 16 E6 epitopes in cervical carcinoma correlates with low expression of HLA class I, LMP2, LMP7, TAP complex and that upregulation of selected MHC class I allele expression induced by IFN-γ correlates with the resolution of cervical intraepithelial lesions or HR-HPV DNA clearance *in vivo* (Evans et al, 2001; Sikorski et al, 2004). Favouring the production of these proteins by treatments based on new molecules, such as IFN-κ, may be useful for the management of cervical cancer and other HPV-associated diseases, even if MHC class I low expression has been recently correlated to an increased survival in HPV-positive tonsillar SCCs (Näsman et al, 2013). In fact, the most immunogenic HPV 16 E6 epitope (peptide $E6_{29-38}$) would be better exposed on cell surface and recognized by the CTLs, activating the immune response against HPV-infected/cancerous cells (immunotherapy). Moreover, the antiviral activity of this new type I IFN, which seems to be acute and strongly mediated by IFN-β, is followed by an antiproliferative effect after a long-term exposure to the molecule.

All these observations and results have to be confirmed with further experiments. The analysis that we performed were a preliminary screening to understand the function of IFN-κ in HPV-infected tumoral cells and its potential utility as new treatment. Our recombinant molecule has been designed for biotechnological production in eucharіotic cells, such as CHO (Chinese hamster ovary) cells. It will be necessary producing and purifying it, in order to treat the same cell lines and reproduce the same results obtained by transfection.

References

Andrei G, Duraffour S, Van den Oord J, Snoeck R (2010) Epithelial raft cultures for investigations of virus growth, pathogenesis and efficacy of antiviral agents. *Antiviral Res* **85:** 431-449

Androphy EJ, Lowy DR, Schiller JT (1987) Bovine papillomavirus E2 trans-activating gene product binds to specific sites in papillomavirus DNA. *Nature* **325:** 70-73

Arias-Pulido H, Peyton CL, Joste NE, Vargas H, Wheeler CM (2006) Human papillomavirus type 16 integration in cervical carcinoma in situ and in invasive cervical cancer. *J Clin Microbiol* **44:** 1755-1762

Badal V, Chuang LS, Tan EH, Badal S, Villa LL, Wheeler CM, Li BF, Bernard HU (2003) CpG methylation of human papillomavirus type 16 DNA in cervical cancer cell lines and in clinical specimens: genomic hypomethylation correlates with carcinogenic progression. *J Virol* **77:** 6227-6234

Balderas-Loaeza A, Anaya-Saavedra G, Ramirez-Amador VA, Guido-Jimenez MC, Kalantari M, Calleja-Macias IE, Bernard HU, Garcia-Carranca A (2007) Human papillomavirus-16 DNA methylation patterns support a causal association of the virus with oral squamous cell carcinomas. *Int J Cancer* **120:** 2165-2169

Barbieri D, Nocera M, Gallinella G, Gentilomi GA, Plazzi M, Costa S, Santini D, Venturoli S (2012) Comparison of HPV sign Genotyping Test with INNO-LiPA HPV Genotyping Extra assay on histologic and cytologic cervical specimens. *Diagn Microbiol Infect Dis* **74:** 43-48

Barzon L, Militello V, Lavezzo E, Franchin E, Peta E, Squarzon L, Trevisan M, Pagni S, Dal Bello F, Toppo S, Palù G (2012) Human papillomavirus genotyping by 454 next generation sequencing technology. *Journal of Clinical Virology* **52:** 93-97

Beglin M, Melar-New M, Laimins L (2009) Human papillomaviruses and the interferon response. *J Interferon Cytokine Res* **29:** 629-635

Bekisz J, Baron S, Balinsky C, Morrow A, Zoon KC (2010) Antiproliferative Properties of Type I and Type II Interferon. *Pharmaceuticals (Basel)* **3:** 994-1015

Brandsma JL, Sun Y, Lizardi PM, Tuck DP, Zelterman D, Haines GK, 3rd, Martel M, Harigopal M, Schofield K, Neapolitano M (2009) Distinct human papillomavirus type 16 methylomes in cervical cells at different stages of premalignancy. *Virology* **389:** 100-107

Buontempo PJ, Jubin RG, Buontempo CA, Wagner NE, Reyes GR, Baroudy BM (2006) Antiviral activity of transiently expressed IFN-kappa is cell-associated. *J Interferon Cytokine Res* **26:** 40-52

Burgers WA, Blanchon L, Pradhan S, de Launoit Y, Kouzarides T, Fuks F (2007) Viral oncoproteins target the DNA methyltransferases. *Oncogene* **26:** 1650-1655

Castellsague X, Diaz M, de Sanjose S, Munoz N, Herrero R, Franceschi S, Peeling RW, Ashley R, Smith JS, Snijders PJ, Meijer CJ, Bosch FX (2006) Worldwide human papillomavirus etiology of cervical adenocarcinoma and its cofactors: implications for screening and prevention. In *J Natl Cancer Inst* Vol. 98, pp 303-315. United States

Castellsagué X, Bosch FX, Muñoz N (2002) Environmental co-factors in HPV carcinogenesis. *Virus Res* **89:** 191-199

Chaiwongkot A, Vinokurova S, Pientong C, Ekalaksananan T, Kongyingyoes B, Kleebkaow P, Chumworathayi B, Patarapadungkit N, Reuschenbach M, von Knebel Doeberitz M (2012) Differential methylation of E2 binding sites in episomal and integrated HPV 16 genomes in preinvasive and invasive cervical lesions. *Int J Cancer*

Chiantore MV, Vannucchi S, Accardi R, Tommasino M, Percario ZA, Vaccari G, Affabris E, Fiorucci G, Romeo G (2012) Interferon-β induces cellular senescence in cutaneous human papilloma virus-transformed human keratinocytes by affecting p53 transactivating activity. *PLoS One* **7:** e36909

Clarke MA, Wentzensen N, Mirabello L, Ghosh A, Wacholder S, Harari A, Lorincz A, Schiffman M, Burk RD (2012) Human papillomavirus DNA methylation as a potential biomarker for cervical cancer. *Cancer Epidemiol Biomarkers Prev* **21:** 2125-2137

Constandinou-Williams C, Collins SI, Roberts S, Young LS, Woodman CB, Murray PG (2010) Is human papillomavirus viral load a clinically useful predictive marker? A longitudinal study. *Cancer Epidemiol Biomarkers Prev* **19:** 832-837

Costa S, Venturoli S, Negri G, Sideri M, Preti M, Pesaresi M, Falasca A, Barbieri D, Zerbini M, Santini D, Sandri MT, Ghiringhello B, Caroppo Venturini N, Syrjanen S, Syrjanen K (2012). Factors predicting the outcome of conservatively treated adenocarcinoma in situ of the uterine cervix: An analysis of 166 cases. *Gynaecologic Oncology* **124**: 490-495

Cricca M, Morselli-Labate AM, Venturoli S, Ambretti S, Gentilomi GA, Gallinella G, Costa S, Musiani M, Zerbini M (2007) Viral DNA load, physical status and E2/E6 ratio as markers to grade HPV16 positive women for high-grade cervical lesions. *Gynecol Oncol* **106:** 549-557

Cuzick J, Bergeron C, von Knebel Doeberitz M, Gravitt P, Jeronimo J, Lorincz AT, J L M Meijer C, Sankaranarayanan R, J F Snijders P, Szarewski A (2012) New technologies and procedures for cervical cancer screening. *Vaccine* **30 Suppl 5:** F107-116

Day PM, Lowy DR, Schiller JT (2003) Papillomaviruses infect cells via a clathrin-dependent pathway. *Virology* **307:** 1-11

de Sanjose S, Quint WG, Alemany L, Geraets DT, Klaustermeier JE, Lloveras B, Tous S, Felix A, Bravo LE, Shin HR, Vallejos CS, de Ruiz PA, Lima MA, Guimera N, Clavero O, Alejo M, Llombart-Bosch A, Cheng-Yang C, Tatti SA, Kasamatsu E, Iljazovic E, Odida M, Prado R, Seoud M, Grce M, Usubutun A, Jain A, Suarez GA, Lombardi LE, Banjo A, Menéndez C, Domingo EJ, Velasco J, Nessa A, Chichareon SC, Qiao YL, Lerma E, Garland SM, Sasagawa T, Ferrera A, Hammouda D, Mariani L, Pelayo A, Steiner I, Oliva E, Meijer CJ, Al-Jassar WF, Cruz E, Wright TC, Puras A, Llave CL, Tzardi M, Agorastos T, Garcia-Barriola V, Clavel C, Ordi J, Andújar M, Castellsagué X, Sánchez GI, Nowakowski AM, Bornstein J, Muñoz N, Bosch FX, Group RISaHTTS (2010) Human papillomavirus genotype attribution in invasive cervical cancer: a retrospective cross-sectional worldwide study. *Lancet Oncol* **11:** 1048-1056

de Villiers EM, Fauquet C, Broker TR, Bernard HU, zur Hausen H (2004) Classification of papillomaviruses. *Virology* **324:** 17-27

De-Castro Arce J, Gockel-Krzikalla E, Rosl F (2012) Silencing of multi-copy HPV16 by viral self-methylation and chromatin occlusion: a model for epigenetic virus-host interaction. In *Hum Mol Genet* Vol. 21, pp 1693-1705. England

Didelot-Rousseau MN, Courgnaud V, Nagot N, Ouedraogo A, Konate I, Mayaud P, Weiss H, Van de Perre P, Segondy M (2006) Comparison of INNO-LiPA HPV Genotyping v2 with PCR product subcloning and sequencing for identification of genital human papillomavirus genotypes in African women. *J Virol Methods* **135:** 181-185

Ding DC, Chiang MH, Lai HC, Hsiung CA, Hsieh CY, Chu TY (2009) Methylation of the long control region of HPV16 is related to the severity of cervical neoplasia. *Eur J Obstet Gynecol Reprod Biol* **147:** 215-220

Doorbar J (2006) Molecular biology of human papillomavirus infection and cervical cancer. *Clin Sci (Lond)* **110:** 525-541

Evans M, Borysiewicz LK, Evans AS, Rowe M, Jones M, Gileadi U, Cerundolo V, Man S (2001) Antigen processing defects in cervical carcinomas limit the presentation of a CTL epitope from human papillomavirus 16 E6. *J Immunol* **167:** 5420-5428

Frazer IH (2009) Interaction of human papillomaviruses with the host immune system: a well evolved relationship. *Virology* **384:** 410-414

Ganguly N, Parihar SP (2009) Human papillomavirus E6 and E7 oncoproteins as risk factors for tumorigenesis. *J Biosci* **34:** 113-123

Gharizadeh B, Ghaderi M, Donnelly D, Amini B, Wallin KL, Nyrén P (2003) Multiple-primer DNA sequencing method. *Electrophoresis* **24:** 1145-1151

Gharizadeh B, Kalantari M, Garcia CA, Johansson B, Nyrén P (2001) Typing of human papillomavirus by pyrosequencing. *Lab Invest* **81:** 673-679

Gharizadeh B, Oggionni M, Zheng B, Akom E, Pourmand N, Ahmadian A, Wallin KL, Nyrén P (2005) Type-specific multiple sequencing primers: a novel strategy for reliable and rapid genotyping of human papillomaviruses by pyrosequencing technology. *J Mol Diagn* **7:** 198-205

Gien LT, Beauchemin MC, Thomas G (2010) Adenocarcinoma: a unique cervical cancer. In *Gynecol Oncol* Vol. 116, pp 140-146. United States

Gravitt PE (2011) The known unknowns of HPV natural history. *J Clin Invest* **121:** 4593-4599

Gravitt PE, Kovacic MB, Herrero R, Schiffman M, Bratti C, Hildesheim A, Morales J, Alfaro M, Sherman ME, Wacholder S, Rodriguez AC, Burk RD (2007) High load for most high risk human papillomavirus genotypes is associated with prevalent cervical cancer precursors but only HPV16 load predicts the development of incident disease. *Int J Cancer* **121:** 2787-2793

Génin P, Vaccaro A, Civas A (2009) The role of differential expression of human interferon--a genes in antiviral immunity. *Cytokine Growth Factor Rev* **20:** 283-295

Haller O, Kochs G, Weber F (2007) Interferon, Mx, and viral countermeasures. *Cytokine Growth Factor Rev* **18:** 425-433

Hegde RS (2002) The papillomavirus E2 proteins: structure, function, and biology. *Annu Rev Biophys Biomol Struct* **31:** 343-360

Holzinger D, Schmitt M, Dyckhoff G, Benner A, Pawlita M, Bosch FX (2012) Viral RNA Patterns and High Viral Load Reliably Define Oropharynx Carcinomas with Active HPV16 Involvement. *Cancer Res* **72:** 4993-5003

Hong D, Ye F, Lu W, Hu Y, Wan X, Chen Y, Xie X (2008) Methylation status of the long control region of HPV 16 in clinical cervical specimens. *Mol Med Report* **1:** 555-560

Hwang LY, Lieu PT, Peterson PA, Yang Y (2001) Functional regulation of immunoproteasomes and transporter associated with antigen processing. *Immunol Res* **24:** 245-272

Höller M, Westin G, Jiricny J, Schaffner W (1988) Sp1 transcription factor binds DNA and activates transcription even when the binding site is CpG methylated. *Genes Dev* **2:** 1127-1135

Kalantari M, Calleja-Macias IE, Tewari D, Hagmar B, Lie K, Barrera-Saldana HA, Wiley DJ, Bernard HU (2004) Conserved methylation patterns of human papillomavirus type 16 DNA in asymptomatic infection and cervical neoplasia. *J Virol* **78:** 12762-12772

Kim JH, Choi YD, Lee JS, Lee JH, Nam JH, Choi C (2010) Assessment of DNA methylation for the detection of cervical neoplasia in liquid-based cytology specimens. In *Gynecol Oncol* Vol. 116, pp 99-104. United States

Kim K, Garner-Hamrick PA, Fisher C, Lee D, Lambert PF (2003) Methylation patterns of papillomavirus DNA, its influence on E2 function, and implications in viral infection. *J Virol* **77:** 12450-12459

Kjær SK, Frederiksen K, Munk C, Iftner T (2010) Long-term absolute risk of cervical intraepithelial neoplasia grade 3 or worse following human papillomavirus infection: role of persistence. *J Natl Cancer Inst* **102:** 1478-1488

Koromilas AE, Li S, Matlashewski G (2001) Control of interferon signaling in human papillomavirus infection. *Cytokine Growth Factor Rev* **12:** 157-170

Kostareli E, Holzinger D, Hess J (2012) New Concepts for Translational Head and Neck Oncology: Lessons from HPV-Related Oropharyngeal Squamous Cell Carcinomas. *Front Oncol* **2:** 36

Kreimer AR, Chaturvedi AK (2011) HPV-associated Oropharyngeal Cancers--Are They Preventable? *Cancer Prev Res (Phila)* **4:** 1346-1349

Kreimer AR, Clifford GM, Boyle P, Franceschi S (2005) Human papillomavirus types in head and neck squamous cell carcinomas worldwide: a systematic review. *Cancer Epidemiol Biomarkers Prev* **14:** 467-475

LaFleur DW, Nardelli B, Tsareva T, Mather D, Feng P, Semenuk M, Taylor K, Buergin M, Chinchilla D, Roshke V, Chen G, Ruben SM, Pitha PM, Coleman TA, Moore PA (2001) Interferon-kappa, a novel type I interferon expressed in human keratinocytes. *J Biol Chem* **276:** 39765-39771

Lazarczyk M, Cassonnet P, Pons C, Jacob Y, Favre M (2009) The EVER proteins as a natural barrier against papillomaviruses: a new insight into the pathogenesis of human papillomavirus infections. *Microbiol Mol Biol Rev* **73:** 348-370

Leemans CR, Braakhuis BJ, Brakenhoff RH (2011) The molecular biology of head and neck cancer. *Nat Rev Cancer* **11:** 9-22

Leo E, Venturoli S, Cricca M, Musiani M, Zerbini M (2009) High-throughput two-step LNA real time PCR assay for the quantitative detection and genotyping of HPV prognostic-risk groups. In *J Clin Virol* Vol. 45, pp 304-310. Netherlands

Lewis H, Webster K, Sanchez-Perez AM, Gaston K (1999) Cellular transcription factors regulate human papillomavirus type 16 gene expression by binding to a subset of the DNA sequences recognized by the viral E2 protein. *J Gen Virol* **80 (Pt 8):** 2087-2096

Li N, Franceschi S, Howell-Jones R, Snijders PJ, Clifford GM (2011) Human papillomavirus type distribution in 30,848 invasive cervical cancers worldwide: Variation by geographical region, histological type and year of publication. *Int J Cancer* **128:** 927-935

Lichtig H, Algrisi M, Botzer LE, Abadi T, Verbitzky Y, Jackman A, Tommasino M, Zehbe I, Sherman L (2006) HPV16 E6 natural variants exhibit different activities in functional assays relevant to the carcinogenic potential of E6. *Virology* **350:** 216-227

Lohavanichbutr P, Houck J, Fan W, Yueh B, Mendez E, Futran N, Doody DR, Upton MP, Farwell DG, Schwartz SM, Zhao LP, Chen C (2009) Genomewide gene expression profiles of HPV-positive and HPV-negative oropharyngeal cancer: potential implications for treatment choices. *Arch Otolaryngol Head Neck Surg* **135:** 180-188

Matovina M, Sabol I, Grubisić G, Gasperov NM, Grce M (2009) Identification of human papillomavirus type 16 integration sites in high-grade precancerous cervical lesions. *Gynecol Oncol* **113:** 120-127

Mehanna H, Beech T, Nicholson T, El-Hariry I, McConkey C, Paleri V, Roberts S (2012) Prevalence of human papillomavirus in oropharyngeal and nonoropharyngeal head and neck cancer-systematic review and meta-analysis of trends by time and region. *Head Neck*

Meissner TB, Li A, Kobayashi KS (2012) NLRC5: a newly discovered MHC class I transactivator (CITA). *Microbes Infect* **14:** 477-484

Miller DL, Puricelli MD, Stack MS (2012) Virology and molecular pathogenesis of HPV (human papillomavirus)-associated oropharyngeal squamous cell carcinoma. *Biochem J* **443:** 339-353

Mirabello L, Schiffman M, Ghosh A, Rodriguez AC, Vasiljevic N, Wentzensen N, Herrero R, Hildesheim A, Wacholder S, Scibior-Bentkowska D, Burk RD, Lorincz AT (2012) Elevated methylation of HPV16 DNA is associated with the development of high grade cervical intraepithelial neoplasia. *Int J Cancer*

Muñoz N, Castellsagué X, de González AB, Gissmann L (2006) Chapter 1: HPV in the etiology of human cancer. *Vaccine* **24 Suppl 3:** S3/1-10

Neefjes J, Jongsma ML, Paul P, Bakke O (2011) Towards a systems understanding of MHC class I and MHC class II antigen presentation. *Nat Rev Immunol* **11:** 823-836

Näsman A, Andersson E, Nordfors C, Grün N, Johansson H, Munck-Wikland E, Massucci G, Dalianis T, Ramqvist T (2013) MHC class I expression in HPV positive and negative tonsillar squamous cell carcinoma in correlation to clinical outcome. *Int J Cancer* **132:** 72-81

Pannone G, Rodolico V, Santoro A, Lo Muzio L, Franco R, Botti G, Aquino G, Pedicillo MC, Cagiano S, Campisi G, Rubini C, Papagerakis S, De Rosa G, Tornesello ML, Buonaguro FM, Staibano S, Bufo P (2012) Evaluation of a combined triple method to detect causative HPV in oral and oropharyngeal squamous cell carcinomas: p16 Immunohistochemistry, Consensus PCR HPV-DNA, and In Situ Hybridization. *Infect Agent Cancer* **7:** 4

Park IS, Chang X, Loyo M, Wu G, Chuang A, Kim MS, Chae YK, Lyford-Pike S, Westra WH, Saunders JR, Sidransky D, Pai SI (2011) Characterization of the methylation patterns in human papillomavirus type 16 viral DNA in head and neck cancers. *Cancer Prev Res (Phila)* **4:** 207-217

Perrons C, Jelley R, Kleter B, Quint W, Brink N (2005) Detection of persistent high risk human papillomavirus infections with hybrid capture II and SPF10/LiPA. *J Clin Virol* **32:** 278-285

Peter KC Goon MAS, Jörg Ebmeyer, Lars Steinsträsser, Tahwinder Upile, Waseem Jerjes, Manuel Bernal-Sprekelsen, Martin Görner, Holger H Sudhoff (2012) HPV & head and neck cancer: a descriptive update. *Head & Neck Oncology* **1:** 36

Pett M, Coleman N (2007) Integration of high-risk human papillomavirus: a key event in cervical carcinogenesis? *J Pathol* **212:** 356-367

Pett MR, Alazawi WO, Roberts I, Dowen S, Smith DI, Stanley MA, Coleman N (2004) Acquisition of high-level chromosomal instability is associated with integration of human papillomavirus type 16 in cervical keratinocytes. *Cancer Res* **64:** 1359-1368

Poljak M, Kocjan BJ (2010) Commercially available assays for multiplex detection of alpha human papillomaviruses. *Expert Rev Anti Infect Ther* **8:** 1139-1162

Qu W, Jiang G, Cruz Y, Chang CJ, Ho GY, Klein RS, Burk RD (1997) PCR detection of human papillomavirus: comparison between MY09/MY11 and GP5+/GP6+ primer systems. *J Clin Microbiol* **35:** 1304-1310

Quint KD, de Koning MN, van Doorn LJ, Quint WG, Pirog EC (2010) HPV genotyping and HPV16 variant analysis in glandular and squamous neoplastic lesions of the uterine cervix. In *Gynecol Oncol* Vol. 117, pp 297-301. United States: 2010 Elsevier Inc

Rajeevan MS, Swan DC, Duncan K, Lee DR, Limor JR, Unger ER (2006) Quantitation of site-specific HPV 16 DNA methylation by pyrosequencing. *J Virol Methods* **138:** 170-176

Rautava J, Kuuskoski J, Syrjanen K, Grenman R, Syrjanen S (2012) HPV genotypes and their prognostic significance in head and neck squamous cell carcinomas. *J Clin Virol* **53:** 116-120

Rigoni-Stern, D. (1842). Fatti statistici relativi alle malattie cancrosi che servirono da base alle poche cose dette dal dott. Giornale. Service propr.pathol.terap.ser. 2: 507–517.

Rincon-Orozco B, Halec G, Rosenberger S, Muschik D, Nindl I, Bachmann A, Ritter TM, Dondog B, Ly R, Bosch FX, Zawatzky R, Rosl F (2009) Epigenetic silencing of interferon-kappa in human papillomavirus type 16-positive cells. *Cancer Res* **69:** 8718-8725

Seoud M, Tjalma WA, Ronsse V (2011) Cervical adenocarcinoma: moving towards better prevention. *Vaccine* **29:** 9148-9158

Sharma A, Méndez E, Yueh B, Lohavanichbutr P, Houck J, Doody DR, Futran ND, Upton MP, Schwartz SM, Chen C (2012) Human papillomavirus-positive oral cavity and oropharyngeal cancer patients do not have better quality-of-life trajectories. *Otolaryngol Head Neck Surg* **146:** 739-745

Sheu BC, Chang WC, Lin HH, Chow SN, Huang SC (2007) Immune concept of human papillomaviruses and related antigens in local cancer milieu of human cervical neoplasia. *J Obstet Gynaecol Res* **33:** 103-113

Sichero L, Simão Sobrinho J, Lina Villa L (2012) Oncogenic potential diverge among human papillomavirus type 16 natural variants. *Virology* **432:** 127-132

Sikorski M, Bobek M, Zrubek H, Marcinkiewicz J (2004) Dynamics of selected MHC class I and II molecule expression in the course of HPV positive CIN treatment with the use of human recombinant IFN-gamma. *Acta Obstet Gynecol Scand* **83:** 299-307

Snellenberg S, Schutze DM, Claassen-Kramer D, Meijer CJ, Snijders PJ, Steenbergen RD (2012) Methylation status of the E2 binding sites of HPV16 in cervical lesions determined with the Luminex(R) xMAP system. *Virology* **422:** 357-365

Spaapen RM, Neefjes J (2012) Immuno-waste exposure and further management. *Nat Immunol* **13:** 109-111

Stanley M (2010) Pathology and epidemiology of HPV infection in females. *Gynecol Oncol* **117:** S5-10

Stanley MA, Pett MR, Coleman N (2007) HPV: from infection to cancer. *Biochem Soc Trans* **35:** 1456-1460

Sun C, Reimers LL, Burk RD (2011) Methylation of HPV16 genome CpG sites is associated with cervix precancer and cancer. *Gynecol Oncol* **121:** 59-63

Syrjanen S (2004) HPV infections and tonsillar carcinoma. *J Clin Pathol* **57:** 449-455

Syrjanen S (2010) The role of human papillomavirus infection in head and neck cancers. *Ann Oncol* **21 Suppl 7:** vii243-245

Syrjänen K, Syrjänen S, Lamberg M, Pyrhönen S, Nuutinen J (1983) Morphological and immunohistochemical evidence suggesting human papillomavirus (HPV) involvement in oral squamous cell carcinogenesis. *Int J Oral Surg* **12:** 418-424

Szalmas A, Konya J (2009) Epigenetic alterations in cervical carcinogenesis. *Semin Cancer Biol* **19:** 144-152

Tawfik El-Mansi M, Cuschieri KS, Morris RG, Williams AR (2006) Prevalence of human papillomavirus types 16 and 18 in cervical adenocarcinoma and its precursors in Scottish patients. *Int J Gynecol Cancer* **16:** 1025-1031

Thain A, Jenkins O, Clarke AR, Gaston K (1996) CpG methylation directly inhibits binding of the human papillomavirus type 16 E2 protein to specific DNA sequences. *J Virol* **70:** 7233-7235

Tornesello ML, Losito S, Benincasa G, Fulciniti F, Botti G, Greggi S, Buonaguro L, Buonaguro FM (2011) Human papillomavirus (HPV) genotypes and HPV16 variants and risk of adenocarcinoma and squamous cell carcinoma of the cervix. In *Gynecol Oncol* Vol. 121, pp 32-42. United States: 2010 Elsevier Inc

van Doorn LJ, Quint W, Kleter B, Molijn A, Colau B, Martin MT, Kravang-In, Torrez-Martinez N, Peyton CL, Wheeler CM (2002) Genotyping of human papillomavirus in liquid cytology cervical specimens by the PGMY line blot assay and the SPF(10) line probe assay. *J Clin Microbiol* **40:** 979-983

Veldhuijzen NJ, Snijders PJ, Reiss P, Meijer CJ, van de Wijgert JH (2010) Factors affecting transmission of mucosal human papillomavirus. *Lancet Infect Dis* **10:** 862-874

Vinokurova S, von Knebel Doeberitz M (2011) Differential methylation of the HPV 16 upstream regulatory region during epithelial differentiation and neoplastic transformation. *PLoS One* **6:** e24451

Vinokurova S, Wentzensen N, Kraus I, Klaes R, Driesch C, Melsheimer P, Kisseljov F, Dürst M, Schneider A, von Knebel Doeberitz M (2008) Type-dependent integration frequency of human papillomavirus genomes in cervical lesions. *Cancer Res* **68:** 307-313

Wentzensen N, Vinokurova S, von Knebel Doeberitz M (2004) Systematic review of genomic integration sites of human papillomavirus genomes in epithelial dysplasia and invasive cancer of the female lower genital tract. *Cancer Res* **64:** 3878-3884

Worden FP, Kumar B, Lee JS, Wolf GT, Cordell KG, Taylor JM, Urba SG, Eisbruch A, Teknos TN, Chepeha DB, Prince ME, Tsien CI, D'Silva NJ, Yang K, Kurnit DM, Mason HL, Miller TH, Wallace NE, Bradford CR, Carey TE (2008) Chemoselection as a strategy for organ preservation in advanced oropharynx cancer: response and survival positively associated with HPV16 copy number. *J Clin Oncol* **26:** 3138-3146

Yugawa T, Kiyono T (2009) Molecular mechanisms of cervical carcinogenesis by high-risk human papillomaviruses: novel functions of E6 and E7 oncoproteins. *Rev Med Virol* **19:** 97-113

Zaino RJ (2000) Glandular lesions of the uterine cervix. *Mod Pathol* **13:** 261-274

Zheng ZM, Baker CC (2006) Papillomavirus genome structure, expression, and post-transcriptional regulation. *Front Biosci* **11:** 2286-2302

Zubach V, Smart G, Ratnam S, Severini A (2012) Novel microsphere-based method for detection and typing of 46 mucosal human papillomavirus types. *J Clin Microbiol* **50:** 460-464

zur Hausen H, Gissmann L, Steiner W, Dippold W, Dreger J (1975) Human papilloma viruses and cancer. *Bibl Haematol*, 43: 569–571